School of Molecular and Cell Biology

University of the Witwatersrand

Johannesburg

Controlling gold nanoparticle biogenesis in the bacterium *Enterobacter* sp. Pb204

A Dissertation submitted to the Faculty of Science of the University of Witwatersrand, Johannesburg, in full fulfilment of the requirements for the degree of Master of Science

October 2018

by

Nicholas Ryan Ho

606903

Supervisor: Dr Kulsum Kondiah

Co-supervisor: Dr Pieter De Maayer

Advisor: Prof. Karl Rumbold

Declaration

I, Nicholas Ryan Ho (606903), am a student registered for the degree of Master of Science (MSc): Biotechnology in the academic year 2018.

I hereby declare the following:

- I am aware that plagiarism (the use of someone else's work without their permission and/or without acknowledging the original source) is wrong.
- I confirm that the work submitted for assessment for the above degree is my own unaided work except where explicitly indicated otherwise.
- I have not submitted this work before for any other degree or examination at any other University.
- I have followed the required conventions in referencing the thoughts and ideas of others.
- I understand that the University of the Witwatersrand may take disciplinary action against me if there is a belief that this is not my own unaided work or that I have failed to acknowledge the source of the ideas or words in my writing.

Signature of candidate 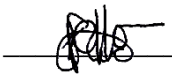 04 day of October 2018

Dedication

To my family

Acknowledgements

My utmost gratitude goes to my supervisor, Dr. Kulsum Kondiah, and my co-supervisor, Dr. Pieter De Maayer. I would like to thank you for all of the guidance, encouragement and your endless patience. Your support has allowed me to achieve what was only a dream when I first entered university. The guidance that you have provided me has not only changed the way that I approach problems in science but also challenges in my own personal life.

I would also like to thank my advisor, Prof. Karl Rumbold, for the use of his lab for the last 4 months of 2017. My research would have been much more difficult if it was not for your generosity in both knowledge and advice. You have become both my mentor and my friend.

To my parents, Charmaine and Patrick Ho, who have supported me though out my entire life, your struggles and hardships have allowed me to pursue my dreams and proved a solid foundation for my future. No words could express the gratitude that I have for you. To Lance Ho, my brother and my first friend, thank you for everything you have done for me. You have been the person who I strive to be like the most in science and in life. My family's love and support throughout my life have given me the tools to be the best possible version of myself. I hope to do you proud.

To all of my friends from first year, Liang Gu, Tyrone Otgaar, Megan Govender and Edward Chen, thank you for all of the memories and good times you have given me. To my friends in the Biology building and room B207 (Helen Walsh, Warren Freeborough, Frances Aryes and everyone else who I have had the privilege to meet), you have made my postgrad life enjoyable. Our many debates have been the highlight of my Masters which have ranged from the net worth of Tony Stark to the possibility of creating teacup mammoths. To my friends outside of the scientific field, you have always been there for discussions about science, current affairs and life in general.

To the members of Environmental Biotechnology Laboratory and Industrial Microbiology and Biotechnology Laboratory, thank you for providing a supportive work environment.

Lastly, I would like to thank the National Research Foundation and the University of the Witwatersrand for the funding for the duration of this project

Abstract

Research into the synthesis of gold nanoparticles (AuNPs) has increased in the past few decades due to their wide range of potential applications, with increased emphasis placed on the greener synthesis of AuNPs. A promising method of synthesis is bacterial synthesis but one of the largest obstacles faced by this method is the large variability in the shape and size of AuNPs. To this end, the aim of this study was to improve the uniformity of AuNPs synthesised by a bacterium isolated from acid mine decant on the West Rand of Gauteng, South Africa, (26°06'26.8"S 27°43'20.2"E) (*Enterobacter* sp. Pb204) through alteration of reaction parameters as well as the determination of possible genetic pathways responsible for AuNP synthesis.

The following reaction parameters: growth media, biocatalyst ratio, temperature, pH and gold ion concentration were altered to determine their influence on AuNP synthesis by *Enterobacter* sp. Pb204. The AuNPs were analysed using ultraviolet-visible spectroscopy, transmission electron microscopy and energy-dispersive X-ray spectroscopy. Following the optimisation of AuNP biogenesis in *Enterobacter* sp. Pb204, the whole genome of the bacterium was sequenced using the Illumina Hiseq (2500, California, USA).

To produce uniformed spherical AuNPs, within a size range of 2 to 15 nm, the following parameters were identified: cell biocatalyst grown LB at a pH of 3, incubated at 37 °C with a chloroauric acid concentration of 1 mM for 24 hours. The whole genome analysis of *Enterobacter* sp. Pb204 revealed that it is a unique strain of *Enterobacter xiangfangensis* LMG 27195^{T} and was therefore named *E. xiangfangensis* Pb204. Further analysis of *E. xiangfangensis* Pb204's genome revealed that it possessed several unique metal resistance genes not found in the type strain. The majority of these genes were found on an integrated conjugative element (ICE). The presence of the ICE element, with the extra cargo genes, in *E. xiangfangensis* Pb204 may play a role in AuNP synthesis.

The results of this dissertation suggest that *E. xiangfangensis* Pb204 has the ability to synthesis uniformed AuNPs under the correct reaction parameters.

Keywords: *Enterobacter xiangfangensis* Pb204, biological synthesis, gold nanoparticles, integrated conjugative element, metal resistance genes

Outputs of the study

1. Poster presentation at the 16th Frontiers of Electron Microscopy in Materials Science International Conference: Ho, N. R., De Maayer, P., and Kondiah, K. (2017). Controlling gold nanoparticle biogenesis in the bacterium *Paenibacillus castaneae*. The 16th Frontiers of Electron Microscopy in Materials Science International Conference (FEMMS), Johannesburg, South Africa.
2. Two articles will be produced from the results of this study and will be submitted for publication in ISI rated journals by May 2018.

Table of Contents

Declaration……i

Dedication……ii

Acknowledgements iii

Abstract……v

Outputs of the study vii

List of figures xii

List of tables xiv

List of abbreviations xv

Chapter 1: Introduction 1

1.1 Background 1

1.2 Knowledge gap 3

1.3 Aims and objectives 6

1.3.1 Main aim 6

1.3.2 Specific objectives 6

1.4 Chapter outline 7

Chapter 2: Literature Review 8

2.1 Gold nanoparticles 8

2.1.1 History of AuNPs 8

2.1.2 Properties of AuNPs 8

2.2 Applications of AuNPs 9

2.2.1 Gene delivery 9

2.2.2 Drug delivery 10

2.2.3 Biodetection 10

2.2.4 Bioimaging 11

2.2.5 Electrical energy production and storage 12

2.2.6 Industrial catalysis 12
2.3 Synthesis of AuNPs 13
2.3.1 Physical synthesis 13
2.3.2 Chemical synthesis 14
2.3.3 Biological synthesis 16
2.3.3.1. Bacterial synthesis 16
2.5 Advantage and disadvantages of biological AuNPs synthesis 18
2.6 Factors influencing size and shape of AuNPs during biological synthesis. 19
2.6.1 Effects of pH 19
2.6.2 Effects of temperature 20
2.6.3 Effects of biomass to gold solution volume 20
2.6.4 Effects of gold ion concentration 21
2.7 Rationale for the current study 21
2.7.1 The genus *Enterobacter* 21
2.7.2 Research rationale 23
Chapter 3: The influence of reaction parameters on the biogenesis of AuNPs in *Enterobacter* sp. Pb204 24
3.1 Introduction 24
3.2 Methodology 25
3.2.1 Materials 25
3.2.2 Identification of *Enterobacter* sp. Pb204 by 16S rRNA sequencing ... 26
3.2.3 Biogenesis of AuNPs by *Enterobacter* sp. Pb204 under variable conditions 27
3.2.4 Characterisation of AuNPs produced by *Enterobacter* sp. Pb204 28
3.2.4.1 UV-Vis spectroscopy 29
3.2.4.2 Transmission Electron Microscopy (TEM) and Energy-dispersive X-ray Spectroscopy (EDS) 29

3.2.4.3 ImageJ: particle size analysis 29
3.3 Results and discussion 30
3.3.1 Identification of *Enterobacter* sp. Pb204 through 16s rRNA gene sequencing 30
3.3.2 The biogenesis of AuNPs by *Enterobacter* sp. Pb204 30
3.3.2.1 The spectral and elemental analysis of AuNPs 30
3.3.3 The influence of reaction parameters on AuNP size, shape and dispersity 33
3.3.3.1 Growth media 33
3.3.3.2 Reaction time 36
3.3.3.3 Concentration and source of biocatalyst 38
3.3.3.4 pH 43
3.3.3.5 Temperature 46
3.3.3.6 Concentration of gold ions 50
3.3.3.7 Summary of optimal parameters for the production of uniform AuNPs in Enterobacter sp Pb204 53
3.4 Conclusion 54
Chapter 4: Linking AuNP synthesis to heavy metal resistance in *Enterobacter sp.* Pb204 55
4.1 Introduction 55
4.2 Methodology 56
4.2.1 Whole genome sequencing of Enterobacter sp. Pb204 56
4.2.2 Comparative genomic analyses to identify genetic factors involved in AuNP synthesis 57
4.3 Results 58
4.3.1 General features of the *Enterobacter* sp. Pb204 genome 58

4.3.2 *Enterobacter* sp. Pb204 belongs to the species *E. xiangfangensis* LMG 27195^{T} 60

4.3.2.1 Comparison of the Enterobacter sp. Pb204 genome with E. xiangfangensis LMG 27195^{T} 61

4.3.3 *In silico* analysis of ICE*Exi*Pb204-encoded heavy metal resistance loci 65

4.3.3.1 Silver resistance pathway 65

4.3.3.3 Copper resistance pathway 66

4.3.3.4 Arsenic resistance pathway 67

4.3.3.5 Zinc resistance pathway 67

4.3.4 Other pathways with a putative role in heavy metal resistance and AuNP synthesis in *E. xiangfangensis* Pb204 67

4.3.5 *E. xiangfangensis* Pb204 unique genes and AuNP synthesis 68

4.4 Conclusion 69

Chapter 5: Overall conclusions and future work 70

5.1 Overall conclusions 70

5.2 Future Work 70

References 72

List of figures

Figure 1.1: A bar graph illustrating the top producers of nanotechnology related products……...……..…….....1

Figure 2.1: A diagrammatic representation of laser ablation..……..…….....14

Figure 2.2: A schematic representation of chemical reduction of gold ions to AuNPs.....15

Figure 2.3: A diagrammatic representation of intracellular and extracellular AuNP synthesis ..……..……...…….17

Figure 3.1: The UV-vis spectra of the AuNPs produced by *Enterobacter* sp. Pb204….……..……...……..31

Figure 3.2: The EDS elemental spectra of the AuNPs produced by *Enterobacter* sp. Pb204…….……..32

Figure 3.3: TEM micrographs of AuNPs produced by *Enterobacter* sp. Pb204 cultured in LB and NB .....……..33

Figure 3.4: A histogram illustrating the size and frequency of the AuNPs produced in the growth media trials …….....34

Figure 3.5: TEM micrographs of AuNPs produced by *Enterobacter* sp. Pb204 cultured in LB media over time …….……36

Figure 3.6: A histogram illustrating the size and frequency of the AuNPs produced in the reaction time trials. ……..…….……..…36

Figure 3.7: TEM micrographs showing gold particle formation when the biocatalyst (CB) was added to gold ions in different concentrations …….…….…….39

Figure 3.8: A histogram illustrating the size and frequency of the AuNPs produced in the CB ratio trials …….40

Figure 3.9: TEM micrographs showing gold particle formation when the cell free biocatalyst (CFB) was added to gold ions in different concentrations.……..41

Figure 3.10: A histogram illustrating the size and frequency of the AuNPs produced in the CFB ratio trials……..……...42

Figure 3.11: TEM micrographs of pH trials ……..…..……..44

Figure 3.12: A histogram illustrating the size and frequency of the AuNPs produced during the pH trials…..……...45

Figure 3.13: TEM micrographs of temperature trials …….……..……48

Figure 3.14: A histogram illustrating the size and frequency of the AuNPs produced during the temperature trials …..……..49

Figure 3.15: TEM micrographs of gold ion concentration trials ……..……51

Figure 3.16: A histogram illustrating the size and frequency of the AuNPs produced in the temperature trials …….....…..52

Figure 3.17: A TEM micrograph showing the production of uniformed spherical AuNPs by Enterobacter sp. Pb204 under optimal parameters determined in the present study …….....…..54

Figure 4.1: Circular map of the chromosome of *Enterobacter* sp. Pb204……58

Figure 4.2: Diagrammatic representation of the ICE found in *E. xiangfangensis* Pb204……65

List of tables

Table 1.1: The twelve principles for green chemistry …….3

Table 2.1: Size and shape variation in the AuNPs synthesised bacteria…….18

Table 2.2: The applications of the genus Enterobacter in biotechnology ……22

Table 3.1: Table showing the reaction parameters used in six different treatments during the biogenesis of AuNPs by *Enterobacter* sp. Pb204….....28

Table 4.1: The size of the genetic material elements…….....59

Table 4.2: Unique genomic islands of *E.xiangfangensis* Pb204….....62

List of abbreviations

Au	-	Gold
AuNP	-	Gold nanoparticle
AuP	-	Gold particle
Bps	-	Base pairs
CB	-	Cell biocatalyst
CFB	-	Cell free biocatalyst
CTAB	-	Hexadecyltrimethylammonium bromide
ICE	-	Integrative and conjugative Element
GFP	-	Green fluorescent protein
$HAuCl_4.3H_2O$	-	Chloroauric acid
HeLa	-	Henrietta Lacks
Kb	-	Kilobase
LB	-	Luria-Bertani
MB	-	Megabase
MWM	-	Molecular weight marker
MRI	-	Magnetic resonance imaging
NB	-	Nutrient broth
NP	-	Nanoparticles
NM	-	Nanomaterials
PEG	-	Polyethylene glycol
PCR	-	Polymerase chain reaction
SPR	-	Surface plasmon resonance
TEM	-	Transmission electron microscopy
THPC	-	Tetrakishydroxymethylphosphonium chloride
TNT	-	Trinitrotoluene
TOPO	-	Trioctylphosphine oxide
USA	-	United States of America
UV-vis	-	Ultraviolet – visual spectroscopy

Chapter 1: Introduction

1.1 Background

Since the first mention of the concept of nanotechnology in 1959 by Richard P. Feynman with the famous words, “There is plenty room at the bottom”, research interest into the field of nanotechnology has increased substantially (Feynman, 1960).

Nanotechnology can be defined as the study of any research or technology that is concerned with at least a single parameter that falls within the range of 1 to 100 nm, or the nanoscale (Jeng *et al.*, 2007; Issa *et al.*, 2013). Today, nanotechnology has progressed into a general purpose technology which can be found in commercially available products such as pregnancy tests (Rojanathanes *et al.*, 2008), anti-bacterial plasters (Vance *et al.*, 2015) and plasma screens (Bourzac, 2013). Several of the world’s economic powers such as China, USA, and European Union have invested heavily into this field (Dong *et al.*, 2016). It is estimated that the global investment on nanotechnology will exceed R40 trillion by the year 2020 (Roco, 2011). Currently, the USA and China are the top producers of nanotechnology related products (Figure 1.1) (Dong *et al.*, 2016).

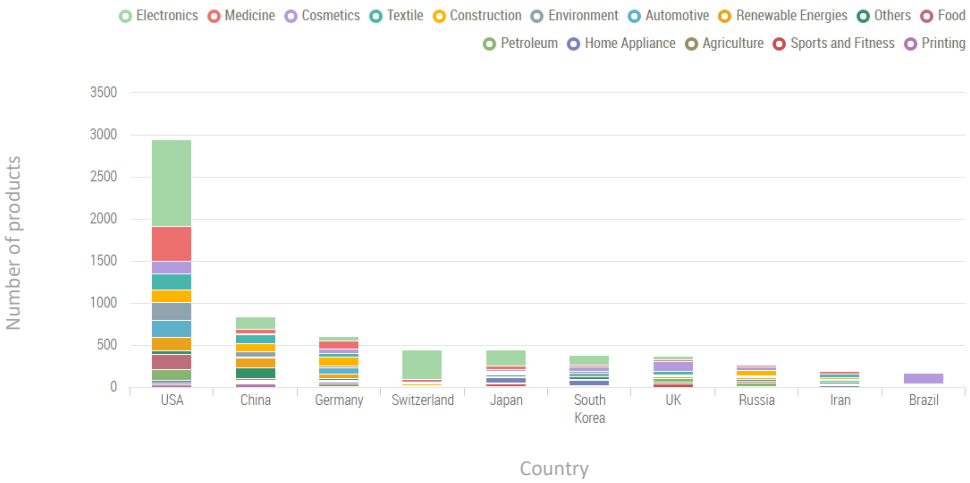

Figure 1.1: A bar graph illustrating the top producers of nanotechnology related products. Image retrieved from http://product.statnano.com/

A central focal point in nanotechnology is the development of nanomaterials (NM) and nanoparticles (NP), due to certain physiochemical properties which are not possessed by the bulk material. (Tiwari *et al*., 2011; Tran and Le, 2013). These potentially useful aspects include, but are not restricted to unique mechanical, electrical, catalytic, optical and magnetic properties (Lin *et al*., 2012). The large surface area to volume ratio, caused by the nanoscale dimensions is key to the unique properties found in NMs and NPs (Issa *et al*., 2013; Tran and Le, 2013). The larger surface area to volume ratio results in a greater number of atoms to be present on the surface. This inherently leads to a change in surface energy, spatial confinement of the electrons and reduced imperfections (Narayanan and Sakthivel, 2010). These novel properties have allowed for nanotechnology to have a profound effect on the innovation in many fields, both globally and locally (Roco, 2011).

Metallic-based NMs and NPs are one of the most promising prospects of nanotechnology, with considerable research being dedicated towards the development of these materials. Approximately 37% of all nano-based products are metal based (Tiwari *et al*., 2011; Vance *et al*., 2015). Particular interest has been garnered towards metallic NPs, with the prevalent use of gold nanoparticles (AuNPs) being well documented. AuNPs have the potential to be used in many fields such as therapeutics (Tiwari *et al*., 2011), catalysis (Haruta, 2003), electronics (Huang *et al*., 2003), remediation (Xiong *et al*., 2010), spectroscopy (Chen *et al*., 2008), microscopy (Chen *et al*., 2008) and fuel cells (Luo *et al*., 2008). This versatility has increased the research into AuNPs and one of the main focuses of these studies is the synthesis of these nanomaterials.

There are 3 main categories in which AuNPs can be synthesised: chemical, physical and biological synthesis. These methods of synthesis will be discussed in further detail in Chapter 2. Although physical and chemical means are regularly used to synthesise AuNPs, there have been concerns regarding the environmental impact and sustainability of these methods (Shedbalkar *et al*., 2014). Chemical synthesis uses toxic chemical reagents and physical synthesis requires a large energy input to

create AuNPs (Sharma *et al*., 2012). These concerns have driven the need for green chemistry in the synthesis of AuNPs. Green chemistry, as defined in the paper by Anastas and Eghbali (2010), is the reduction or removal of toxic substances in the design of chemical products or processes. The 12 principles of green chemistry are outlined in Table 1 below.

Table 1.1: The twelve principles for green chemistry

1. Design chemical process to prevent the production or use of hazardous materials	2. Atom economy should always maximise the use of all materials for the chemical process
3. Design chemical process to use less hazardous chemical synthesis	4. Design chemical process to produce safer end products
5. Use safer solvents and auxiliaries in chemical process	6. Design chemical process to be energy efficient
7. Use renewable feedstocks in chemical process	8. Reduce derivatives in chemical process
9. Catalytic reagents should be incorporated into chemical process where possible	10. Design chemical products for degradation
11. Real-time analysis for pollution prevention	12. Design for safer chemistry to prevent accidents

The table above was adapted from (Anastas and Eghbali, 2010)

The most promising alternative to conventional AuNP chemical synthesis is a biological synthesis, as the use of the latter fulfills most of the principles of green chemistry. Biological synthesis relies on the biomolecules of a biotic system to produce the AuNPs (Shedbalkar *et al*., 2014). This eliminates the concerns of the toxicity which is unavoidable in chemical synthesis (Shedbalkar *et al*., 2014). Many biological organisms have displayed the ability to synthesise AuNPs, such as plants (Ahmed and Ikram, 2016), archaea (Konishi *et al*., 2007), viruses (Slocik *et al*., 2005), fungi (Shedbalkar *et al*., 2014) and bacteria (Sharma *et al*., 2012). Literature presents numerous and diverse systems involved in the biological synthesis of AuNPs. However, the fundamental aspects of such processes in individual organism remains speculated (He *et al*.,2007; Shedbalkar *et al*., 2014).

1.2 Knowledge gap

The practical application and efficacy of AuNPs have been previously exhibited in molecular research (Tiwari *et al*., 2011), diagnostics (Narayanan *et al*., 2011),

catalysis (Haruta, 2005) and therapeutics (Dreaden *et al*., 2012). Owing to their versatility and ability for biological functionalisation, the synthesis of these AuNPs have been extensively investigated. However, the current production methods are not sustainable for industrial and commercial production (Narayanan and Sakthivel, 2010). Conventional synthesis methods use toxic chemicals or require high energy inputs which may have long-term implications for human safety and the environment (Narayanan and Sakthivel, 2010).

The need for greener AuNP synthesis methods has contributed towards the increased research effort into biological AuNP synthesis (Nangia *et al*., 2009). One such biological system which may potentially be capable of alleviating some shortfalls of AuNP synthesis is the use of a bacterial synthesis host, or bacterial AuNP synthesis (Nangia *et al*., 2009). The high proliferation rate of certain bacterial species is promising for the generation of large amounts of AuNPs without the risks of toxic chemical use (Pantidos and Horsfall, 2014).

Bacteria from the genus *Enterobacter* have been exploited for many biotechnological applications from microbial fuel cells (Rezaei *et al*., 2009) to biocatalysis (Pudge *et al*., 2003). *Enterobacter* strains have been isolated from heavy metal contaminated gold mine regions in South Dakota (Rastogi *et al*., 2010) and Johannesburg (van Marwijk *et al.,* 2009). The high metal concentration found in mines and surrounding areas would put selective pressure on the bacterial communities found in these areas (Diaz-Ravina and Baath 1996; Rajbanshi, 2008). The bacterial communities would adapt to the conditions and acquire mechanisms to resist the high metal concentrations such as metal efflux systems or extracellular precipitation (Diaz-Ravina and Baath 1996; Rajbanshi, 2008). A connection has been observed between heavy metal resistant bacteria and metallic NP formation (Ramanathan *et al*., 2013). The bacterial isolate used in the present study belongs to the genus of *Enterobacter*. It was cultured from acid mine decant sourced from uranium mine tailings in the West Rand of Gauteng, South Africa, (26°06'26.8"S 27°43'20.2"E). This isolate has previously been shown to possess heavy metal resistance and the ability to synthesise AuNPs (Hiebner 2017; Vallabh 2017).

The lack of knowledge on the pathways responsible for AuNP bacterial biogenesis is clearly evident in current literature (He *et al*., 2007). A large number of published reports terminate with a simple speculated reason for the occurrence of AuNP biogenesis in a particular bacterial strain. This may have implications for the efficacy of the optimisation process. Identifying possible genetic pathways involved in AuNP biogenesis, from quantitative experimental data, will provide a more holistic overview of bacterial AuNP biogenesis. A better understanding of the biological catalyst system may aid in improving the production of biologically derived AuNPs, leading towards practical application of these unique NMs.

1.3 Aims and objectives

1.3.1 Main aim

The aim of this project was to optimise the size and shape uniformity of biologically derived AuNPs in *Enterobacter* sp. Pb204, through the manipulation of certain reaction parameters. Moreover, the project aimed to cursorily identify the potential genetic pathways responsible for AuNP production to obtain a greater understanding of the AuNP biogenesis process of *Enterobacter* sp. Pb204.

1.3.2 Specific objectives

1. To expose *Enterobacter* sp. Pb204 to 1 mM chloroauric acid ($HAuCl_4.3H_2O$) and confirm the formation of AuNPs through elemental analysis.
2. To determine the influence of growth medium, pH, temperature, reaction time, cell concentration and metal concentration on AuNP biogenesis through sequential optimization and monitoring of particle size, shape and dispersity.
3. To sequence the whole genome of *Enterobacter* sp. Pb204 to elucidate possible pathways for the AuNP synthesis.

1.4 Chapter outline

The structure of the dissertation is presented as follows:

Chapter 1 is a brief introduction to the research area covered by the study. It also outlines the problem statement as well as the main aim and specific objectives that are needed to address the problem statement.

Chapter 2 presents a detailed review of the state of current literature with regards to AuNPs, including the application of AuNPs, the synthesis of AuNPs, the factors which affect bacterial synthesis and the rationale for the present study.

Chapter 3 focuses on the effects that reaction parameters of growth medium, reaction time, biocatalyst ratio, environmental pH, temperature, and gold ion concentration have on the biogenesis of AuNP in the *Enterobacter* sp. Pb204.

Chapter 4 expands on the genomic analysis of *Enterobacter* sp. Pb204 for the purpose of elucidating possible genetic pathways related to AuNP synthesis

Chapter 5 presents a general conclusion based on the specific objectives and future recommendations derived from the present study.

Chapter 2: Literature Review

2.1 Gold nanoparticles

2.1.1 History of AuNPs

Though scientific research in AuNPs has only been developed in the past few decades (Dreaden *et al*., 2012), the existence of AuNPs, or "soluble" gold, in human society dates as far back as fourth century AD in China and Egypt (Daniel and Astruc, 2004). Artisans through-out the Middle Ages used AuNPs in fluid form, or colloidal gold, to produce deep ruby colour in ceramics and glass (Daniel and Astruc, 2004). One of the oldest and most well-known uses of AuNPs in glass, is in the Lycurgus Cup. The Romans had unknowingly produced AuNPs when they made the glass of the Lycurgus Cup (Freestone *et al*., 2007). This cup is unique in that light shone on the outside of the cup made the glass appear jade green colour, while light shone from within made the glass appear ruby red (Barber *et al*., 1990; Freestone *et al*., 2007).

The first to recognise that the colour of AuNPs was caused by their small size and the unique light scattering properties was Michael Faraday (Faraday, 1857). This phenomenon was later referred to as the Faraday-Tyndall effect (Tweney 2006). Since this first mention of the unique optical properties of AuNPs, research on these nanoparticles has drastically increased (Eustis and El-Sayed, 2006).

2.1.2 Properties of AuNPs

One of the main reasons for the interest of AuNP research is due to its novel properties which can be exploited by researchers (Tiwari *et al*., 2011). One such unique property that AuNPs are renowned for is the surface plasmon resonance, or SPR, of the material. SPR can be defined as the oscillation of the cloud of electrons found on the surface when excited by visible light (Srivastava and Mukhopadhyay 2015).

In AuNPs, the cloud of electrons is confined to a much smaller space than that of the bulk material. This results in changes to the spectra of light that the gold absorbs and reflects, thereby altering the colour of the AuNPs from the traditional yellow colour of its bulk material. Larger AuNPs absorb a greater amount of optical waves in the red spectrum (700 nm), while simultaneously reflecting less in the blue frequency range (450 nm) appearing purple in colour. Contrastingly, smaller AuNPs absorb more blue light and reflect more red light resulting in a red colour (Elbakry *et al*., 2009; Zeng *et al*., 2011).

The catalytic properties of gold are also altered in its NP form (Grisel *et al*., 2002). As a bulk material, gold is considered chemically inert in terms of chemisorption of hydrogen and oxygen. However, at the nanoscale, gold is considerably different (Grisel *et al*., 2002). Nanoscale gold acquires the ability to react with oxygen and hydrogen which has allowed AuNPs to catalyse a wide range of reactions from the oxidation of propene to propene oxide to carbon monoxide oxidation (Lopez *et al*., 2004; Sinha *et al*., 2004).

2.2 Applications of AuNPs

The new properties acquired by gold, when in the nanoscale, has allowed AuNPs to be used in a wide range of biotechnological and industrial applications (Tiwari *et al*., 2011). These include gene therapy, drug delivery, bioimaging, biodetection, energy storage, energy production and industrial catalysis (Tiwari *et al*., 2011).

2.2.1 Gene delivery

AuNPs have been functionalised to carry genetic material and may be useful for gene therapy (Chen *et al*., 2006; Tiwari *et al*., 2011). Functionalisation is the attachment of a biomolecule (e.g. DNA) to the AuNP which gives the AuNP specific functions (Tiwari *et al*., 2011). When compared to current vectors, AuNPs exhibit better cell membrane penetration and are less cytotoxic (Pissuwan *et al*., 2011) making them much more effective for gene therapy. Gold nanorods coated with polyethylene glycol (PEG) have been previously functionalised with DNA

plasmids which encoded for green fluorescent protein (GFP) (Chen *et al*., 2006). These were then allowed to penetrate HeLa cells and infrared radiation was used to detach the GFP DNA sequences. After 48 hours the cell showed the production of GFP suggesting that AuNPs may be a feasible gene therapy system (Chen *et al*., 2006).

Antisense RNA has also been attached to the surface of AuNPs to regulate gene expression (Elbakry *et al*., 2009; Pissuwan *et al*., 2011). Antisense technology has made significant progress but the delivery of the siRNA remains an issue due to low transfection rate of the target cells. AuNPs have shown to increase the half-life of the siRNA up to 6 times and lengthen the time of the gene knock out when compared to free RNA duplexes (Elbakry *et al*., 2009).

2.2.2 Drug delivery

Much like the functionalisation of AuNPs with DNA, therapeutic agents such as antibiotics, vaccines or anti-cancer drugs can be attached to its surface (Niikura *et al*., 2013; Yang *et al*., 2005a). The use of AuNPs, as a vector, allows for a significantly improved efficacy of the attached therapeutic agent (Niikura *et al*., 2013). This is because the AuNPs can be targeted to specific cells and tend to demonstrate improved cellular penetration surface (Niikura *et al*., 2013; Yang *et al*., 2005a). In this regard, Brown *et al.* (2010) reported that the anticancer drug oxaliplatin shows a 5 fold increase cytotoxicity to lung cancer cells (A549 cell line) and colon cancer cells (HT29) when functionalised to AuNPs when compared with unmodified oxaliplatin.

2.2.3 Biodetection

There is a wide range of inorganic molecules that AuNPs can be used to detect (Xia *et al.*, 2010). Notable molecules include heavy metals (Sugunan *et al*., 2005), arsenic (Dai and Compton, 2006), cocaine (Liu and Lu, 2006), cyanide (Shang *et al*., 2009), trinitrotoluene (TNT) (Dasary *et al*., 2009) or banned narcotics (Luo *et al*., 2012).

Recently, colourimetric and fluorescence assays have been developed for multiplex detection utilising AuNPs. In the study conducted by Luo *et al*. (2012), unmodified AuNPs and aptamers conjugated with fluorescent molecules (aminomethyl-coumarin, carboxy-X-rhodamine and carboxyfluorescein) were used in a multiplex aptasensor for the detection of cocaine, thrombin and adenosine. The success of this sensor was only possible due to the unique chemical and optical properties of AuNPs. Briefly, AuNPs and tagged aptamers were attracted to each other in the presence of NaCl which caused a salt-induced attraction between the AuNPs, quenching the fluorescence of the aptamers and resulting in an overall red colour in the AuNPs. However, in the presence of the aptamers' target, the aptamers would dissociate from the AuNPs and bind to the target, causing a colour change from red to blue indicating a positive reaction and the fluorescence of the aptamer indicates which specific molecule is present (Luo *et al.*, 2012).

AuNPs have the potential to be a robust system for the detection of microorganisms, e.g. bacteria. *Cryptosporidium parvum* has been successfully identified using AuNPs that are functionalised with its heat shock protein 70 in a colourimetric assay (Javier *et al*., 2009). Immuno-based assays have also detected *Staphylococcus aureus* in food samples by using AuNPs that are conjugated with cell wall protein targeting antibodies (Huang, 2006).

2.2.4 Bioimaging

Diagnostics and imaging have utilised AuNPs to improve the quality of dye in the selective detection of target tumour cells, due to functionalisation with anti-tumour markers and increase the resolution of the imaging (Badawi and Ahmed, 2014). AuNPs have been used in conjunction with iron nanoparticles to lower the iron nanoparticle cytotoxicity, as well as to target specific cells for increased efficiency of tumour imaging in magnetic resonance imaging (MRI) (Narayanan *et al*., 2011).

Gold nanorods, when functionalised with PEG, have been used as a contrast agent in computed tomography. The gold nanorods have been shown to be more effective than the current iodine contrast agent as the gold nanoparticles can be functionalised

to have specific ligands or antibodies which allows them to target specific organs (Kim *et al*., 2007). Imaging of extracellular structures can also be improved by AuNPs through the functionalisation of antibodies which bind to specific structures on the cell surface (Tiwari *et al*., 2011).

2.2.5 Electrical energy production and storage

The unique optical and physical properties of AuNPs have been exploited to produce electrical energy in the form of photovoltaic cells (Su *et al*., 2012; Li *et al*., 2013). The SPRs of AuNPs have been used to separate charges on titanium dioxide (TiO_2) films under visible light radiation (Su *et al*., 2012). This separation of charges has allowed researchers to create negative charge potential and anodic current which has the potential to be used in plasmon-sensitised solar cells and plasmonic solar cells (Ratchford *et al*., 2017).

Energy storage also has the potential to be improved by AuNPs (Su *et al*., 2012; Ratchford *et al*., 2017). In the study conducted by Lu *et al*. (2010), lithium-air rechargeable batteries had been improved through the use of gold/platinum nanoparticles (Pt/AuNPs). The Pt/AuNPs improved the kinetic rate of the oxygen evolution reaction and oxygen reduction reaction within the batteries greatly increasing the discharge voltage. Research on the use of AuNPs in capacitors has also yielded promising results (Huang *et al*., 2003; Park *et al*., 2006). The recent study conducted by Tan *et al*. (2017) found that introducing AuNPs into nano-Co_3O_4 reduced the internal resistance of the charge transmission in the capacitor. It was noted that nano-Co_3O_4 decorated with the AuNPs exhibited higher specific capacitance than that of a pristine Co_3O_4 capacitor.

2.2.6 Industrial catalysis

There is a direct correlation in the reduction in the size of gold to an increase in its catalytic ability (Grisel *et al*., 2002; Daniel and Astruc, 2004). This novel catalytic capacity has been used in several industrial processes (Daniel and Astruc, 2004). AuNPs inlaid with TiO_2 can be exploited further for the production of hydrogen gas through its photocatalytic activity (Murdoch *et al*., 2011). The presence of the

AuNPs aids in the trapping of photo-excited electrons and transferring them to the hydrogen ions to form the hydrogen gas. This concept has been previously reported in several studies (Rosseler *et al*., 2010; Murdoch *et al*., 2011; Su *et al*., 2014; Wu *et al*., 2016).

2.3 Synthesis of AuNPs

The synthesis of AuNPs can be classed into two categories: the "bottom-up" approach or the "top-down" approach (Wang and Xia, 2004). The "bottom-up" synthesis method refers to when the NPs are formed from atoms and molecules that nucleate and grow to form the NPs. The "top-down" synthesis involves the breakdown of larger bulk material to form the smaller NPs (Wang and Xia, 2004). These approaches can be placed into three categories in which AuNPs can be synthesised which are chemical, biological and physical synthesis (Herizchi *et al*., 2016).

2.3.1 Physical synthesis

Physical synthesis is a "top-down" approach that produces AuNPs through heat energy, mechanical pressure, radiation or electrical energy to cause condensation, melting, abrasion or evaporation of the bulk material (Narayanan and Sakthivel 2010; Dhand *et al*., 2015). This form of synthesis is one of the oldest methods of producing AuNPs. One of the first methods of physically creating AuNPs was by melt mixing whereby AuNPs were created when dissolved in glass (Ruivo *et al*., 2008). Currently, the application of laser technology is now at the forefront of this research (Mafuné *et al*., 2001). A diagrammatic representation of this process can be seen in Figure 2.1.

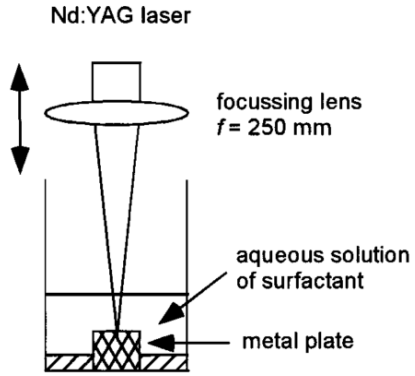

Figure 2.1: A diagrammatic representation of laser ablation. Laser ablation has resulted in the synthesis of size-specific nanoparticles that range between 1 – 5 nm (Mafuné *et al*., 2001).

As demonstrated in Figure 2.1, the high-intensity radiation from the YAG lasers is used to create size specific nanoparticles through laser ablation of bulk gold material (Mafuné *et al*., 2001; Kabashin *et al*., 2003). The AuNPs are produced by the plasma generated at the laser's focal point and the extreme pressure and temperature created by the plasma is thought to be responsible for the formation of the AuNPs (Dell'Aglio *et al*., 2016). These methods have been shown to produce monodispersed NPs. However, the high energy consumption and high gold waste during production have raised economic concerns about this synthesis method (Narayanan and Sakthivel, 2010; Ndeh *et al*., 2017).

2.3.2 Chemical synthesis

One of the simplest methods used to produce AuNPs is through chemical synthesis (Narayanan and Sakthivel, 2010). Chemical synthesis can incorporate both the "top-down" and the "bottom-up" approaches (Wang and Xia, 2004). The top-down method of chemical synthesis uses chemical degradation of the bulk gold to create AuNPs, but there is a greater chance of surface imperfections (Thakkar *et al*., 2010). The bottom-up approach has therefore been favoured. Bottom-up chemical synthesis employs chemical reducing agents to reduce the metals to form the AuNPs and chemical capping agents to stabilise the AuNPs (Zeng *et al*., 2011).

Currently, most AuNPs are produced through chemical synthesis (Ahmed and Ikram, 2016). This method has the advantage of an easily controlled synthesis of AuNP, both in size and shape, as well as the production of cost-effective, repeatable runs of AuNPs (Hiramatsu and Osterloh, 2004). A schematic of this process is presented in Figure 2.2.

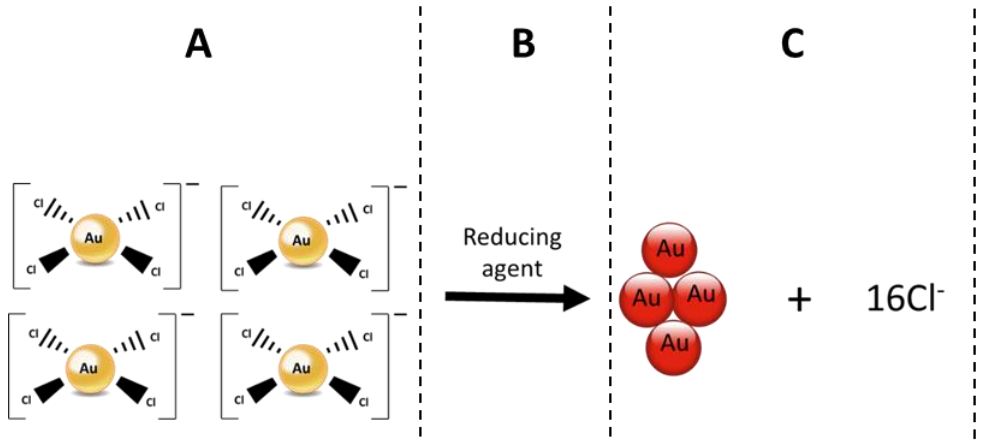

Figure 2.2: A schematic representation of chemical reduction of gold ions to AuNPs (adapted from (Murphy, 2014)). This method utilises the bottom up approach where the AuNP (C) grows from the reduction of gold ions (A) using a reducing agent (B).

Figure 2.2 presents an outline of the most widely used method of producing AuNPs. Here, the reduction of chloroauric acid ($HAuCl_4.H_2O$) (Figure 2.2A) is instigated by a reducing agent such as hexadecyltrimethylammonium bromide (CTAB) (Figure 2.2B). This reaction subsequently produces the nanoparticles (Figure 2.2C) whose final nanoparticle size, shape and concentration are controlled by altering the chemical additives and other environmental parameters in the methodology (Hiramatsu and Osterloh, 2004; Zeng *et al*., 2011). For example, the shape of the AuNPs can be controlled by altering the seed solution. In a study conducted by Nikoobakht and El-Sayed (2003), it was observed that the formation of noncylindrical nanorods, spherical particles and φ-shaped particles can be changed to gold nanorods by altering the seed solution from citrate-capped seed to CTAB capped seed in the chloroauric acid. The size of the AuNPs could also be controlled by changing the nucleation and growth steps.

Although chemical synthesis is one of the most popular methods used to synthesise AuNPs, it does have its disadvantages. One of the largest drawbacks is the requirement of toxic chemicals to reduce the gold from the gold salt solutions. Chemicals such as sodium borohydride, hydroxylamine, trioctylphosphine oxide (TOPO), tetrakishydroxymethylphosphonium chloride (THPC), toluene or chloroform have all had inquiries about their direct impact on the environment (Xie *et al*., 2007). Another concern is the effect that chemicals, such as in CTAB capped AuNPs, may have on the health of an individual if the nanomaterial were to be deployed in therapeutic applications (Lau *et al*., 2012). The CTAB cap on the AuNP has been observed to be cytotoxic towards human erythrocytes (Lau *et al*., 2012), while mouse model studies have shown that CTAB on its own will adversely affect the weight of mice (Isomaa *et al*., 1976).

2.3.3 Biological synthesis

Recently, biological synthesis of AuNPs has gained much interest due the increased need for green science (Shedbalkar *et al*., 2014). In lieu of harsh chemical reductants, biotic systems use naturally active biomolecules, e.g. proteins, as the capping and reducing agent (He *et al*., 2007; Xie *et al*., 2007; Shedbalkar *et al*., 2014) to form AuNPs. Several organisms such as Archaea (Konishi *et al*., 2007), plants (Ahmed and Ikram, 2016), fungi (Shedbalkar *et al*., 2014), viruses (Slocik *et al*., 2005), and bacteria (Sharma *et al*., 2012) have been observed to produce AuNPs. The work presented in this thesis focuses on bacterial synthesis which will be discussed further.

2.3.3.1. Bacterial synthesis

One of the most researched organisms for the production of AuNPs is through the use of bacteria. Compared to other organisms they are relatively simple to culture, propagate and genetically modify (Kalishwaralal *et al*., 2010). Numerous studies have reported on the reduction of chloroauric acid to AuNPs using bacterial species including *Bacillus subtilis* (Deplanche and Macaskie, 2008), *Rhodopseudomonas capsulata* (He *et al*., 2007) and *Brevibacterium casei* (Kalishwaralal *et al*., 2010).

Within bacterial systems, AuNPs can either be formed extracellularly or intracellularly which depends on the location of the reducing component (Li *et al*., 2011). Figure 2.3 demonstrates a schematic of the two processes.

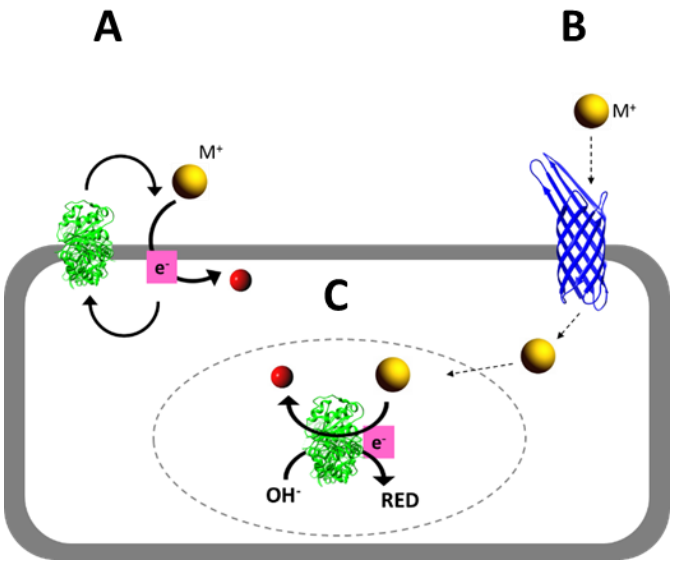

Figure 2.3: A diagrammatic representation of intracellular and extracellular AuNP synthesis. The gold ions are either reduced at the surface of the bacteria (extracellular) or within the bacteria (intracellular) (adapted from Shedbalkar *et al*., 2014). Structure (A) is a membrane bound protein which reduces the Au ions to form the AuNPs extracellularly and structure (B) is transmembrane protein which transports Au ion into the cell to structure (C) which reduces the Au ions to form the AuNPs intracellularly.

The true mechanism of bacterial AuNP biogenesis is largely speculated in current literature (He *et al*., 2007; Li *et al*., 2011). However, several potential mechanisms of action have been postulated (Figure 2.3). One such process is the hypothesised reduction of metal cations at the cell wall of the bacteria by a reducing biomolecule (Figure 2.3A). Here, extracellular synthesis requires the presence of reducing agents, found either on the cell surface or as secreted soluble biomolecules. Alternatively, intracellular synthesis involves the shuttling of the metal cations through, possibly, an influx pump (Figure 2.3B) following which, the formation of

nanoparticles is initiated by reducing agent biomolecules found within the bacterial cell (Li *et al*., 2011).

2.5 Advantage and disadvantages of biological AuNPs synthesis

The greatest advantage of biological synthesis is that it offers an environmentally friendly alternative to the chemical-based synthesis, which requires highly toxic compounds in the production of AuNPs (Narayanan and Sakthivel, 2010). Toxic reducing or capping agents used in chemical synthesis (Kabashin *et al*., 2003; Chandran *et al*., 2014) are replaced by natural biocompatible biomolecules. Biogenic AuNPs are especially desirable for therapeutic applications because the particles do not have the toxic chemical species attached to the surface (Tiwari *et al*., 2011). Furthermore, a biological system could potentially be more sustainable, leading to long-term cost efficiency, when compared to physical or chemical synthesis (Kalishwaralal *et al*., 2010). However, unlike chemical synthesis where it is relatively easy to control the shape and size of the AuNPs, this is difficult to achieve in biosynthesis (Chandran *et al*., 2014). Many studies (Table 2.1) have noted the large variability in the AuNPs produced which has hampered its introduction in the field of nanotechnology as a viable route of synthesis.

Table 2.1: Size and shape variation in the AuNPs synthesised by bacteria.

Microbe	Shapes	Size range (nm)	Source
Marinobacter pelagius	Triangles and spheres	1 – 20	Sharma *et al*., 2012
Shewanella algae	Spheres and variety of nanoplates	100 -200	Ogi *et al*., 2010
Geobacillus sp. ID17	Quasi-hexagons crystals	4 – 48	Correa-Llantén *et al*., 2013
Escherichia coli	Triangular plates and quasi-hexagonal plates	25 – 33	Du *et al*., 2007
R. capsulata	Triangles and spheres	50 – 400	He *et al*., 2007
Actinobacter spp.	Quasi-spheres, triangular plates, hexagonal plates, hexagonal crystals, irregular plates	50 -500	Bharde *et al*., 2007

An overview of bacterial AuNP biogenesis studies demonstrates a wide variety of AuNP synthesis processes in terms of the microbial host, and overall shape and size

range of the produced AuNPs (Table 2.1). Overall the shape of the resultant AuNPs does not appear to be dictated by bacterial species. For example, triangular-shaped AuNPs have been produced by *Marinobacter pelagius* (Sharma *et al.*, 2012), *Escherichia coli* (Du *et al*., 2007) and *Actinobacter* spp (Bharde *et al*., 2007). The size range of bacterial derived AuNPs appears to fall within a size range of 1 nm to 500 nm (Table 2.1). This suggests that certain external environmental factors also contribute to the physical properties of biologically derived AuNPs. This concept will be expanded on in the following subsections.

2.6 Factors influencing size and shape of AuNPs during biological synthesis

Size and shape uniformity, as well as monodispersity of nanoparticles, are crucial parameters to optimise. This is because, in the nanodimension, the physical properties of the nanoparticles are inherently related to the size of the particle (Sau *et al*., 2010). A slight change in size or shape results in exponential changes in quantum effects (Link and El-Sayed, 1999). This can have serious potential implications for nanoparticles used in optics, MRI and biomedical applications (Huang and El-Sayed, 2010). It is, therefore, a necessity to develop processes that lead to the synthesis of AuNPs of controlled size, shape and dispersity. Similar to physical and chemical synthetic routes, there are a number of parameters that are reported to directly influence the uniformity and dispersion of biogenic AuNPs. These include pH, temperature, reaction time and gold concentration (Gericke and Pinches, 2006). These factors are discussed in further detail below, with emphasis on bacterial biosynthesis.

2.6.1 Effects of pH

The environmental pH of the biosynthesis reaction has been shown to contribute significantly to the resulting AuNPs from the reduction of gold salt solutions (Gericke and Pinches 2006; El-Deeb *et al.,* 2014; Shantkriti and Rani, 2014). Several studies have observed that altering the pH of the reaction mixture will cause a change in the shape and size of the resultant AuNPs (He *et al*., 2007; Shantkriti and Rani, 2014). In *R. capsulata*, a decrease in pH resulted in the preferential synthesis of triangular shaped nanoparticles, with a size range of 50 nm to 400 nm,

over spherical nanoparticles, with a size range of 10 nm to 20 nm (He *et al*., 2007). Erasmus *et al.* (2014) reported that when *Thermus scotoductus* was exposed to higher environmental pH conditions, a greater number of smaller, spherical AuNPs were formed. Similarly, El-Deeb *et al*. (2014) observed an increase in the size range of spherical AuNPs from 10 – 20 nm to 10 – 45 nm when pH was increased from 7 to 10 using *Alcaligenes faecalis*. *Zooglea ramigera* also produces larger AuNPs at higher pH, but this was in conjunction with an increase in NP shape variety (Srivastava and Mukhopadhyay, 2015).

2.6.2 Effects of temperature

The effects of temperature on the biological synthesis of AuNPs has been well documented (Erasmus *et al*., 2014; El-Deeb *et al*., 2014; Wadhwani *et al*., 2014). It was concluded for *Acinetobacter* sp. SW30, a bacterial strain isolated from German sewage sludge, that an increase in overall reaction temperature (from 30 °C to 50 °C), resulted in an increased rate of synthesis of AuNPs (Wadhwani *et al*., 2014). Additionally, in a study conducted by El-Deeb *et al.* (2014), an increased temperature resulted in smaller nanoparticles produced by the bacterium *A. faecalis*. At 60 °C, the size of AuNPs ranged from 15 – 55 nm while at 10 °C the AuNP's ranged from 10 – 40 nm. A directly proportional relationship between temperature and production rates of AuNPs is also evident. As the temperature of the vessel is increased, many metabolic reaction rates are also increased, forcing more gold ions to be seeded into nuclei rather than undergo secondary reduction to larger AuNPs (El-Deeb *et al*., 2014). This observation has also been made in *T. scotoductus* (Erasmus *et al*., 2014) and *Streptomyces* spp. (Zonooz *et al*., 2012).

2.6.3 Effects of biomass to gold solution volume

The ratio of biomass to gold salt solution has been observed to alter the size of the nanoparticles in AuNPs synthesised by *Aloe vera* extracts (Chandran *et al*., 2006). In the aforementioned study, the greater concentration of dried biomass added to the reaction mix resulted in an improved amount of spherical AuNPs being produced. Shape-dependence on biomass concentration was also observed in *Magnolia kobus* and *Diopyros kaki* systems, whereby a lower concentration of

biomass resulted in hexagonal and triangular AuNPs but a higher concentration resulted in a preference towards spherical AuNPs (Song and Kim, 2009). The exact mechanisms of action regarding biomass to gold salt solution ratio effects on AuNPs have not been elucidated in bacteria. However, previously published literature strongly suggests that the biomass may have a direct effect on the size and shape of the AuNPs (Pimprikar *et al.,* 2009).

2.6.4 Effects of gold ion concentration

The size of AuNPs and their rate of production is known to be influenced by the concentration of gold ions in solution. Lower concentrations of $HAuCl_4$ are more easily reduced, while too high a concentration can become toxic to bacterial cells (Karthikeyan and Beveridge 2002; Reith *et al*., 2009). At low concentrations of $HAuCl_4$ (0.5 – 1 mM), *Z. ramigera* was reported to form small AuNPs <80 nm in diameter (Srivastava and Mukhopadhyay, 2015). As the concentration increased to 2.5 mM $HAuCl_4$, larger nanoparticles ranging between 240 – 360 nm in size were observed. The authors suggested that more availability of gold ions at higher concentrations leads to aggregation of gold particles, hence the increased particle sizes. Srinath and Rai (2015) also observed aggregation of AuNPs into larger particles after exposing *Enterobacter aerogenes* to 1.5 mM gold solution.

An increase in the size of the AuNPs produced by *A. faecalis* accompanied by an increased reaction rate was reported for higher concentrations of gold solution by El-Deeb *et al*. (2014). This could be attributed to fewer substrate molecules being present at lower concentrations as compared to biological reducing proteins limiting the rate of bioreduction.

2.7 Rationale for the current study

2.7.1 The genus *Enterobacter*

Members of the genus *Enterobacter* are common Gram-negative, non-spore forming, rod-shaped and motile bacteria from the family *Enterobacteriaceae* (Grimont and Grimont, 2006). These bacteria can be found to inhabit a wide range

of environments such as sewage, water, food products, soil, hospitals, human skin, gastrointestinal tract of animals, surface of vegetables, mines and several other environments (Grimont and Grimont, 2006; Rastogi *et al*., 2010; van Marwijk *et al*., 2009). Some *Enterobacter* species are pathogenic to humans and will cause opportunistic infections in immunocompromised individuals (Shaker *et al.,* 2007). Although a few strains from the genus are opportunistic pathogens, bacteria from this genus have been shown to be highly versatile and can be used in many applications in biotechnology, some of which are outlined in Table 2.2.

Table 2.2: The applications of the genus *Enterobacter* in biotechnology

Species	Field	Role	Reference
E. cloacae	Bioremediation	Degradation of chlorpyrifos (pesticide)	Singh *et al*., 2004
	Alternative power	Microbial fuel cell anodic bio catalysis	Rezaei *et al*., 2009
	Nanoparticle synthesis	Biosynthesis of silver nanoparticles	Shahverdi *et al*., 2007
	Decommissioning of munitions	Degradation of hexahydro-1,3,5-trinitro-1,3,5-s-triazine (RDX explosive)	Pudge *et al*., 2003
E. aerogenes	Alternative power	Biohydrogen production	Nakashimada *et al*., 2002
	Solvent production	2, 3-Butanediol production	Blomqvist *et al*., 1993

The biotechnological applications of *Enterobacter* species are vast and multi-disciplinary (Table 2.2). Demonstrating the highly desirable property of bioelectrogenesis, *Enterobacter* strains have been incorporated as microbial fuel cell anodic biocatalysts (Rezaei *et al*., 2009) and biohydrogen producers (Nakashimada *et al*., 2002). In addition, the robustness of these bacteria has allowed

them to be used in bioremediation for the breakdown of recalcitrant and toxic compounds (Pudge *et al*., 2003; Singh *et al*., 2004). Promisingly, the biogenesis of silver nanoparticles has been documented for *E. cloacae* (Shahverdi *et al*., 2007).

Members of the genus have been found in metal-contaminated environments including gold mines, such as the Homestake gold mine in Johannesburg (van Marwijk *et al*., 2009), as well as in South Dakota (Rastogi *et al*., 2010). The ability of these and other organisms to resist heavy metal toxicity is favourable for the biogenic production of metallic nanoparticles. ATPase dependent pathways are thought to be responsible for reducing and/or precipitating the metal ions, which are brought into the cell, into non-toxic metal nanoclusters (Narayan and Sakthivel, 2010).

The particular isolate (of *Enterobacter* sp.) of interest in this thesis was obtained from acid mine decant on the West Rand of Gauteng, South Africa. Studies by the Environmental Biotechnology Research Group (Wits) have shown its ability to withstand lead, zinc and manganese (Kondiah 2013; Chinhoga 2016; Vallabh 2017). Furthermore, the research group has also successfully demonstrated the synthesis of biogenic AuNPs using this isolate which was misidentified as *Paenibacillus castaneae* in that particular study (Hiebner, 2017).

2.7.2 Research rationale

There is a driving force for researchers to innovate and develop greener methods for the large-scale production of nanomaterials, like AuNPs, for industrial applications. Bacterial synthesis would appear to be the most viable process for replacing the popular chemical synthesis of AuNPs. This has led to an increase in research to identify new bacteria whose bioreduction mechanisms can be altered to synthesise uniformly shaped and sized AuNPs and other metallic nanoparticles. One such bacterium is *Enterobacter* sp. Pb204 which has been shown by the Environmental Biotechnology Research Group at the University of the Witwatersrand to possess the ability to synthesise AuNPs.

Chapter 3: The influence of reaction parameters on the biogenesis of AuNPs in *Enterobacter* sp. Pb204

3.1 Introduction

The uniformity of the shape and size of AuNPs has a direct implication in their subsequent applications (Eustis and El-Sayed 2006). This is due to the fact that AuNPs properties are strongly determined by their morphology (Eustis and El-Sayed, 2006; Li *et al*., 2014). When there is a change in the shape or size of the AuNP, a different set of physicochemical properties can be observed (Li *et al*., 2014). In the study by Sönnichsen *et al*. (2002), it was found that there was a significant reduction in the plasmon dephasing rate when the shape of the AuNPs was changed from a nanosphere to a nanorod. It was deduced that the change in the shape of the AuNPs, altered the surface area to volume ratio which resulted in the suppression of interband damping. These results suggest that nanorods have the potential to be used in a range of optical applications due to the large local-field enhancement and high light-scattering efficiencies. In a study conducted by Jain *et al*. (2006), it was found that the size of spherical AuNPs influences its optical properties. When the nanospheres were increased from 20 nm to 80 nm in diameter, a significant increase in the magnitude of extinction, as well as the relative contribution of scattering to extinction, in the AuNPs was observed.

A review of the current literature revealed that a change in certain parameters of the synthesis process such as environmental pH, biomass ratios and temperature are reported to result in AuNP shape and size variability (Noruzi *et al*., 2011; He *et al*., 2007; Konishi *et al*., 2007). This has been reported widely for fungi or plants (Gericke and Pinches, 2006; Shedbalkar *et al*., 2014; Singh and Srivastava 2015) and a few bacterial taxa (He *et al*., 2007; Li *et al*., 2016) with studies usually focusing on pH and/or temperature at most. These studies have shown that changing the pH will alter the shape and the size of the AuNPs produced. However, changes to the topographical characteristics of the AuNPs can vary between the organisms (Gericke and Pinches, 2006; Singh and Srivastava, 2015). It was found that an increase in pH, increased the size of the AuNPs in black cardamom

(Singh and Srivastava, 2015) and fungal isolates (Gericke and Pinches, 2006), while the opposite was observed in the study conducted by He *et al*., (2007) on the bacterium *R. capsulata*. The effects of temperature on the AuNPs synthesis appears to be shared between bacteria, fungi and plant-based organisms, whereby an increase in environmental temperature causes an increase in the size and diversity of the shapes in the synthesised AuNPs (Gericke and Pinches, 2006; Ghosh *et al*., 2012).

The bacterial strain of choice in the present study was isolated from acid mine decant from a uranium mine West Rand of Gauteng, South Africa (26°06'26.8"S 27°43'20.2"E). This chapter describes the preliminary identification of Pb204 by 16S rRNA sequencing. Furthermore, Pb204 was shown to produce AuNPs when exposed to Au (III) ions and the influence of the reaction parameters: growth media, reaction time, biomass ratios, environmental pH, temperature and Au (III) concentration on their size and shape were evaluated.

3.2 Methodology

3.2.1 Materials

DNA extraction was performed using the Promega Wizard® Genomic DNA Purification Kit (Wisconsin, USA) and Gelred was used for the visualisation of the DNA and were bought from Sigma (Missouri, USA). The PCR reagents were sourced from New England Biolabs (Massachusetts, USA). The reagents and materials for the metabolic characterisation were all purchased from Sigma (Missouri, USA). All of the reagents used in the AuNP biogenesis experimentation were purchased from Sigma (Missouri, USA). The chloride trihydrate ($HAuCl_4 \cdot 3H_2O$) was purchased as >99% pure and sterilised using 0.20 μm membrane filter (GVS Filter Technology, Maine, USA).

3.2.2 Identification of *Enterobacter* sp. Pb204 by 16S rRNA sequencing

3.2.2.1 Extraction of genomic DNA from Enterobacter sp. Pb204

The genomic DNA of *Enterobacter* sp. Pb204 was extracted using the Promega Wizard® Genomic DNA Purification Kit as per the manufacturer's instructions for bacterial genome extractions (Promega, Wisconsin, USA). The Wizard® Genomic Purification Kit is a five step purification which briefly entails: cell membrane lysis, nuclei lysis, protein separation, DNA concentration and desalting through isopropanol and ethanol precipitation and finally the rehydration and re-suspension of the precipitated genomic DNA in the Wizard® Genomic rehydration buffer. The purity of the DNA was assessed using the ND 1000 Nanodrop spectrometer (Thermo Fisher Scientific, Massachusetts, USA) and quantified using Qubit® dsDNA Broad Range assay kit on the Qubit® 2.0 fluorometer (Thermo Fisher Scientific, Massachusetts, USA). Extracted genomic DNA together with Thermo Fisher Scientific 100 bp plus DNA ladder (Thermo Fisher Scientific, Massachusetts, USA) was visualised on a 1% agarose gel stained with GelRed (Biotium Inc., California, USA). Images were captured using the ChemiDoc™ XRS+ System (Biorad, California, USA) and analysed with ImageLab software (Biorad, California, USA).

3.2.2.2 Sequencing of the 16S rRNA gene from Enterobacter sp. Pb204

The 16S rRNA gene of *Enterobacter* sp. Pb204 was amplified from the extracted genomic DNA by PCR using the universal 16S rRNA primer set 8F and 1492R (Inqaba Biotec, Pretoria, RSA). Amplification was performed in a 50 µl reaction vessel using Phusion® High-Fidelity DNA Polymerase (New England Biolabs, Massachusetts, USA) in the Bio-Rad T-100 thermal cycler (Bio-Rad, California, USA). The cycling conditions included: an initial denaturation step at 98 ºC for 30 s, 35 cycles of 98 °C for 10 seconds, 58 °C for 30 seconds and 72 °C for 60 seconds and a final extension at 72 °C for 10 minutes. Amplified products were analysed on a 1% agarose gel stained with GelRed as described in section 3.2.2.1 (page 26). Products of the correct size were purified without excision using the GeneJET PCR Purification Kit (Thermo Fisher Scientific, Massachusetts, USA)

and the services of Inqaba Biotec (Pty) Ltd were used for sequencing. The sequence data of the 16S rRNA was aligned using Basic Local Alignment Search Tool (BLAST) of NCBI to identify regions of local similarity (Altschul *et al.,* 1990).

3.2.3 Biogenesis of AuNPs by *Enterobacter* sp. Pb204 under variable conditions

3.2.3.1 Biogenesis of AuNPs by Enterobacter sp. Pb204

A glycerol stock of *Enterobacter* sp. Pb204 was used to isolate single colonies by streaking out on Luria-Bertani (LB) agar plates and incubating at 37 ^{o}C overnight. A pre-inoculum was prepared by inoculating a single colony in LB broth that was incubated overnight with shaking at 37 ^{o}C. The pre-inoculum was diluted 1% (w/v) in broth and cultured for 24 hours at 37 ^{o}C with shaking to accumulate biomass. The cells were separated from the supernatant by centrifugation at 5000 × *g* for 15 minutes in a Sorvall Legend XTR Centrifuge (Thermo Fisher Scientific, Massachusetts). Both the cell pellet (herewith referred to as cell biocatalyst - CB) and supernatant (herewith referred to as cell-free biocatalyst - CFB) were retained for AuNP synthesis. The CB was washed twice in de-ionised water and the CFB further centrifuged at 15 000 × *g* for 15 minutes to remove any cell debris. The CB and CFB were individually exposed to 50 ml of 1 mM $HAuCl_4.3H_2O$ with shaking for 24 hours at 37 °C according to the method of He *et al*. (2007). AuNPs production was subsequently monitored by visual observation for colour change and by ultraviolet-visible (UV-Vis) spectroscopy and transmission electron microscopy (TEM).

The above described experimental procedure was followed to study the influence of growth media using either LB or nutrient broth (NB), CB vs CFB and reaction parameters i.e. reaction time, pH, temperature, the concentration of biocatalyst and precursor gold ions on the biogenesis of AuNPs with slight modification. Modification involved varying the parameter of interest while maintaining all other reaction conditions. Reaction parameters were varied in a sequential manner building on a previously optimised parameter (P_{OPT}) as indicated in Table 3.1.

Respective treatments were performed in triplicate using the same batch of culture to indicate repeatability. Additionally, a control sample that consisted of either CB or CFB in de-ionised water lacking precursor gold ions were subjected to identical conditions.

Table 3.1: Table showing the reaction parameters used in six different treatments during the biogenesis of AuNPs by *Enterobacter* sp. Pb204.

Treatment	Growth media	CB vs CFB	Biocatalyst (% w/v or ml:ml)	pH	Temperature (ºC)	$HAuCl_4$ (mM)
1	NB LB	CB/CFB	2/50	3	37	1
2	LB_{OPT}	CB CFB	10; 2; 1 0.5:1; 1:1; 2:1	3	37	1
3	LB_{OPT}	CB_{OPT}	2 $_{OPT}$	3; 5; 7; 9	37	1
4	LB_{OPT}	CB_{OPT}	2 $_{OPT}$	3_{OPT}	25; 37; 50	1
5	LB_{OPT}	CB_{OPT}	2 $_{OPT}$	3_{OPT}	37_{OPT}	0.4; 0.6; 1
6	LB_{OPT}	CB_{OPT}	2 $_{OPT}$	3_{OPT}	37_{OPT}	1_{OPT}

P_{OPT}- optimised parameter.

The parameters highlighted in red indicate the parameter being evaluated in a particular treatment.

3.2.4 Characterisation of AuNPs produced by *Enterobacter* sp. Pb204

The production of AuNPs can often be visualised with a change in colour of solution from yellow to red-blue depending on the size of the NPs formed. Each treatment was observed for the occurrence of a colour change during the progress of the reaction. Thereafter, representative samples were collected and analysed using UV-Vis spectroscopy and TEM. A total of three or more samples from each replicate were analysed for shape, size and dispersity of AuNPs.

3.2.4.1 UV-Vis spectroscopy

AuNPs will produce an absorption peak between 520 nm and 580 nm (Haiss *et al.*, 2007) depending on their size. All samples collected from the different treatments were subjected to a wavelength scan between 400 nm - 900 nm on a Jasco V-630 UV-vis spectrophotometer (Jasco Analytical Instruments, Maryland, USA).

3.2.4.2 Transmission Electron Microscopy (TEM) and Energy-dispersive X-ray Spectroscopy (EDS)

Transmission electron microscopy was used to characterise the size and shape of the AuNPs synthesised during each treatment. A volume of 100 µl of each experimental and control sample was drop-cast onto holey carbon-coated 200 mesh copper TEM grid (SPI, Pennsylvania, USA) and allowed to dry overnight at ambient room temperature. Micrographs of the grids were taken on a JOEL 2100 TEM (JOEL Ltd, Tokyo, Japan) with a Gatan SC1000 Orius camera (Gatan Inc, California, USA) at 200 kV. An elemental analysis was conducted using the Oxford Inca X-Max^{N} EDS detector fitted on the TEM (Oxford Instruments, Oxfordshire, UK).

.

3.2.4.3 ImageJ: particle size analysis

The size of the AuNPs was analysed using ImageJ Image Processing and Analysis Software (NIH, Maryland, USA) on the TEM micrographs. This particle analysis tool was used to determine the size of the AuNPs in the TEM micrograph (Rice *et al.*, 2013).

3.3 Results and discussion

Enterobacter sp. Pb204 (used in the present study) was first isolated from acid mine decant collected from a uranium mine in the West Rand of Gauteng, South Africa (26°06'26.8"S 27°43'20.2"E). It was cultured on lead-supplemented LB agar plates and has been reported to be resistant to metals such as lead, cobalt, nickel, manganese and zinc (Kondiah, 2013). The present study reports on the biogenesis of AuNPs by *Enterobacter* sp. Pb204 and their variation in size and morphology when produced under different reaction conditions.

3.3.1 Identification of *Enterobacter* sp. Pb204 through 16s rRNA gene sequencing

The sequence of the almost full-length 16s rRNA gene was compared to those in the nucleotide collection (nr/nt) database on NCBI server and found to align most closely with others from the genus *Enterobacter*. *Enterobacter* is a genus of bacteria which are non-spore forming, Gram negative, rod shaped, motile and facultative anaerobic of the family *Enterobacteriaceae* (Nirbhavane *et al.*, 2017). *Enterobacter* sp. Pb204 had the best alignment with *Enterobacter* sp. B13 (NCBI Accession number of 16S sequence). This strain was isolated from the soil and mud samples collected from the riverside nearby Trabzon, Su¨rmene, Turkey (Eminoğlu *et al*., 2016). It has been observed that the bacteria found in this genus *Enterobacter* have shown resistance to heavy metals such as lead, cadmium, zinc, nickel and manganese (Banerjee *et al*., 2015). This heavy metal resistance has also been found in the South African isolate *Enterobacter* sp. Pb204 in a previous study conducted Kondiah (2013).

3.3.2 The biogenesis of AuNPs by *Enterobacter* sp. Pb204

3.3.2.1 The spectral and elemental analysis of AuNPs

Representative data for UV-vis spectral and EDS analysis of the AuNPs produced are shown in Figure 3.1 and 3.2, respectively. A peak at 527 nm was observed for CB while a broad peak at 577 nm was determined for CFB. These findings correlate

to that previously reported for AuNPs in literature (He *et al*., 2007) showing that AuNPs were successfully synthesised by *Enterobacter* sp. Pb204. The peak observed at 500 nm to 600 nm in the UV/Vis spectra is due to the unique SPR of AuNPs which have an absorbance maxima between 500 nm to 600 nm (Amendola *et al*., 2017). All of the AuNPs shown in the subsequent results share similar data for the UV-vis spectra and EDS analysis.

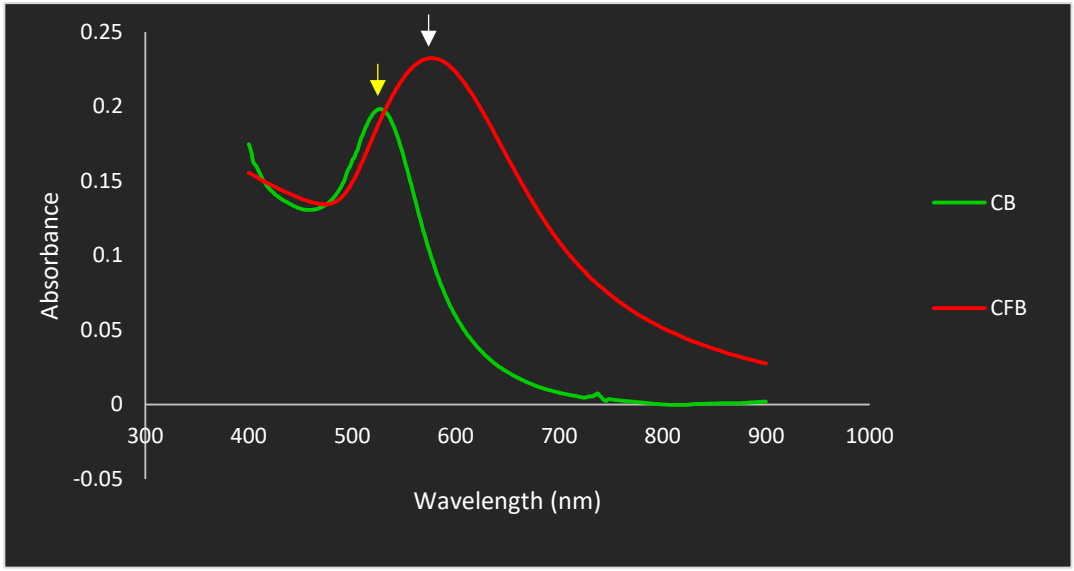

Figure 3.1: The UV-vis spectra of the AuNPs produced by *Enterobacter* sp. Pb204. The CFB had a maximum absorbance at 577 nm (white arrow) and the CB had a maximum absorbance at 527 nm (yellow arrow).

The broadness of the peak in the UV-vis spectra can indicate the polydispersity of the AuNPs (Oliveira *et al*., 2017). The narrower the peak is, the greater the uniformity is for the AuNPs synthesised with the opposite being true for broader peaks (Oliveira *et al*., 2017). In a more polydispersed AuNP mixture, the differing shaped and sized AuNPs have different absorption maxima resulting in a widened peak in the UV-vis spectra (Sau *et al*., 2001; Amendola *et al*., 2017). This trend was observed when the CFB of *Enterobacter* sp. Pb204 was used for AuNP synthesis (Figure 3.1). A much broader peak than that for CB is obtained indicating a higher degree of polydispersity when AuNPs are synthesised using CFB.

The position of maximum absorbance for the peak has also been shown to indicate the size of the AuNPs synthesised (Amendola *et al*., 2017). Larger AuNP will cause a blue-shift in the UV-vis spectra due to the increased space in which the electrons can oscillate in the AuNPs (Dubey *et al*., 2010; Amendola *et al*., 2017). Gold nanoparticles produced by the CB (Figure 3.1) have a lower absorbance maxima implying the occurrence of smaller sized nanoparticles compared to those formed using the CFB.

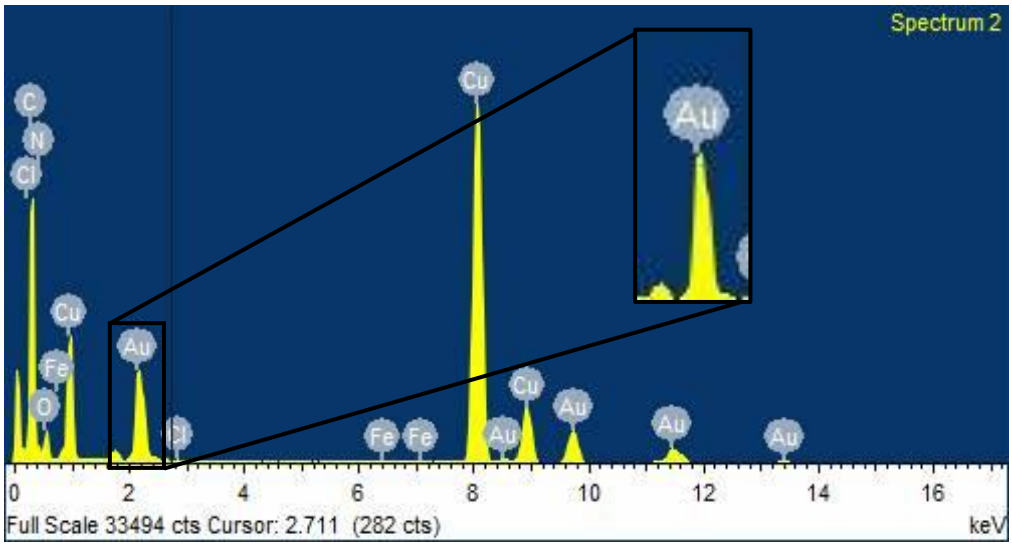

Figure 3.2: The EDS elemental spectra of the AuNPs produced by *Enterobacter* sp. Pb204. A distinct signal for Au was observed for the AuNP synthesis by *Enterobacter* sp. Pb204 (CFB sample).

The atomic structure of all elements will produce distinct peaks on its electromagnetic emission spectrum when excited by x-ray radiation which can be identified by the EDS (Holmes *et al.,* 1995). The NPs produced by *Enterobacter* sp. Pb204 exhibited peaks of Au shown in the EDS spectrum (Figure 3.2) further confirming their elemental nature. The EDS spectra also shows that there is a high quantity of AuNPs which is seen as multiple small peaks for Au throughout the spectra (Figure 3.2) (Menon *et al.,* 2017). The peaks observed for calcium, oxygen, nitrogen and chlorine can be attributed to the biological material surrounding the AuNPs. Iron, copper and carbon which may originate from the carbon, copper sample grid and the steel sample holder were also detected.

3.3.3 The influence of reaction parameters on AuNP size, shape and dispersity

3.3.3.1 Growth media

The TEM analysis coupled with EDS revealed that *Enterobacter* sp. Pb204 successfully reduced the gold (III) ions in solution for both the NB and LB media. When *Enterobacter* sp. Pb204 was grown in LB media, both the CB and CFB resulted in the production of AuNPs (Figure 3.3 A and B). For LB with the CB, the AuNPs produced ranged between 5 nm to 30 nm while that of LB with CFB fell within a size range of 30 nm to 90 nm (Figure 3.3).

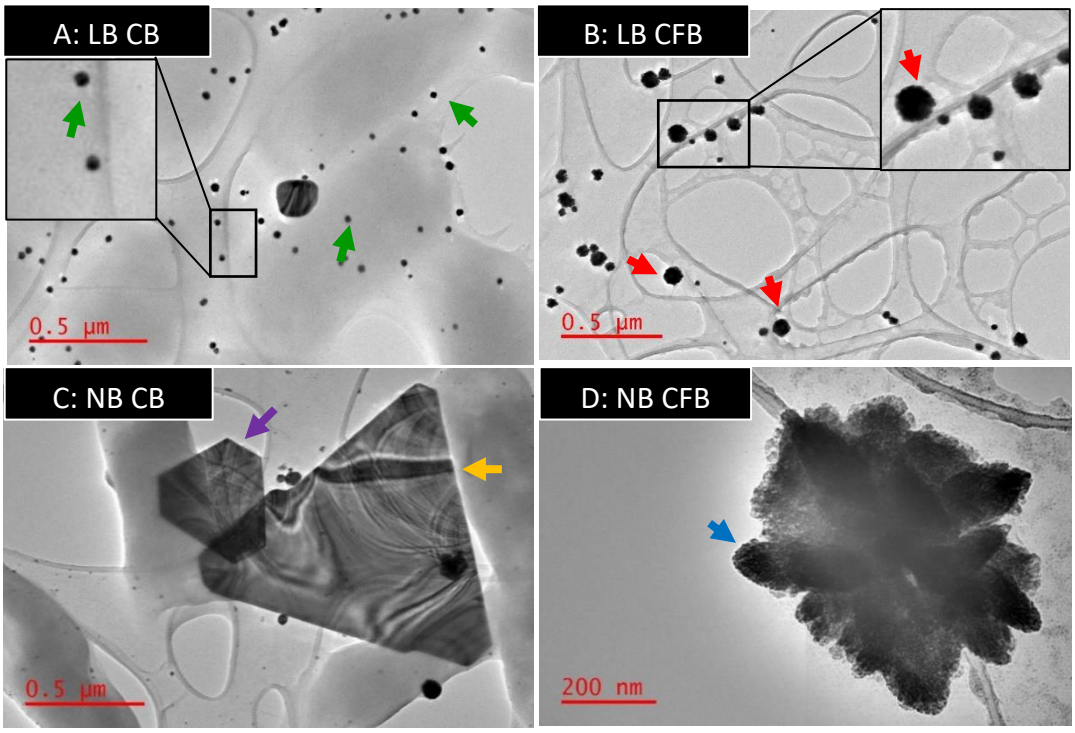

Figure 3.3: TEM micrographs of AuNPs produced by *Enterobacter* sp. Pb204 cultured in LB and NB. Small spherical AuNPs which have been highlighted by the green arrows were produced by the LB CB (A) while larger amorphous AuNPs or "nano-urchins" which are indicated by the red arrows were produced by the LB CFB (B). Large geometric shapes of Au particles such as hexagonal (purple arrow) and triangular (orange arrow) can be seen in the NB CB (C). A large Au particle

with no discernible shape, indicated by the blue arrow was observed in the NB CFB (D).

The CB of *Enterobacter* sp. Pb204 cultured in NB produced a mixture of AuNPs and larger gold particles (Figure 3.4 C) ranging from the nanoscale (12 nm) to the microscale (686 nm) (Figure 3.4).

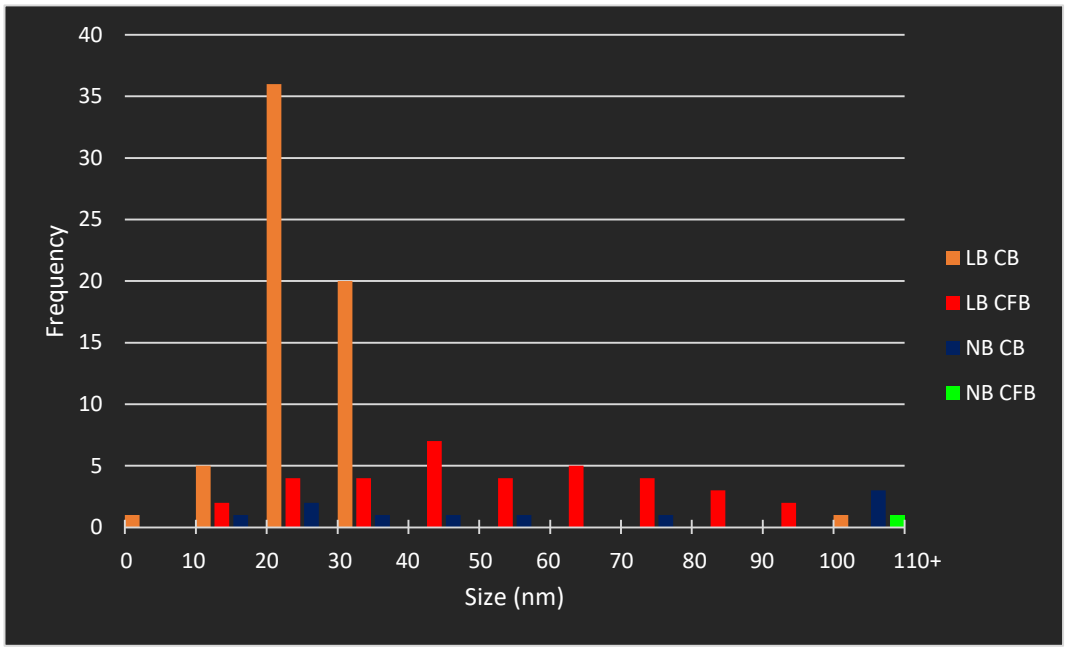

Figure 3.4: A histogram illustrating the size and frequency of the AuNPs produced in the growth media trials. The volume of media for each synthesis was standardised.

The large difference in size and shape of the particles formed could be as a result of the type of growth media that was used for bacterial growth. It has been well documented that macromolecular composition of the bacterial cell, the mass fraction of DNA, RNA and proteins, are dependent on the growth rate of the bacteria allowed by the nutrients in growth medium (Klumpp *et al*., 2009; Scott *et al*., 2010). Global parameters in the bacterial cell, such as the concentration of ribosomes and RNA polymerase, are all growth rate-dependent (Klumpp *et al*., 2009). In a study by Low *et al*. (2013), it was found that *Escherichia coli* ATCC 8739 has a higher growth rate when grown in LB media compared to NB media. It

can be surmised that with an increased growth rate, by using LB as a culture medium for *Enterobacter* sp. Pb204, there was a corresponding increase in the abundance of the biomolecules (proteins) responsible for AuNP synthesis. The increased number of bacterial cells and biomolecules would lead to an increase in the number of binding sites for Au (III) and speed up the rate of reduction of gold ion, respectively leading to numerous nucleation events. These nucleation events would favour the production of isotropic/spherical AuNPs as seen in Figure 3.3 A.

The large triangular and hexagon plates observed in Figure 3.3 C where *Enterobacter* sp. Pb204 was cultured in NB media are referred to as anisotropic AuNPs which are nanoparticles that possess asymmetric axes (Burrows *et al*., 2016). They are formed when there is preferential growth during the synthesis process (Sajanlal *et al*., 2011). Preferential growth occurs when a particular plane in the AuNP is selectively reduced and stabilised, causing an increase in growth in a particular direction (Wei and Zamborini, 2004). This kind of growth is kinetically favoured as opposed to thermodynamically favoured (Sajanlal *et al*., 2011). Although they lack monodispersity, these types of anisotropic AuNPs have the potential to be used in sensing, catalysis, imaging, and photothermal therapy (Li *et al*., 2014). For example, in a study by Bi and Lu (2008), gold nanoplates showed a higher catalytic activity in liberating hydrogen gas from formaldehyde when compared to spherical AuNPs.

Spherical AuNPs necessary for use as biomarkers on lab-on-chip type assays are simply synthesised by chemical reduction of metal salts (Wuithschick *et al*., 2015). Fine-tuning their size and shape can easily be achieved by controlling the precursor metal ion concentration, reducing agents and stabilizers (Wuithschick *et al*., 2015). On the other hand, achieving similar results in a biological system appears to be more complex. The present study was focused on outlining a set of parameters that would result in the formation of isotropic AuNPs by *Enterobacter* sp. Pb204 for application in diagnostic assays. Hence, LB media was selected for the subsequent experimentation as it resulted in a high yield of spherical AuNPs of similar size.

3.3.3.2 Reaction time

During chemical synthesis, the length of reaction time can be controlled to fine-tune the shape of isotropic nanoparticles. Reaction time influences the size and shape of nanoparticles, whether the growth mechanism is based on Ostwald ripening, coalescence or intraparticle growth of colloidal Au particles into larger anisotropes (Thanh *et al*., 2014). When the CB of *Enterobacter* sp. Pb204 was used to reduce Au (III), spherical AuNPs between 2-15 nm were produced within 24 hours (Figure 3.5 A and Figure 3.6). Extending the reaction time to 72 hours resulted in the production of anisotropic AuNPs (Figure 3.5 B) together with larger gold particles (Figure 3.6).

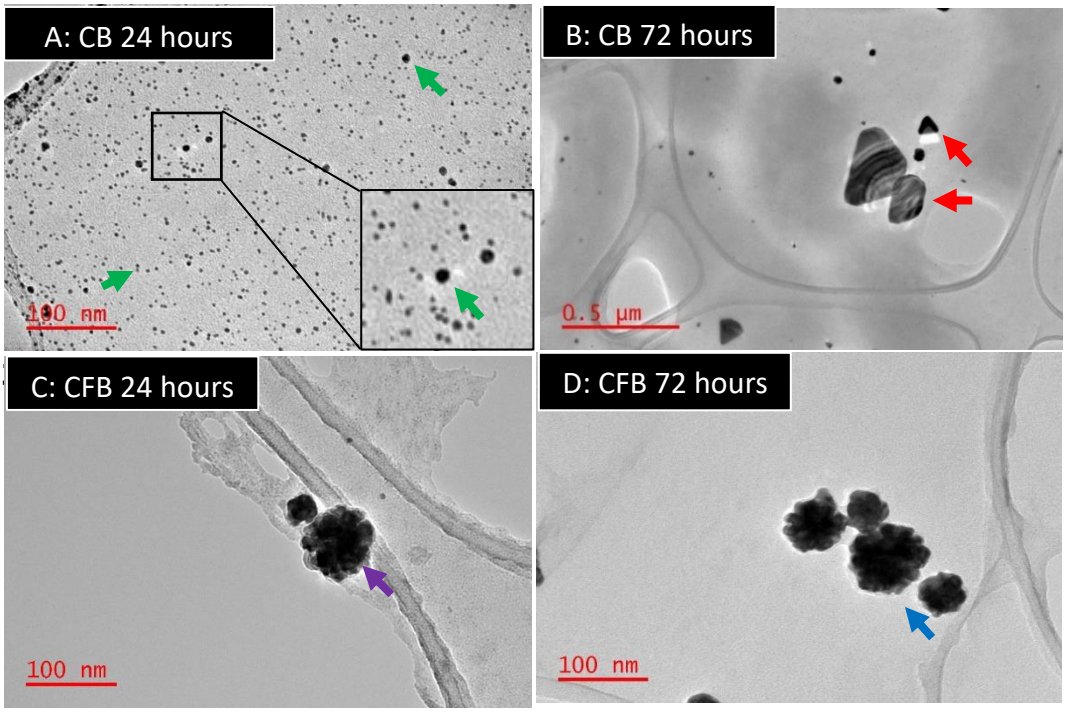

Figure 3.5: TEM micrographs of AuNPs produced by *Enterobacter* sp. Pb204 cultured in LB media over time. Small spherical AuNPs (green arrows) were produced by the CB after 24 hours (A) while large AuNPs, highlighted by the red arrows, were produced after 72 hours (B). Amorphous AuNPs or "nano-urchins" indicated by the purple and blue arrows, were synthesised by the CFB after 24 (C) and 72 (D) hours.

Similar results were observed for the fungus *Trichoderma viride* where considerably larger AuNPs were produced by the filtrate in a 72 hour reaction as compared to the 24 hour reaction (Kumari *et al*., 2016). It was speculated that the smaller AuNPs might fuse to form larger AuNPs which then fuse further to form the gold prisms during the longer period of crystal growth. The same relationship between size and reaction time has also been reported by Chandran *et al*. (2006) when *Aloe vera* plant extract was used to synthesise AuNPs.

Although the mechanism of nanoparticle nucleation and growth in biological systems is poorly understood, it appears to correlate to that described for the chemical mode of synthesis. Several mechanisms of nucleation and growth that include LaMer nucleation, Finke-Watzky two-step mechanism, Ostwald ripening, digestive ripening, coalescence and orientated attachment, and intraparticle growth point to the bonding together of either gold ions or atoms in different planes to form these anisotropic structures over time (Thanh *et al*., 2014).

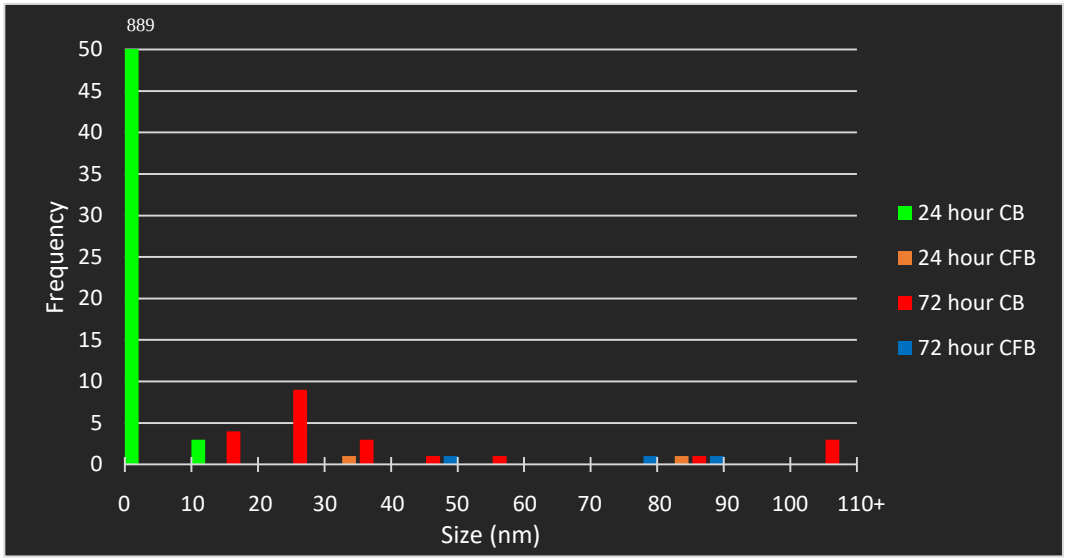

Figure 3.6: A histogram illustrating the size and frequency of the AuNPs produced in the reaction time trials. The volume of media for each synthesis was standardised.

Using the CFB of *Enterobacter* sp. Pb204 over 24 or 72 hours produced similarly shaped and sized nano-urchins (Figure 3.5 C and D). This could be due to the

reduced concentration of secreted biomolecules present in addition to the influence of reaction time. The lower concentration of secreted (extracellular) biomolecules involved in NP biosynthesis as opposed to those present within the CB would lead to fewer nucleation events and subsequently allow for more growth and particle aggregation over time. This would yield fewer and larger AuNPs as represented in Figure 3.7. Subsequently, all downstream biosynthesis was carried out over 24 hours to maintain uniformity in size, shape, and yield of the AuNPs.

3.3.3.3 Concentration and source of biocatalyst

Gold nanoparticles can be produced intracellularly (Du *et al*., 2007; Feng *et al*., 2007; Correa-Lantén *et al*., 2013) or extracellularly (He *et al*., 2007; Johnston *et al*., 2013; Erasmus *et al*., 2014) by bacteria (Figure 2.3 section 2.3.3.2 page 15). The localisation of the biomolecules involved in the reduction of Au (III) to AuNPs influences whether nanoparticle formation takes place within the cell or on the exterior of the cell wall. Furthermore, the rate of reduction will be dependent on, among other factors, the concentration of biomolecules present to begin nucleation.

The most uniform AuNPs in terms of shape (spheres) and size were synthesised when CB was diluted 2% (w/v) in $HAuCl_4^-$ (Figure 3.7). These particles fell within a range of 2-15 nm (Figure 3.8). At a lower concentration of biocatalyst (1% (w/v)) large anisotropic Au particles mixed with smaller AuNPs could be observed (Figures 3.7 and 3.8). This is likely as a result of less metal binding sites available for Au (III) binding (Varia *et al*., 2016) and therefore fewer nucleation sites while leaving room for nanoparticle growth by Ostwald ripening.

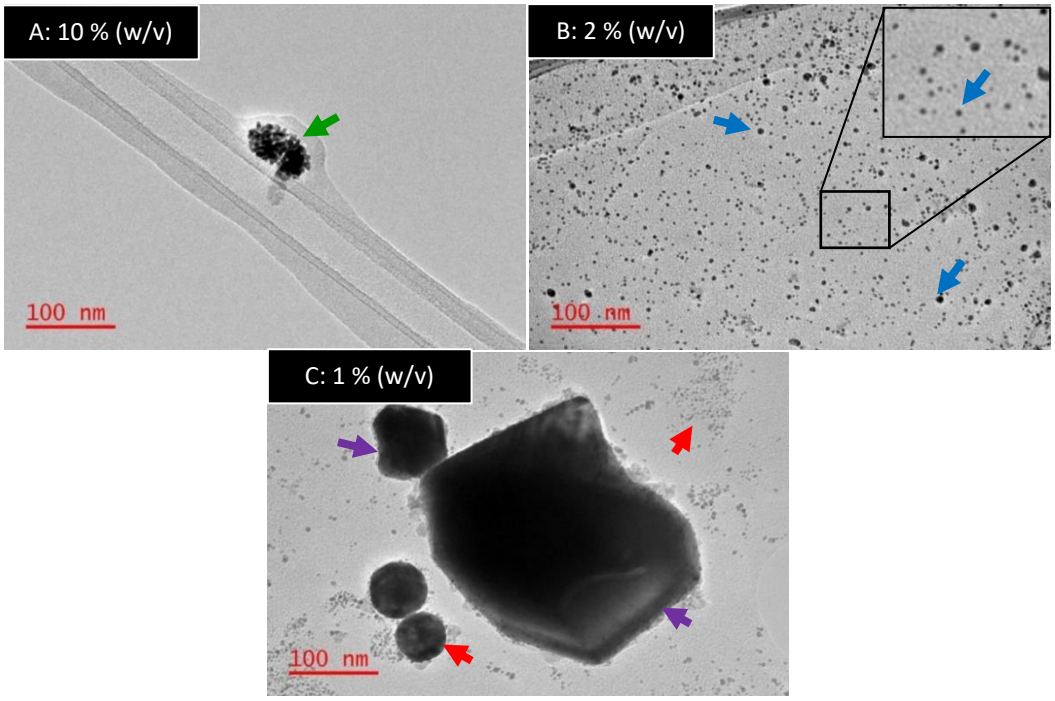

Figure 3.7: TEM micrographs showing gold particle formation when the biocatalyst (CB) was added to gold ions in different concentrations: Few AuNPs with a less discernible shape, green arrow, were produced when CB was diluted 10% (w/v) (A). The most uniform AuNPs which were spherical in shape, blue arrows were produced when CB was diluted 2% (w/v) (B). A mixture of AuNPs (red arrows) and anisotropic microscale Au particles (purple arrows) were observed when CB was diluted 1% (w/v) (C).

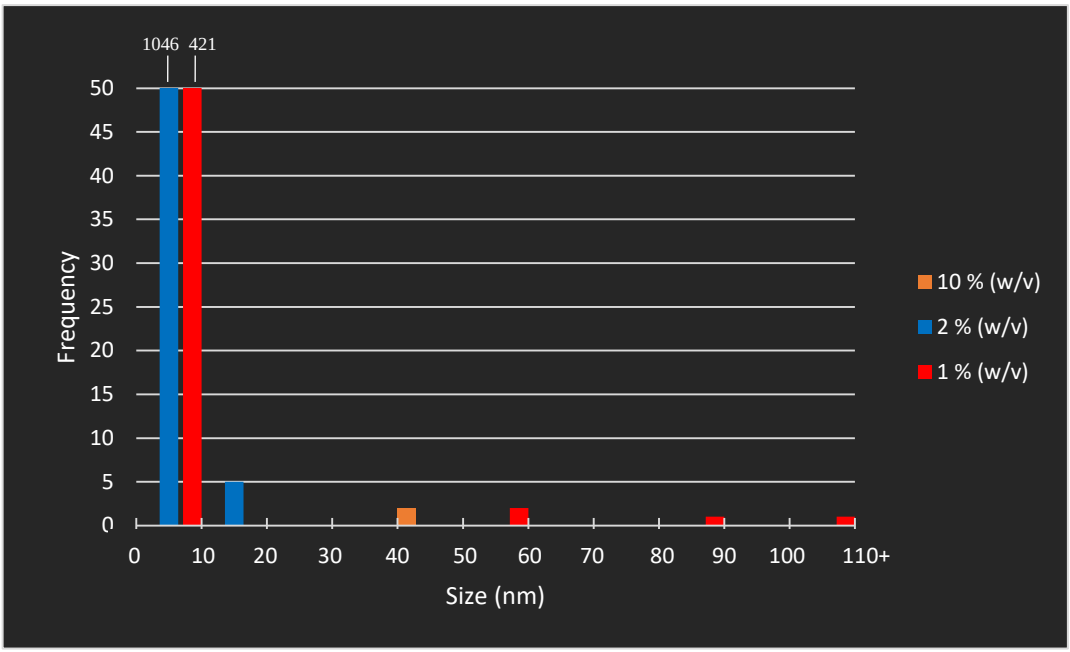

Figure 3.8: A histogram illustrating the size and frequency of the AuNPs produced in the CB ratio trials. The volume of media for each synthesis was standardised.

When CFB was used to reduce Au (III), irrespective of the concentrations used, all of the Au particles and AuNPs produced appeared anisotropic in shape (Figure 3.9) and the yield of the AuNPs were significantly fewer in number (Figure 3.7) than when the CB was used.

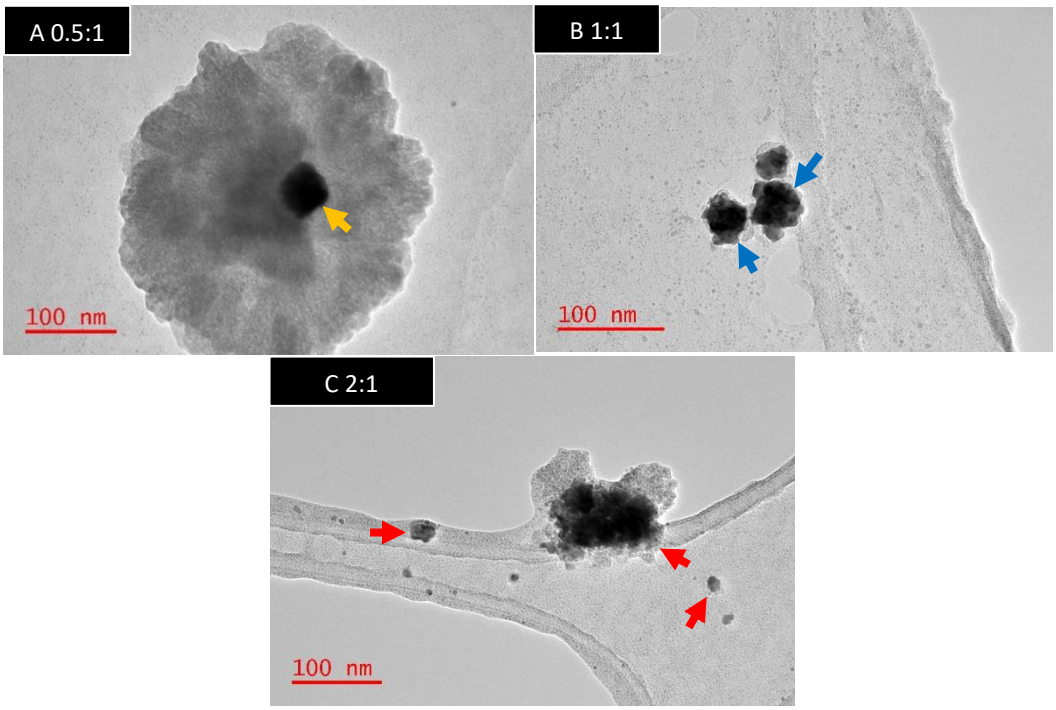

Figure 3.9: TEM micrographs showing gold particle formation when the cell-free biocatalyst (CFB) was added to gold ions in different concentrations. Large anisotropic Au particles indicated by the orange arrow, were observed when CFB was diluted to a ratio of 0.5:1 (A). Nano-urchin AuNPs shown by the blue arrows were observed when CFB was diluted a ratio of 1:1 (B). Interspersed between the nano-urchins, smaller AuNPs marked with the red arrows could be observed when CFB was diluted to a ratio of 2:1 (C).

The majority of the smaller AuNPs were formed using the CFB at a 2:1 ratio in $HAuCl_4^-$; however this treatment also produced larger gold particles. Although the AuNPs produced by the 1:1 ratio of CFB were more uniform in size, ranging between 35 – 59 nm in diameter according to ImageJ Analysis (Figure 3.10), the particles formed nano-urchins (Figure 3.9 B).

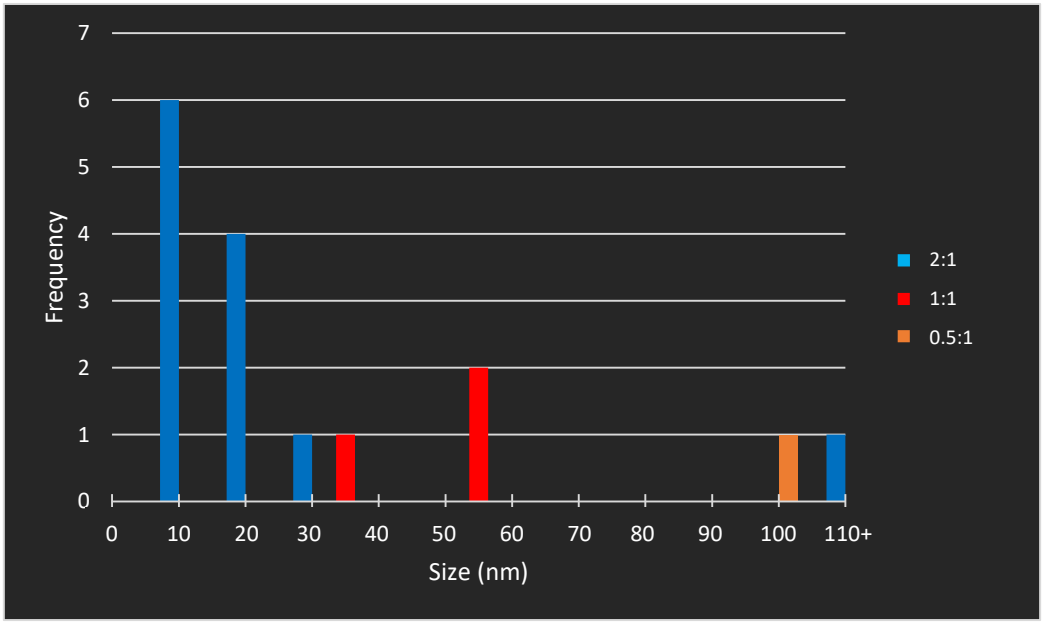

Figure 3.10: A histogram illustrating the size and frequency of the AuNPs produced in the CFB ratio trials The volume of media for each synthesis was standardised.

The findings from the CFB and CB treatments correlate to those reported by Pimprikar *et al*. (2009) where a 2% (w/v) ratio of *Yarrowia lipolytica* biocatalyst produced smaller AuNPs compared to larger AuNPs observed when using the biocatalyst at 1% (w/v) and 2:1 ratios. The change in shape and size was attributed to the low concentration of reducing and capping agent which would not be sufficient to reduce the high concentration of gold ions present (Pimprikar *et al*., 2009; Das *et al*., 2010). At lower dilutions, there is a greater abundance of reducing agent compared to the concentration of gold ions, which would increase the rate of reduction. The increased rate of reduction would provide more Au^0 monomers thereby leading to an increase in the rate of nucleation (Das *et al*., 2010; Wuithschick *et al*., 2015).

Furthermore, the lower yield of AuNPs formed by the CFB when compared to CB infers that although both intracellular and extracellular biogenesis occurs, *Enterobacter* sp. Pb204 prefers to use an intracellular mechanism for tolerance to gold ions through the formation of AuNPs. Although extracellular production of

AuNPs is more appealing for applications in optoelectronics, electronics, bioimaging and in sensor technology due to the reduced need for additional processing steps (Narayan and Sakthivel 2010), AuNPs formed intracellularly are likely to be more monodispersed and suited towards industrial applications.

Following these findings, it is suggested that using CB at a dilution of 2% (w/v) produces high yields of largely monodispersed AuNPs compared to the other ratios tested, subsequent experimentation was conducted using these parameters.

3.3.3.4 pH

Solution pH is one of the most important factors influencing metal sorption and therefore nanoparticle formation. Protons in solution are known to affect the charged anionic functional groups present in the cell wall of bacteria that act as binding sites for metal cations as well as the solubility of the metal ions (Paknikar *et al*., 2003; Das *et al*., 2008). Figure 3.12 shows an increase in the polydispersity of the nanoparticles produced with an increase in pH. At a pH of 3 (Figure 3.11 A), uniform spherical particles of up to 14 nm in diameter were produced (Figure 3.12). When the pH was increased to 5, larger geometric shaped nanoparticles were observed (Figure 3.11 B). Dendritic forms of the AuNPs occurred at neutral pH while large aggregates dominated at pH 9 (Figure 3.11 C and D, respectively).

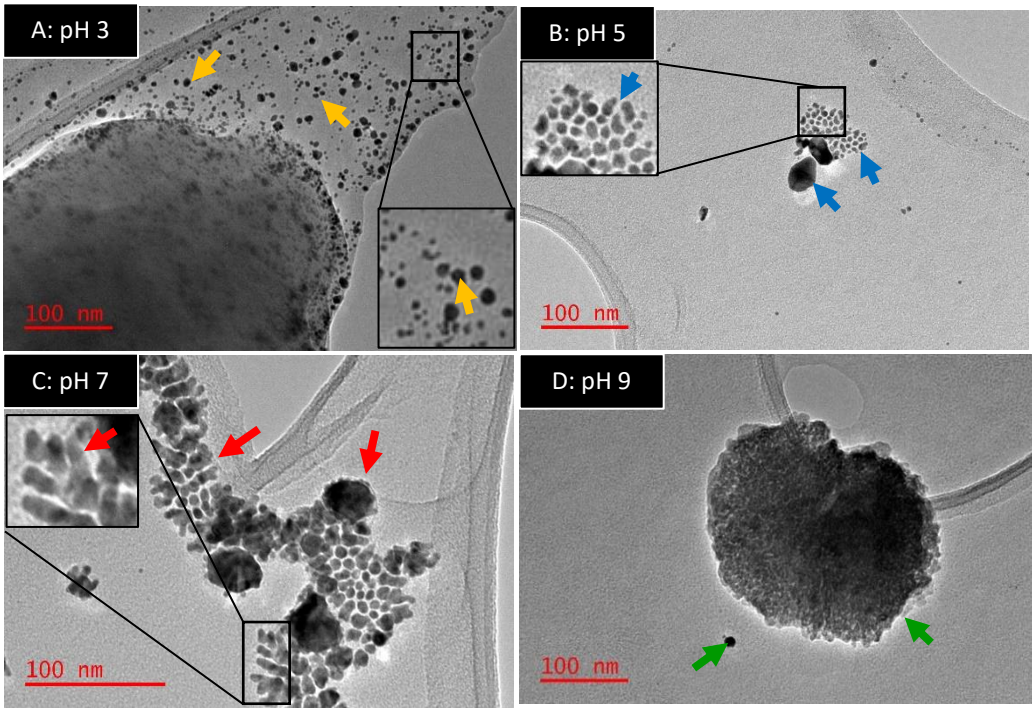

Figure 3.11: TEM micrographs of pH trials: The most uniform, spherical AuNPs (orange arrows) were observed in the reaction mixture with a pH of 3 (A). AuNPs that were more geometric in nature, indicated by blue arrows, were observed at pH 5 (B) while AuNPs that are "dendritic" in shape, highlighted by red arrows were present at pH 7 (C). Large aggregates likely built from small single spherical AuNPs, green arrows formed at pH 9 (D).

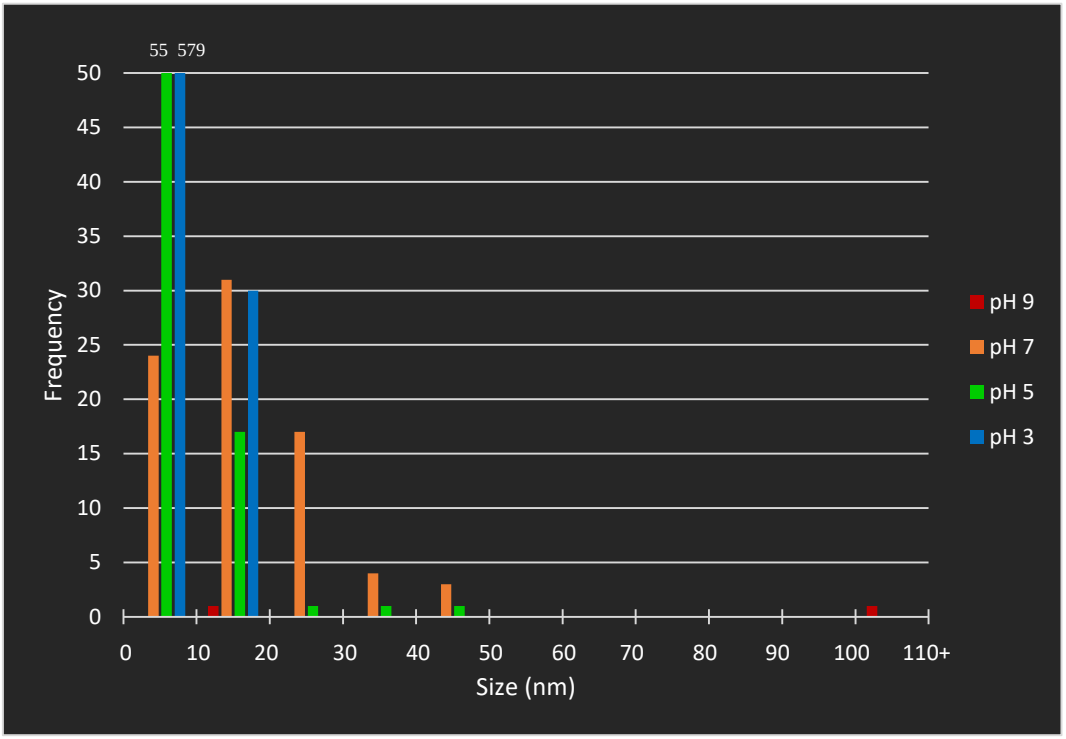

Figure 3.12: A histogram illustrating the size and frequency of the AuNPs produced during the pH trials. The volume of media for each synthesis was standardised.

The trend where a lower pH promotes the synthesis of smaller, spherical AuNPs has been reported in *E. coli* and *Desulfovibrio desulfuricans* (Deplanche and Macaskie, 2008). The authors reported that smaller AuNPs were produced at a pH of 2 and increased in size as the pH was raised from 6 - 9. Similar findings were also obtained when the fungus *Verticillium luteoalbum* produced spherical AuNPs that were less than 10 nm in size at pH 3, but the size and the diversity of the shapes of the AuNPs increased as the pH was raised (Gericke and Pinches, 2006).

Varia *et al*. (2016) proposed a four-step mechanism used by *Shewanella putrefaciens*, a Gram-negative dissimilating metal-reducing bacteria, to produce AuNPs. Briefly, $AuCl_4^-$ ions are transported from the bulk solution to the cell wall, traveling through the cell wall to protein metal recognition, sorption, and nucleation sites. Thereafter, they undergo reduction by membrane proteins leading to the formation of Au^0 monomers that behave as nucleation sites for Au^0 crystallisation and subsequent nanoparticle formation. A key aspect of this mechanism is the binding of metal ions to protein recognition motifs; these motifs must be anionic in

nature for metal cation binding to occur. The peptidoglycan, phospholipids, and lipopolysaccharides of the cell wall of Gram-negative bacteria like *Enterobacter* sp. Pb204 are the primary components responsible for metal-binding capability (Vijayaraghavan and Yun, 2008). Furthermore, extracellular polysaccharides (EPS) which can be found in the genus *Enterobacter* are also able to bind metal ions (Iyer *et al*., 2004, 2005; Vijayaraghavan and Yun 2008).

It is thought that a lower pH protonates the functional groups of the reducing agents (proteins) due to the increased concentration of H^+ ions in solution (Gericke and Pinches, 2006; Reith *et al*., 2009). The highly protonated functional groups will attract the negatively charged gold ions which would increase the rate of reduction (Reith *et al*., 2009). An increased rate of reduction would increase the rate of nucleation which favours the production of small spherical AuNPs (Gericke and Pinches, 2006; Wuithschick *et al*., 2015). Reith *et al*. (2009) found that the bacterium *Cupriavidus metallidurans* was capable of absorbing a greater amount of gold ions from the environment for bio-mineralisation at a lower pH (Reith *et al.*, 2009).

Tuning the size and shape of AuNPs using pH is unpredictable. Although there are studies that support the findings presented here, there are other reports where contrasting behaviour has been observed. Larger AuNPs have been produced at lower pH with smaller, spherical particles being formed at higher pH in *A. faecalis* (El-deeb *et al*., 2014), *T. scotodoctus* (Erasmus *et al*., 2014) and *R. capsulata* (He *et al*., 2007). Despite these findings, under the conditions used in the present study, uniformly spherical AuNPs ranging in size from 2-14 nm were produced by the CB of *Enterobacter* sp. Pb204 at pH 3 and this parameter was selected for subsequent experimentation.

3.3.3.5 Temperature

Homogeneous nucleation refers to the uniform formation of nuclei during the reduction of Au (III) to Au (0) while heterogeneous nucleation forms at structural inhomogeneities such as grain boundaries and surfaces (Thanh *et al*., 2014).

Homogenous nucleation favours thermodynamically controlled growth of all crystal facets and subsequent formation of spherical or near-spherical structures (Sajanlal *et al.,* 2011). On the other hand, under a kinetically controlled manner, anisotropic nanoparticles are formed as a result of preferential and directional growth (Thanh *et al.,* 2014).

As the temperature at which reduction of gold occurred was increased from 25 ^{o}C to 50 ^{o}C, the size and shape of AuNPs changed (Figure 3.13). Sphere-like AuNPs ranging in size from 2-20 nm were produced at 25 ^{o}C; the majority of which lay in the 5-9 nm range as shown in Figure 3.15. More uniform AuNPs in terms of size and shape were produced at 37 ^{o}C as seen in Figure 3.13 B. ImageJ analysis revealed that the highest yield of AuNPs with a diameter between 2-9 nm was achieved at this temperature. The most variation in size and shape was seen at a temperature of 50 °C (Figure 3.13 C). Microscale gold particles and large anisotropic hexagonal and triangular AuNPs about 245 nm in size could be seen mixed with smaller AuNPs ranging between 4 nm – 44 nm (Figure 3.14).

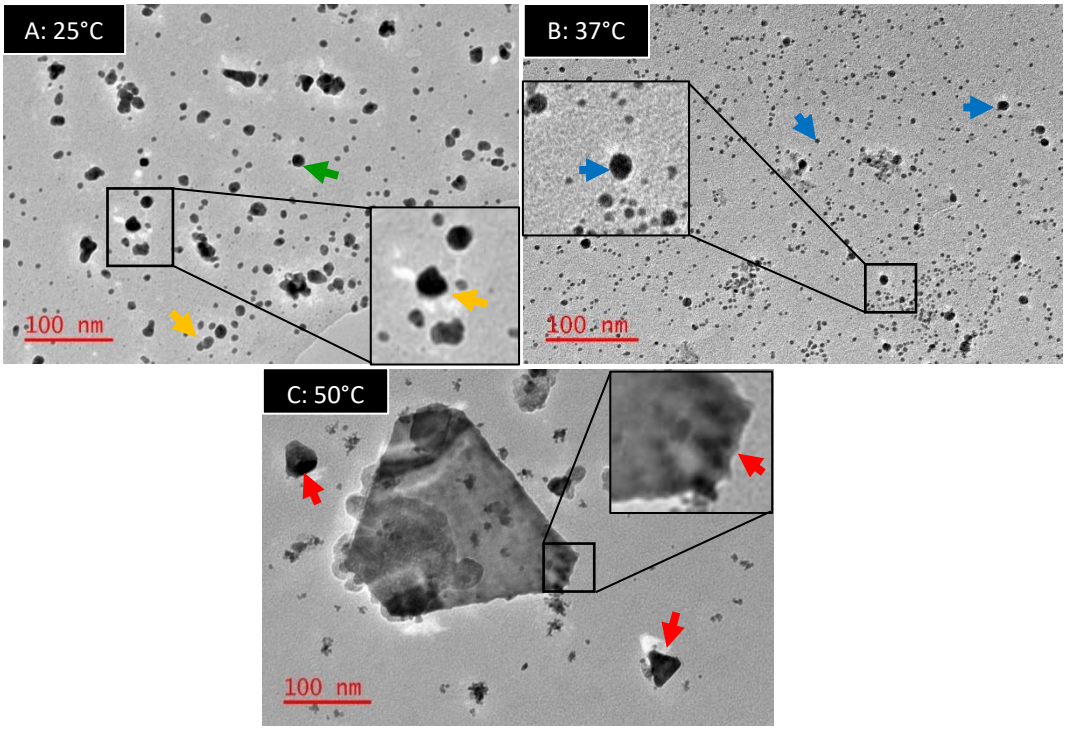

Figure 3.13: TEM micrographs of temperature trials. Marginally large quasi-spheres (orange arrows) and spheres (green arrows) were produced at 25 °C (A) while uniformly spherical AuNPs (blue arrows) were observed at 37 °C (B). Large AuNPs with geometric shapes such as hexagons and triangles as indicated by the red arrows were produced at 50 °C (C). The edges of the gold particles formed at 50 °C appeared rougher than similar particles observed during previous treatment.

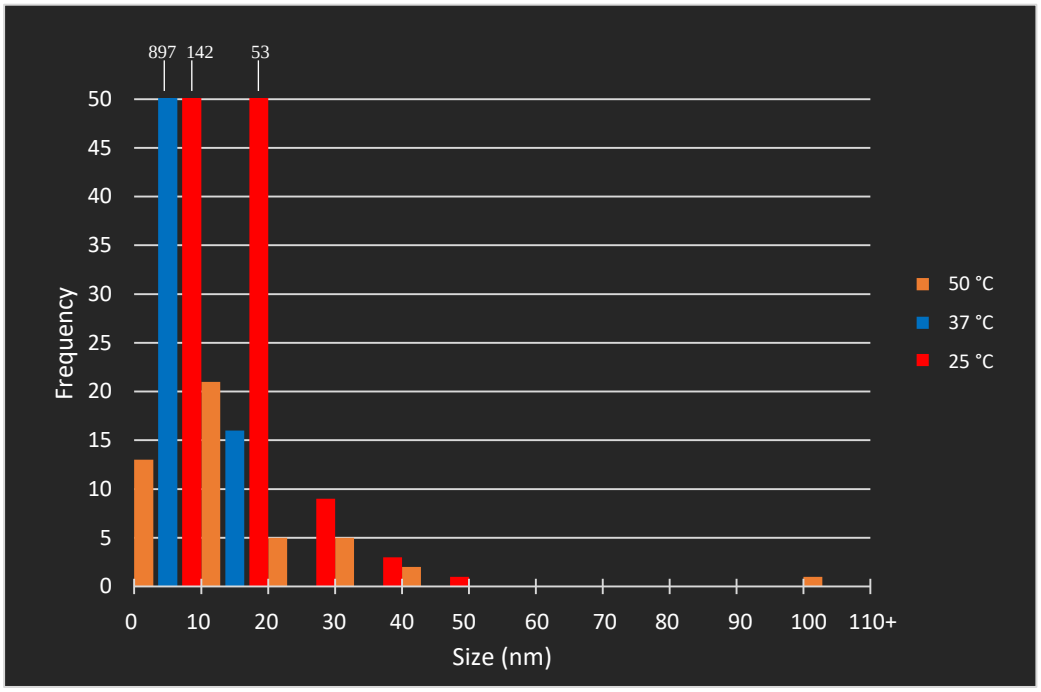

Figure 3.14: A histogram illustrating the size and frequency of the AuNPs produced during the temperature trials. The volume of media for each synthesis was standardised.

The findings from the present study suggest that at a lower temperature, AuNP formation by *Enterobacter* sp. Pb204 is thermodynamically controlled resulting in the biosynthesis of low-energy spherical particles. As the temperature is increased and surface-energy is overcome, AuNP is driven kinetically resulting in the formation of anisotropic AuNPs. The thermodynamic and kinetic aspects act in synergy to determine nanoparticle shape, but the general mechanism for the formation of these morphologies is not fully understood (Sajanlal *et al.*, 2011).

It is speculated that higher temperatures increase the rate of reduction by the reducing agent in the biotic system such as *P. aeruginosa* (Timoszyk *et al.*, 2017), *V. luteoalbum* (Gericke and Pinches, 2006) or *T. viride* (Kumari *et al*., 2016), where similar findings were reported. A filtrate of *T. viride* was reported to produce large triangular AuNPs which exceeded 500 nm in size at 50 °C, while increasing the temperatures from 25 °C to 50 °C caused a change from spherical AuNPs to large

triangular, hexagonal and pentagonal nanoplates in *V. luteoalbum*. In chemical synthesis, higher reduction rates are linked to the synthesis of anisotropic AuNPs while lower reduction rates result in a greater number of spherical AuNPs (Li *et al*., 2004). It can, therefore, be argued that in biological synthesis, lower temperatures reduce the rate of reduction favouring the production of spherical AuNPs while higher temperature yield more asymmetric AuNPs (Gericke and Pinches, 2006; Grzelczak *et al*., 2008).

From these findings, the optimal temperature for the biosynthesis of monodispersed AuNPs by *Enterobacter* sp. Pb204 was found to be 37 °C and used in all subsequent experimentation.

3.3.3.6 Concentration of gold ions

Similar to the kinetics of most chemical reactions, during the biosynthesis of AuNPs, the concentration of Au (III) within the solution becomes a rate-limiting factor. The majority of studies performed on the biological production of AuNPs have used a concentration of 1 mM gold ions (Gericke and Pinches 2006; He *et al*., 2007). Present findings indicate that when the concentration of Au (III) is lower than 1 mM, low yields of AuNPs lacking a discernible shape are produced. The LaMer mechanism (LaMer and Dinegar 1950; LaMer 1952) of nucleation and growth follows three stages. A rapid initial increase in the concentration of monomers in solution is followed by "burst nucleation" that leads to a reduction in monomer concentration. Finally, a diffusion-dependent growth of the nanoparticle is achieved. It may be inferred that at concentrations below 1 mM, there are too few Au (III) ions in solution that can be biologically reduced for nucleation. As a consequence, most of the ions are used during nucleation, leaving little room for growth by Ostwald ripening, coalescence or intraparticle ripening. This results in few nanoparticles which have a short-lived growth cycle hence the appearance of small amorphous AuNPs evident in Figure 3.15 A and B.

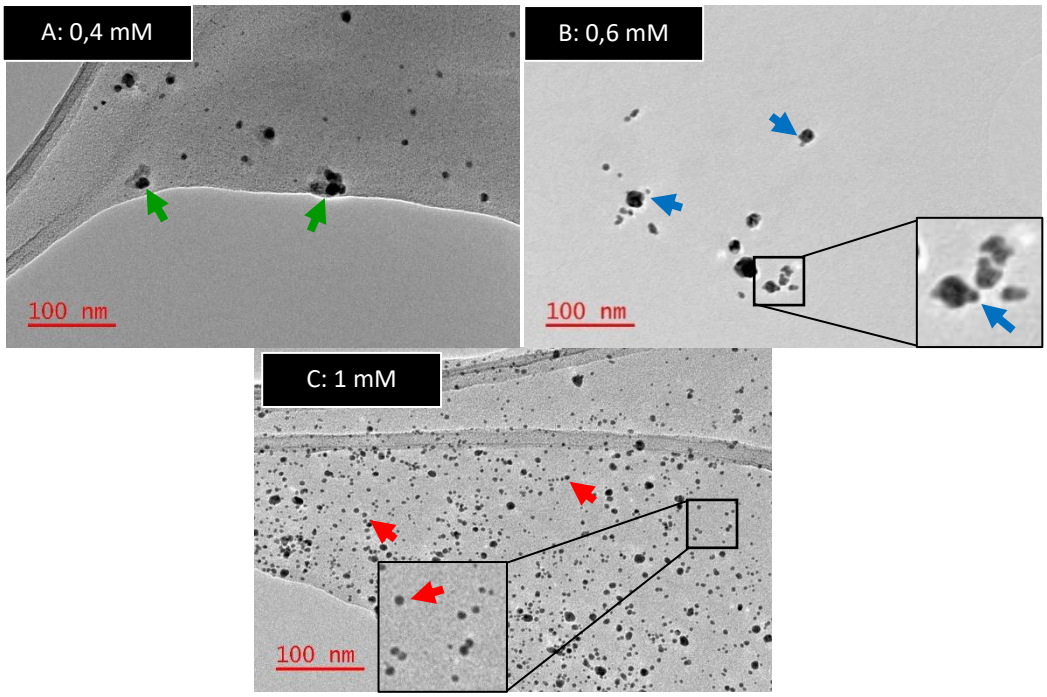

Figure 3.15: TEM micrographs of gold ion concentration trials. Small AuNPs lacking a distinct shape (green and blue arrows) were observed when 0.4 mM (A) and 0.6 mM (B) gold (III) ions were added to the reaction. A high yield of spherical AuNPs (red arrows) was present in the reaction containing 1 mM gold (III) ions (C).

At a concentration of 1 mM, there appear to be sufficient Au (III) ions to produce small (2-13 nm, Figure 3.16) AuNPs that are spherical in shape (Figure 3.15 C). Studies that evaluated higher concentrations of Au (III) report that small spherical AuNPs of increasing size are produced when the concentration was increased from 1 mM to 5 mM in *A. faecalis* (El-Deeb *et al*., 2014) and *T. scotodoctus* (Erasmus *et al.*, 2014). Furthermore, at concentrations >5 mM, large triangular and hexagonal nanosheets dominate leading to rupturing of the bacterial cells (Erasmus *et al.*, 2014).

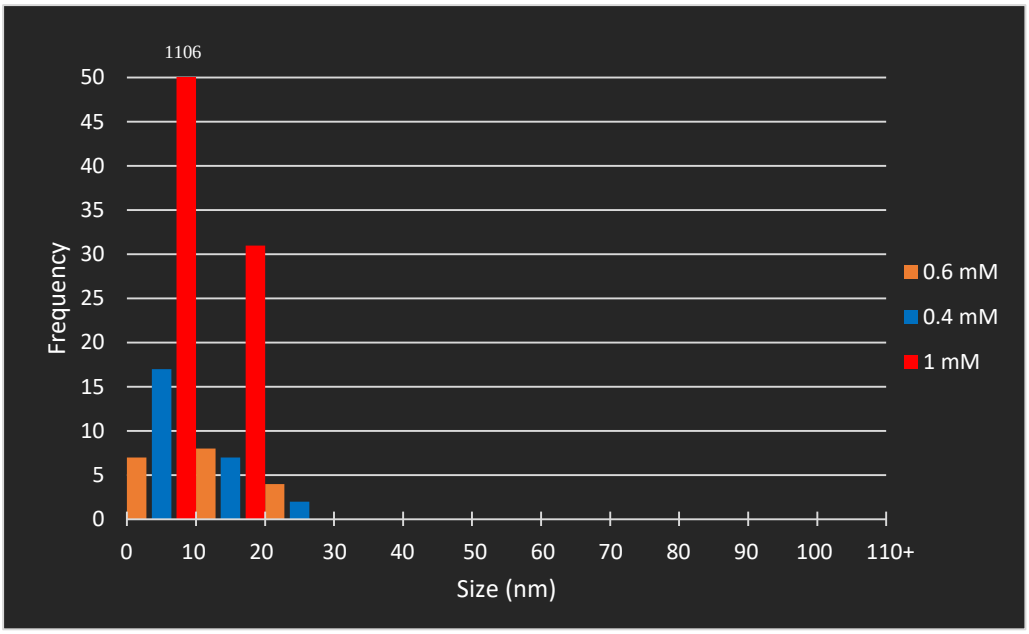

Figure 3.16: A histogram illustrating the size and frequency of the AuNPs produced in the temperature trials. The volume of media for each synthesis was standardised**.**

Although higher concentrations of Au (III) were not evaluated in the present study, *Enterobacter* sp. Pb204 would likely produce larger anisotropic AuNPs as reported for *A. faecalis* and *T. scotodoctus*. Based on the Turkevich method (Enustun and Turkevich, 1963) for the chemical synthesis of monodisperse AuNPs, Polte *et al*., (2010) described a four-step seeded growth mechanism. It begins with "burst nucleation" followed by coalescence and a diffusional growth step that is completed with the rapid consumption of the remaining gold precursor retaining the number of particles as well as constant polydispersity. The rate at which further gold (III) ions are added to the seeding solution would not increase nucleation events but rather increase the size of the AuNPs (Polte *et al*., 2010; Wuithschick *et al*., 2015). Alternatively, increasing the rate of nucleation by increasing the number of seed nanoparticles from Au^0 monomers favours the synthesis of smaller spherical AuNPs (Grzelczak *et al*., 2008; Das *et al*., 2010; Sajanlal *et al*., 2011; Wuithschick *et al*., 2015). Since nanoparticle formation is, in essence, a chemical reaction regardless of the source of the reducing agent (chemical vs biological), it can be assumed that the biological route of AuNP production would follow a similar

mechanism of seeded growth. Thus, controlling the concentration of Au (III) could be used to tune the size and shape of biogenic AuNPs.

3.3.3.7 Summary of optimal parameters for the production of uniform AuNPs in Enterobacter sp Pb204

The findings of the present study confirm that reaction parameters such as growth medium, the concentration of biocatalyst or gold ions, pH, temperature and reaction time influence the size, shape, monodispersity, and yield of AuNPs produced by *Enterobacter* sp. Pb204. Consequently, AuNPs for different types of applications can be tuned by selecting the most appropriate reaction parameters that will achieve the desired result. For the present study, the focus was on the delineation of a set of conditions under which *Enterobacter* sp. Pb204 would yield small, spherical nanoparticles. These nanoparticles are intended for application in diagnostic assays within the biomedical industry. Table 3.1 (Section 3.2.3., page 27) summarises the optimal parameters required for *Enterobacter* sp Pb204 to produce spherical AuNPs between 2-15 nm in diameter. These nanoparticles, which can be seen in figure 3.17, are formed when 2% (w/v) CB (cultured in LB broth) is used to reduce 1 mM $HAuCl_4$ (pH 3) at 37 ^oC for 24 hours.

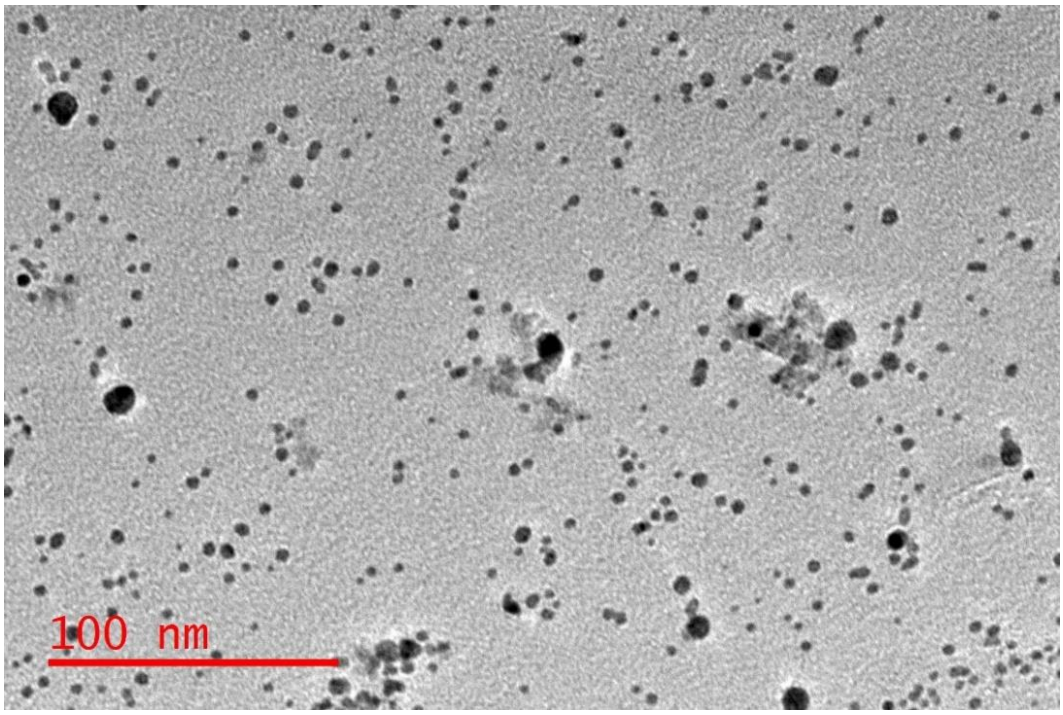

Figure 3.17: A TEM micrograph showing the production of uniformed spherical AuNPs by *Enterobacter* sp. Pb204 under optimal parameters determined in the present study. The optimal parameters are as follows: 2% (w/v) CB (cultured in LB broth) at a concentration of 1 mM $HAuCl_4$ (pH 3) at 37 ^oC for 24 hours.

3.4 Conclusion

The bacterial isolate *Enterobacter* sp. Pb204 is able to produce AuNPs from precursor metal ions. These AuNPs can be fine-tuned to form small, uniformly distributed, spherical particles by controlling reaction parameters such as growth media, reaction time, biocatalyst ratio, environmental pH, incubation temperature and metal concentration. This would suggest that *Enterobacter* sp. Pb204 is a viable biotic system for the production of AuNPs for application in various industries such as the biomedical industry or electronics industry.

Chapter 4: Linking AuNP synthesis to heavy metal resistance in *Enterobacter sp.* Pb204

4.1 Introduction

While there has been extensive research on the bacterial synthesis of NPs, the exact molecular mechanisms for synthesis of these nanoparticles are not yet fully understood. The most commonly accepted mechanism for the intracellular reduction of soluble Au and, in turn, the biosynthesis and stabilisation of the AuNPs involves proteins which contain tryptophan, cysteine, and tyrosine (Gole *et al*., 2001; Sastry *et al*., 2003). It is thought that these amino acid residues bind to the surface of AuNPs which reduce and stabilise the AuNPs (Suresh *et al*., 2011). In *R. capsulata* the use of NADH dependent reductase for the reduction of Au^{3+} to the AuNPs has been suggested (He *et al*., 2007). However, the exact nature of the NAD/NADH dependent reduction process is yet to be elucidated.

Recent studies have suggested that certain genetic pathways may play a role in NP synthesis in bacteria (Johnston *et al.,* 2013). Some of these studies have provided evidence to suggest that there may be a possible connection between heavy metal resistance and NP formation, including the biogenesis of AuNPs (Ramanathan *et al*., 2013). For example, the gold resistant bacteria *Delftia acidovorans,* possesses a specific cluster of genes that encode for a nonribosomal peptide synthetase/polyketide synthase called delftibactin, identified as the protein responsible for AuNP synthesis (Johnston *et al*., 2013). This metallophore protein is secreted extracellularly by *D. acidovorans* as a secondary metabolite and protects the bacterium from the harmful effects of soluble Au. To accomplish this, the protein detoxifies the soluble gold through chemical reduction and subsequently produces AuNPs (Johnston *et al*., 2013). *S. typhimurium* has been found to possess several metal resistance pathways including one specifically geared towards gold resistance by actively transporting gold ions outside of the cell (Pontel *et al*., 2007; Reith *et al*., 2009). Here, the Au resistance pathway is controlled by the GolS transcription factor that forms part of the MerR family, a group of transcription regulators that respond to environmental stress stimuli which include heavy metals

(Checa *et al*., 2007; Pontel *et al*., 2007). This transcription regulator is highly specific to gold ions (Checa *et al*., 2007). Both GolT and GolB, the proteins regulated by GolS, have been classified as a putative efflux P-type ATPase and metallochaperone, respectively. These proteins complexes actively transport gold ions out to the exterior of the cell to regulate the concentration of gold ions in the cytoplasm (Pontel *et al*., 2007; Reith *et al*., 2009).

As discussed in Chapter 3, *Enterobacter* sp. Pb204 was isolated from acid mine drainage decant from the West Rand of Gauteng, South Africa, (26°06'26.8"S 27°43'20.2"E). Furthermore, as shown in Chapter 3, this strain can effectively produce spherical AuNPs under specific reaction parameters. These spherical AuNPs have the potential to be used in a wide range of applications from drug delivery to biosensors (Tiwari *et al*., 2011). In this chapter, the complete genome of *Enterobacter* sp. Pb204 has been sequenced, with the aim of identifying potential molecular pathways involved in the synthesis of AuNPs. The genomic analysis showed that strain Pb204 belongs to the species *Enterobacter xiangfangensis* LMG 27195^{T}. Comparative genomic analyses identified several pathways which are predicted to play a role in heavy metal resistance, and their role in AuNP synthesis is postulated upon.

4.2 Methodology

4.2.1 Whole genome sequencing of Enterobacter sp. Pb204

Genomic DNA was extracted from *Enterobacter* sp. Pb204 using the Promega Wizard® Genomic DNA Purification Kit as per the manufacturer's instructions (Promega, Wisconsin, USA). The Wizard® Genomic Purification Kit is a five step purification which briefly entails: cell membrane lysis, nuclei lysis, protein separation, DNA concentration and desalting through isopropanol and ethanol precipitation and finally the rehydration and re-suspension of the precipitated genomic DNA in the Wizard® Genomic rehydration buffer. The genomic DNA was checked for quality and quantity using the ND 1000 Nanodrop spectrometer (Thermo Fisher Scientific, Massachusetts, USA). Subsequently, it was shipped to

Mr DNA (Texas, USA) and sequenced using the Illumina HiSeq 2500 (Illumina, California, USA) using the Nextera DNA Sample preparation kit (Illumina, California, USA). The quality of the raw sequence data from the HiSeq was assessed using the FastQC application (Illumina, California, USA). The FastQ toolkit (Illumina, California, USA) application was then used to trim the Nextera adapters and filter reads which were below a mean Phred quality score of 26, from the sequence data. The trimmed and filtered reads were subsequently *de novo* assembled using SPAdes (Bankevich *et al*., 2012). The processed genome was then compared to other genomes of the genus *Enterobacter* using the Genome-to-Genome Distance Calculator (http://ggdc.dsmz.de/home.php). Once the genome with the highest identity was found, the contigs from *Enterobacter* sp. Pb204 were further scaffolded against this complete genome using the MeDuSa scaffolder (Bosi *et al*., 2015). Manual curation of the assembled scaffolds was undertaken to obtain a complete genome sequence. The Rapid Annotations using Subsystems Technology (RAST) (Aziz *et al*., 2008) server and Prokka genome annotation application (Seeman, 2014) were used to annotate the complete assembled genome of *Enterobacter* sp. Pb204.

4.2.2 Comparative genomic analyses to identify genetic factors involved in AuNP synthesis

The annotated genome of *Enterobacter* sp. Pb204 was searched for putative genetic factors involved in AuNP synthesis using the protein sequences of known pathways for the biosynthesis of nanoparticles. This was done by local tBlastN analyses in Bioedit v. 7.2.5 (Hall, 1999) with the amino acid sequences of 96 proteins with a role in AuNP synthesis (Hall, 1999). Furthermore, the subsystem classification of the RAST (Aziz *et al*., 2008) genome annotation was used to assess categories of proteins known to be involved in nanoparticle biosynthesis, such as heavy metal resistance pathways.

The genome of *Enterobacter* sp. Pb204 was again compared to that of the closest relative (section 4.2.1, page 54), *Enterobacter xiangfangensis* LMG 27195^{T}. This was done on the assumption that, while *Enterobacter* sp. Pb204 is derived from acid

mine decant, it would contain the likely pathways for AuNP synthesis which would be expected to be absent from the latter strain, which was isolated from sourdough (Gu *et al.,* 2014). The genomes of these two organisms were aligned using Mauve v 2.4.0 (Darling *et al*., 2011). Furthermore, pair-wise localised BlastP comparisons using Bioedit v. 7.2.5 (Hall, 1999) were undertaken, where orthologues were assumed for those proteins sharing an amino acid identity greater than 50% and an alignment length of 70% or more. The processed data from the BlastP comparison was then used to determine the unique proteins in *Enterobacter* sp. Pb204. These proteins were then functionally annotated on the basis of the RAST server (Aziz *et al*., 2008) data as well as BlastP analysis against the NCBI non-redundant protein database (Altschul *et al.,* 1990).

4.3 Results

4.3.1 General features of the *Enterobacter* sp. Pb204 genome.

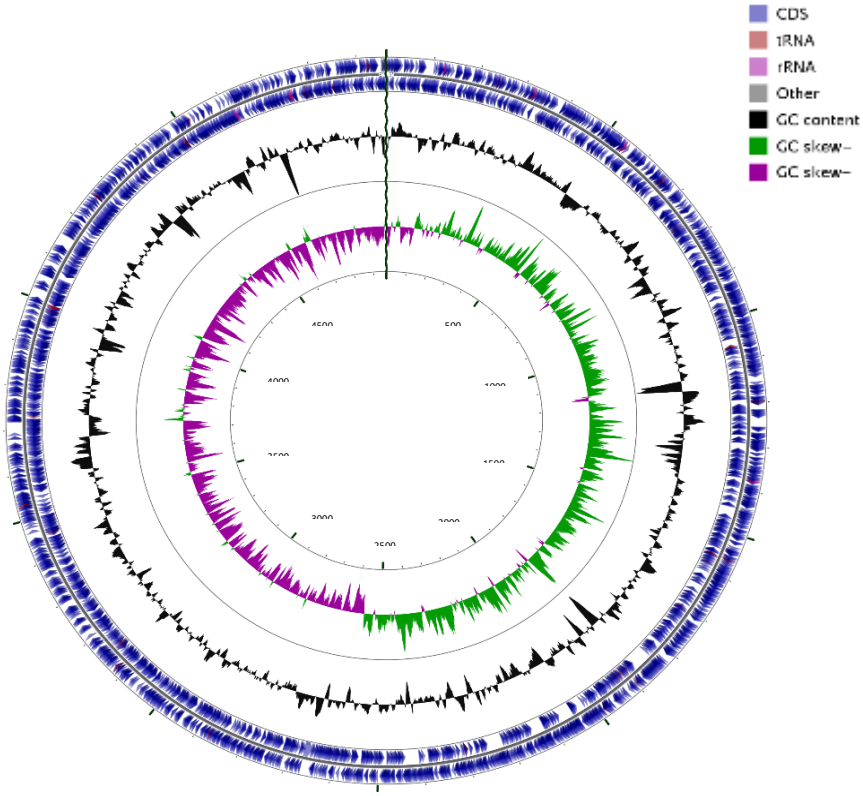

Figure 4.1: Circular map of the chromosome of *Enterobacter* sp. Pb204. the diagram was generated using CGview (Grant and Stothard 2008). The outer blue

ring denotes the direct strand coding DNA sequences, the inner blue ring denotes the complementary strand coding DNA sequences, red arrows denote the tRNA sequences and the purple arrows rRNA sequences. The black inner ring shows the GC content in a 1000 bp window, the green and purple rings represents the GC skew in the direct and complementary strands, respectively.

Paired-end sequencing of the *Enterobacter* sp. Pb204 genome using the Illumina HiSeq 2500 (Illumina, California, USA) platform yielded 6,373,398 read pairs with a maximum length of 151 bp. FastQC (www.bioinformatics.babraham.ac.uk/projects/fastqc/) treatment resulted in a final dataset of 6,067,324 paired reads which were used in subsequent genome assembly with SPAdes (Bankevich *et al*., 2012). *De novo* assembly yielded a total of 70 contigs with a total length of 4.94 megabases and a genome coverage of ~389x. The scaffolding of the draft contigs of Pb204 against the complete genome of *E. xiangfangensis* LMG 27195^T resulted in scaffolding of the Pb204 genome into 19 scaffolds. Manual curation allowed the closure of all gaps.

Table 4.1: The size of the genetic material elements

Genetic material element	Size (base pairs)	G+C content (%)	Distinctly encoded proteins
Genome	4956155	55.35	4610
Plasmid 1	3458	36.41	3
Plasmid 2	4096	55.52	4

The complete genome of *Enterobacter* sp. Pb204 is comprised of two circular small plasmids and a chromosome with a total size of ~ 4.96 megabases (Figure 4.1; Table 4.1). This is similar to what is typically observed (4.5-5 megabases) for members of the family *Enterobacteriaceae* (Brenner and Farmer, 2005) and similar as to what has been observed for members of the genus *Enterobacter* (Ren *et al*., 2010; DeAngelis *et al*., 2011; Shin *et al*., 2012). The average GC content is 55.35%, which also falls within the typical range (38-60%) for the *Enterobacteriaceae* (Brenner

and Farmer, 2005). Structural annotation of the genome with RAST (Aziz *et al*., 2008), showed that the chromosome codes for 4,610 distinct proteins, while three and four proteins are encoded on plasmid 1 and plasmid 2, respectively.

4.3.2 *Enterobacter* sp. Pb204 belongs to the species *E. xiangfangensis* LMG 27195^{T}

The 16S rRNA gene comparisons allowed for the delineation of strain Pb204 to the genus *Enterobacter*. However, the high identities values of the *Enterobacter* sp. Pb204 16S rRNA gene sequence to those of other *Enterobacter* species (> 96% nucleotide identity which correlates to the species cut-off value) did not allow for classification of Pb204 to the species level.

The genome sequence of *Enterobacter* sp. Pb204 was compared to those of available *Enterobacter* type strains, using the Genome-to-Genome Distance Calculator. This tool allows for digital DNA-DNA Hybridization (dDDH) values to be calculated between two comparator organisms. These dDDH values equate to wet-lab DNA-DNA hybridization results, where DDH values >70% indicate that two organisms belong to the same species (Auch *et al*., 2010). *Enterobacter* sp. Pb204 shared >70% dDDH values only with *Enterobacter xiangfangensis* LMG 27195^{T} (76% dDDH), indicating that *Enterobacter* sp. Pb204 represents a novel strain of this species.

E. xiangfangensis LMG 27195^{T} was first isolated by Gu *et al.*, (2014) from sourdough from the province of Heilongjiang in China. This bacterial species is phylogenetically related to *Enterobacter hormaechei*, *Enterobacter cancerogenus*, *Enterobacter asburiae*, *Enterobacter mori* LMG 25706^{T} and *Enterobacter ludwigii*, EN-119^{T}, having a 16S rRNA sequence homology above 98% with all of the above mentioned species (Gu *et al.*, 2014). *E. xiangfangensis* LMG 27195^{T}, is a non-spore forming, Gram negative, motile, rod-shaped bacterium. It is approximately 0.8 μm to 1.5 μm in size and is generally found as single cells. *E. xiangfangensis* LMG 27195^{T} is a facultative aerobe that produces acid from the fermentation of glycerol, L-arabinose, D-galactose, D-mannitol, D-glucose, D-fructose, D-mannose, D-

sorbitol, D-ribose, D-xylose, N-acetylglucosamine, methyl α-D-glucopyranoside, L-rhamnose, maltose, salicin, cellobiose, arbutin, lactose, melibiose, sucrose, trehalose, raffinose, gentiobiose, D-lyxose and D-fucose (Gu *et al*., 2014).

4.3.2.1 Comparison of the Enterobacter sp. Pb204 genome with E. xiangfangensis LMG 27195^T

Given that *E. xiangfangensis* LMG 27195^T was isolated from Chinese sourdough, while *E. xiangfangensis* Pb204 was isolated from acid mine drainage from a uranium mine, a genome comparison was undertaken to identify potential differences between them that may account for AuNP biosynthesis in strain Pb204. Comparison of the genomes of the two strains shows that the genome of *E. xiangfangensis* Pb204 is ~ 300 kilobases larger than that of the type strain. Genes in these additional genome regions may potentially be involved in allowing Pb204 to survive in the uranium mine environment. Furthermore, proteins may be encoded in these regions which are involved in nanoparticle biosynthesis. As such, the genomes of *E. xiangfangensis* Pb204 and LMG 27195^T were further compared to elucidate the roles of proteins encoded by these additional genomic regions. This was undertaken by pairwise BlastP (Altschul *et al.*, 1990) comparison to identify orthologous and non-orthologous proteins.

In total, 510 proteins (~ 10% of the genomic proteins) are unique to *E xiangfangensis* Pb204, while *E. xiangfangensis* LMG 27195^T codes for 256 proteins (~ 6% of total protein content) without representative orthologues in Pb204. By contrast, 3,894 proteins are core to both genomes. The majority of genomic regions unique to Pb204 represent phages integrated within the chromosome of this strain (Table 4.2). Similarly, the majority of genomic islands unique to *E. xiangfangensis* LMG 27195^T are of phage origin. The genomic islands differ in G+C content from the chromosome by between 15.78% below the genomic average and 5.25% above the genomic average G+C content, indicating that many of these genomic islands have likely been derived through horizontal gene transfer

events. The genomic islands *of E. xiangfangensis* encode 510 distinct proteins in total, accounting for 11.1% of the total proteins unique to *E. xiangfangensis* Pb204.

Table 4.2: Unique genomic islands of *E.xiangfangensis* Pb204

Genomic island	Size (kb)	CDS number	G+C content	G+C deviation from the chromosome	Codes for
IS1	7.2	5	60.60	5.25	Drug resistance
IS2	4.4	4	52.56	-2.79	Beta fimbria
IS3	7.0	7	56.16	0.81	Sialic acid metabolism
IS4	7.1	8	57.17	1.82	Type 1 pilus
IS5	29.9	37	50.73	-4.62	Integrated phage
IS6	13.8	14	41.56	-13.79	Mobile element
IS7	70.3	83	53.31	-2.04	Secondary flagellar (*flag*-2) system
IS8	9.7	7	55.08	-0.27	Lactose metabolism
IS9	16.8	16	59.48	4.13	Sugar metabolism
IS10	12.6	10	42.38	-12.97	Mannose metabolism
IS11	16.5	19	52	-3.35	Integrated phage
IS12	6.8	18	53.48	-1.87	Integrated phage
IS13	12.8	17	55.41	0.06	Integrated phage
IS14	7.8	9	59.34	3.99	Hypothetical protein coding region
IS15	23.1	15	53.7	-1.65	Pathogenicity
IS16	8.2	8	54.45	-0.9	Hypothetical protein coding region
IS17	8.9	8	54.61	-0.74	CRISPR

IS18	14.5	9	56.92	1.57	Drug resistance
IS19	5.8	5	51.04	-4.31	Sucrose metabolism
IS20	4.4	3	53.11	-2.24	Sugar metabolism
IS21	19.1	22	51.14	-4.21	Integrated phage
IS22	10.4	9	56.3	0.95	Fructose metabolism
IS23	16.2	22	47.42	-7.93	Nickle/cobalt resistance
IS24	14.1	19	53.62	-1.73	Integrated phage
IS25	6.7	9	56.71	1.36	Maltose metabolism
IS26	19.6	12	45.6	-9.75	Hypothetical protein coding region
IS27	6.4	5	53.85	-1.5	Hypothetical protein coding region
IS28	7.0	7	56.3	0.95	Hypothetical protein coding region
IS29	93.2	96	54.85	-0.5	Integrative conjugative element
IS30	9.7	7	39.57	-15.78	Hypothetical protein coding region

Among the genomic islands identified in *E. xiangfangensis* Pb204 is a ~ 93.2 kilobases region which has a G+C content of 54.85% (0.5% below the total genomic G+C content) and codes for 96 distinct proteins. This island shows hallmarks of integrative and conjugative elements (ICE). ICEs are mobile genetic elements which integrate into bacterial chromosomes (De Maayer *et al.*, 2015; Johnson and Grossman, 2015). ICE regions are fairly diverse and can range between approximately 20 kilobases to over 500 kilobases in a bacterial genome (Johnson and Grossman, 2015). ICE regions are usually composed of three modules which

are essential for the functioning of the element (De Maayer *et al*., 2015). These modules have genes which code for proteins involved in the excision, transfer, and maintenance of the ICE element in the host genome (De Maayer *et al*., 2015; Johnson and Grossman, 2015). Along with the 3 core modules, the ICE element contain extra cargo genes (Wozniak and Waldor, 2010; Johnson and Grossman, 2015). These cargo genes can affect the phenotype of the bacteria as they encode proteins which are involved in secondary metabolite production, pathogenesis, metabolic adaptation and metal and antibiotic resistance (Burrus *et al*., 2002; Wozniak and Waldor, 2010; Johnson and Grossman, 2015). These extra genes on the ICE element allow bacteria to inhabit niche environments such as areas with high concentrations of heavy metal ions (De Maayer *et al*., 2015).

The *E. xiangfangensis* Pb204 ICE, here named ICE*Exi*Pb204 in accordance with ICE nomenclature, was structurally and functionally annotated. This element contains 52 proteins which are predicted to be involved the excision, transfer, and maintenance of ICE*Exi*Pb204 (Figure 4.2). In addition, ICE*Exi*Pb204 encodes 50 proteins which are not involved in the functioning of the ICE but can be considered to form part of the ICE cargo. Of interest is that among these cargo genes are several which code for proteins involved in copper, zinc, silver and arsenic resistance (Figure 4.2). Twenty-eight of the 50 cargo genes are predicted to be involved in heavy metal resistance, suggesting that a major function of ICE*Exi*Pb204 is its contribution towards the heavy metal resistance of *E. xiangfangensis* Pb204. Given the importance of this phenotype in NP biosynthesis, we further elucidated these heavy metal resistance gene loci.

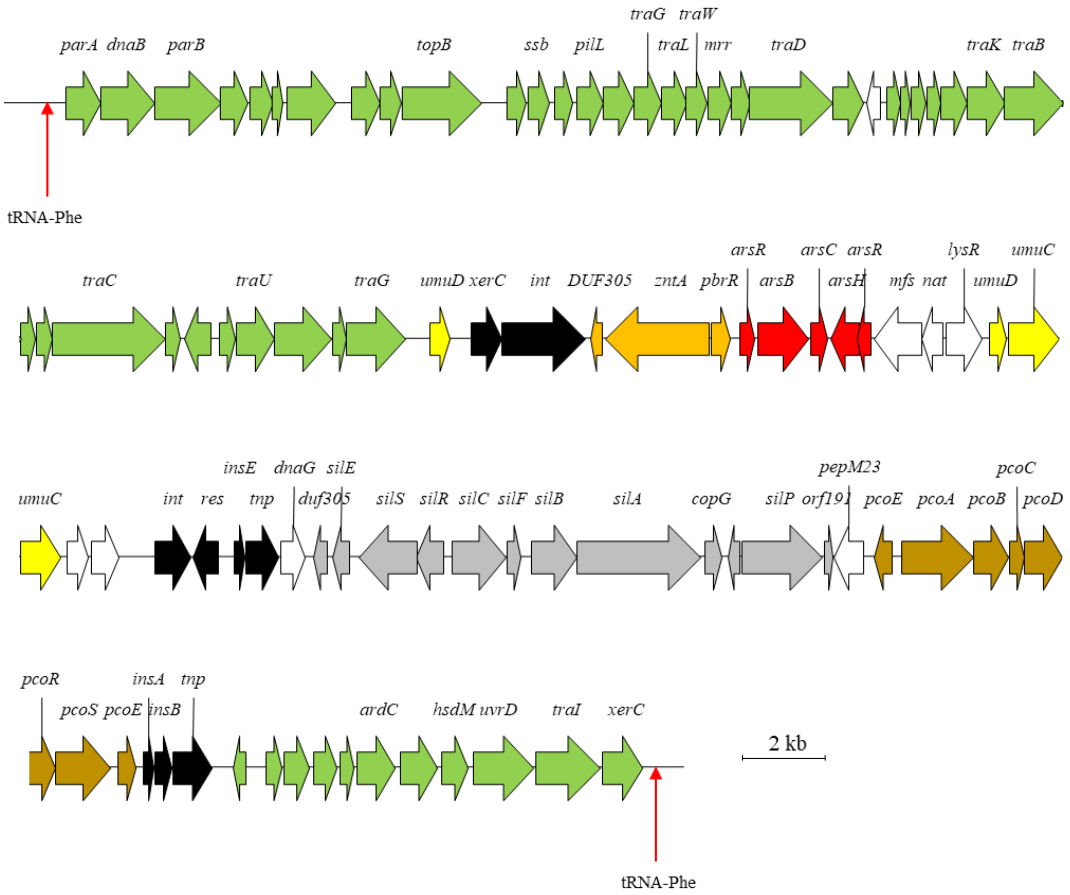

Figure 4.2: **Diagrammatic representation of the ICE found in *E. xiangfangensis* Pb204**. Genes coding for proteins involved in silver resistance are shown in grey, copper resistance in brown, arsenic resistance in red, zinc resistance in orange, *umu* stress pathway in yellow, insertion sequences in black and the green represents other proteins related to the ICE element.

4.3.3 *In silico* analysis of ICE*Exi*Pb204-encoded heavy metal resistance loci

Four distinct loci with predicted roles in heavy metal resistance could be identified in the ICE*Exi*Pb204 on the basis of orthology to characterised heavy metal resistance pathways in other bacterial taxa. These are described in more detail below:

4.3.3.1 Silver resistance pathway

The *sil* pathway, is responsible for providing silver resistance in many bacteria including *Escherichia coli* (Sütterlin *et al.*, 2014), *Pseudomonas stutzeri*

(Haefeli et *al*., 1984), *Enterobacter cloacae* (Percival *et al*., 2008) and *Salmonella typhimurium* (Woods *et al.*, 2009). The *sil* pathway acts as a silver ion efflux system (Silver, 2003) and is typically comprised of an operon consisting of nine genes, *silERSCFBA-orf105-silP* (Randall *et al*., 2015). SilS is a membrane kinase sensor which detects the silver ions and actives the transcription regulator SilR (Silver, 2003). The SilSR complex regulates the synthesis of a periplasmic silver ion binding protein, SilE, and two efflux systems, SilABC and SilP (Randall *et al*., 2015). SilABC is a tripartite chemiosmotic RND silver/hydrogen ion transport system while SilP is a P-type ATPase (Silver, 2003). Both these systems pump the silver ions out of the cell (Gupta *et al*., 1999; Silver, 2003). The full *sil* operon is present in *E. xiangfangensis* Pb204 (Figure 4.2) and the encoded proteins share 97.37% average amino acid identity with those in *Salmonella enterica* subsp. enterica serovar Typhimurium YU39.

4.3.3.3 Copper resistance pathway

A predicted copper resistance pathway was also found in ICE*Exi*Pb204. The *pco* operon encodes for a copper resistance system similar to that of the *sil* pathway (Bondarczuk and Piotrowska-Seget, 2013). It comprises of eight genes, *pcoEABCDRSE*. PcoRS represents a sensor/regulator complex much like the SilRS complex. It regulates the production of the copper efflux proteins (Bondarczuk and Piotrowska-Seget, 2013). PcoABC is the main copper ion efflux system and PcoD is thought to be responsible for copper uptake across the inner membrane (Rouch and brown, 1997; Bondarczuk and Piotrowska-Seget, 2013; Nies and Herzberg, 2013). The exact function of periplasmic protein PcoE is still unknown but *pcoE* is heavily induced by copper ions which indicate that it plays a role in copper resistance (Zimmermann *et al.*, 2012). This pathway has been found in *E. coli* (Huffman *et al*., 2002) and *Cupriavidus metallidurans* (Monchy *et al*., 2006). The eight proteins encoded by the *E. xiangfangensis* Pb204 *pco* locus share an average protein identity of 99.66% with those found in *Klebsiella pneumoniae* CG43.

4.3.3.4 Arsenic resistance pathway

Genes for arsenic resistance were also identified in ICE*Exi*Pb204. Here, parts of the *ars* pathway, coding for an arsenic transport system and an arsenic oxidase (Yang and Rosen, 2016), were present. The *arsB* and *arsC* genes found in *E. xiangfangensis* Pb204 code for an arsenic efflux system which transports the arsenic out of the cell (Yang *et al*., 2012). The *arsH* gene encodes a methylarsenite oxidase which oxidises MAs(III) and other trivalent organoarsenicals (Yang and Rosen, 2016). Both these system work together to reduce the concentration of arsenic within the cell (Levy, 1992; Yang and Rosen, 2016). The *ars* pathway has been characterised in several bacterial taxa, including *Sinorhizobium meliloti* (Yang *et al.*, 2005b), *Corynebacterium glutamicum* (Ordóñez *et al*., 2005) and *Staphylococcus aureus* (Ji and Silver, 1992). The ArsAB and ArsH proteins share 97.23% average amino acid identity with orthologous proteins in *Salmonella enterica s*ubsp. *enterica* CFSAN002050.

4.3.3.5 Zinc resistance pathway

ICE*Exi*Pb204 also encodes a predicted zinc resistance pathway (Figure 4.2). The *zntA* gene codes for a protein which belongs to the P-type ATPases family (Lu *et al*., 2016). Members of this family hydrolyse ATP to actively transport cations and lipids across the cell membrane in bacteria (Palmgren and Nissen, 2011). The ZntA P-type ATPases actively transports zinc, lead and cadmium ions out of the cell (Lu *et al.*, 2016). The ZntA orthologue encoded on the ICE*Exi*Pb204 shares 100% amino acid identity with that in *Salmonella enterica* subsp. *enterica* CFSAN001083. Adjacent to *zntA* in the ICE*Exi*Pb204 is a gene, *pbrR*, which is likely to encode a transcriptional factor which regulates the expression of *zntA* (Borremans *et al.*, 2001).

4.3.4 Other pathways with a putative role in heavy metal resistance and AuNP synthesis in *E. xiangfangensis* Pb204

The genome of *E. xiangfangensis* Pb204 was further searched for orthologues of proteins which have been shown to be involved in AuNP synthesis and gold resistance. This analysis showed that for two of these known AuNP biosynthesis

mechanisms, no orthologues could be found, namely delftibactin and the *gol* gold resistance pathway. However, a locus comprising of four genes coding for the proteins Pb204_CDS3676-3679, which are predicted to be involved in cobalt and nickel resistance, was found on the chromosome. These proteins encode for the nickle/cobalt resistance proteins NirA, NirB, NirC and NirD (Park *et al.,* 2008). It is thought that these four proteins are transmembrane and transporter proteins that have a high affinity for nickel (Park *et al.,* 2008). The NirA, NirB, NirC, and NirD found in *E. xiangfangensis* Pb204 have an amino acid identity of 92.42% with the proteins found in *Klebsiella oxytoca* CCUG 15788.

4.3.5 *E. xiangfangensis* Pb204 unique genes and AuNP synthesis

E. xiangfangensis Pb204 appears not to have pathways which are directly involved in the production of AuNPs such as delftibactin. This lack of AuNP synthesis and gold resistance pathways can be explained by the fact that gold is a rare element, so exposure to gold would be equally rare for bacteria (Reith *et al*., 2009). The economic value of gold also is a contributing factor to the low exposure of gold to bacteria as mining corporations strive to maximize the extraction of gold from the mines (Gajigo *et al*., 2012). This efficient extraction of gold prevents or lowers the wastage of gold which makes it less likely for bacteria to come into contact with gold (Gajigo *et al*., 2012). In literature, there is a consensus that NAD^+/NADH dependent reductase plays an important role in the synthesis of AuNPs but it can be argued that this mechanism does not provide a full explanation for the synthesis of AuNPs (Durán *et al*., 2011). The NAD^+/NADH dependent reductase family is a diverse group of proteins that have a wide range of functions so identifying those reductases involved in gold reduction on the genome of *E. xiangfangensis* Pb204 would be very difficult (Durán *et al*., 2011; Spaans *et al*., 2015).

Although no pathways which are directly linked to AuNPs synthesis were found in *E. xiangfangensis* Pb204, there were several metal resistance pathways that were identified. The majority of these are found on a predicted ICE element, ICE*Exi*Pb204. The presence of this element with its cargo of heavy metal resistance genes confirms the notion that *E. xiangfangensis* Pb204 has adapted to heavy metal

environments of the mine which generally have high concentrations of metal such as lead, zinc, copper, mercury, nickel, arsenic and uranium (Kondiah, 2013; Fashola *et al*., 2016).

A brief literature review reveals that proteins involved in the metabolic pathways that infer certain heavy metal resistance can be bi-functional towards other heavy metals (Nies 2003; Wiesemann *et al*., 2013). For example, it was found in a study by Wiesemann *et al.* (2013) that a copper resistance pathway in *C. metallidurans* also contributed towards its resistance to gold ions. When the *copABCD* complex, which is functionally the same as *pcoABCD*, was deleted from *C. metallidurans*, its resistance to gold ions was significantly reduced. It is thus possible that the pathway involved in resistance to heavy metals other than gold may play a role in Au resistance in *E. xiangfangensis* Pb204. Whether these resistance pathways also play a direct role in AuNP synthesis remains to be elucidated. It is also possible that additional proteins which are encoded on the genome, but could not directly linked to AuNP synthesis on the basis of *in silico* analyses, could play a role in AuNP synthesis.

4.4 Conclusion

From the genomic analysis of the bacterial isolate of this study, it was found that it was a unique strain of the bacterium *E. xiangfangensis* LMG 27195^{T} and has been named *E. xiangfangensis* Pb204. *E. xiangfangensis* Pb204 has many genetic pathways which are not found in *xiangfangensis* LMG 27195^{T}. A few of these unique genetic pathways are metal resistance pathways and are mainly found on a mobile genetic element in the form of an ICE element (ICE*Exi*Pb204). These unique pathways may be implicated in the biogenesis of AuNPs of *E. xiangfangensis* Pb204.

Chapter 5: Overall conclusions and future work

5.1 Overall conclusions

This study aimed to control the biogenesis of AuNPs in the bacteria *E. xiangfangensis* Pb204. Most research into biological synthesis AuNPs only identify novel biotic systems to synthesis AuNPs or only investigate the effect of one or two reaction parameters on the synthesis of AuNPs. The findings from Chapter 3 of this dissertation showed that the synthesis of AuNPs by *E. xiangfangensis* Pb204 can be influenced by a wide range of reaction parameters. These reaction parameters can be altered and can be used to control the synthesis of AuNPs by *E. xiangfangensi* Pb204 in order to create uniformed AuNPs. It was found that the use of CB of *E. xiangfangensis* Pb204 which is grown in LB at a 2% (w/v) ratio, at a pH of 3, incubated at a temperature of 37 °C for 24 hours with a chloroauric acid concentration of 1 mM will yield uniformed spherical AuNPs.

To further elucidate the ability of *E. xiangfangensis* Pb204 to produce AuNPs, whole genome sequencing was conducted on *E. xiangfangensis* Pb204. The genomic data produced by the whole genome sequencing revealed that *E. xiangfangensis* Pb204 was a unique strain of *E. xiangfangensis* LMG 26783^{T} which was isolated from sourdough in Heilongjiang Province, China. *E. xiangfangensis* Pb204's genome was approximately 300 kilobases larger than that of the type strain *E. xiangfangensis* LMG 26783^{T}. Further examination of the genomic data found that *E. xiangfangensis* Pb204 had many pathways which can confer resistance to silver, copper, zinc and cadmium, which were found on an ICE element. This would imply that *E. xiangfangensis* Pb204 has been conditioned for heavy metal contaminated conditions and may represent an important driver for the capacity of this strain to synthesise AuNPs.

5.2 Future Work

The uniform spherical AuNPs produced by *E. xiangfangensis* Pb204 could be used in future nanotechnological research projects. For example, the spherical AuNPs can be functionalised with attachment of biomolecules through biotin-streptavidin

binding. These functionalised biologically synthesised AuNPs could then be used in studies that investigate AuNP based drug delivery systems, AuNP based biosensors and many other AuNP based applications. Transcriptomics could also be done to further elucidate the molecular mechanisms involved in the synthesis of AuNPs by *E. xiangfangensis* Pb204, where the expression of genes by *E. xiangfangensis* Pb204 before and after exposure to chloroauric acid could be determined. The transcriptomic data could potentially reveal whether the gold ions cause any changes in the expression profiles which may identify any specific up- or down-regulated pathways in the presence of gold ions. This could provide invaluable insights into AuNP synthesis pathways employed by *E. xiangfangensis* Pb204, and furthermore fill a substantial gap in our understanding and exploitation of bacterial nanoparticle biosynthesis.

References

Ahmed, S., and Ikram, S. (2016). Biosynthesis of gold nanoparticles: a green approach. *Journal of Photochemistry and Photobiology B: Biology*, *161*, 141-153.

Altschul, S. F., Gish, W., Miller, W., Myers, E. W., and Lipman, D. J. (1990). Basic local alignment search tool. *Journal of molecular biology*, *215*(3), 403-410.

Amendola, V., Pilot, R., Frasconi, M., Maragò, O. M., and Iatì, M. A. (2017). Surface plasmon resonance in gold nanoparticles: a review. *Journal of Physics: Condensed Matter*, *29*(20), 203002.

Anastas, P., and Eghbali, N. (2010). Green chemistry: principles and practice. *Chemical Society Reviews*, *39*(1), 301-312.

Auch, A. F., Jan, M., Klenk, H. P., and Göker, M. (2010). Digital DNA-DNA hybridization for microbial species delineation by means of genome-to-genome sequence comparison. *Standards in Genomic Sciences*, *2*(1), 117-134.

Aziz, R. K., Bartels, D., Best, A. A., DeJongh, M., Disz, T., Edwards, R. A., Formsma, K., Gerdes, S., Glass, E.M., Kubal, M., and Meyer, F. (2008). The RAST Server: rapid annotations using subsystems technology. *BMC Genomics*, *9*(1), 75.

Badawi, M. I., and Ahmed, M. M. (2014). Gold nanoparticles as high-resolution imaging contrast agents for early cancer diagnoses: Computational study. *International Journal of Chemical And Applied Biological Sciences 1*, 12-17.

Banerjee, G., Pandey, S., Ray, A. K., and Kumar, R. (2015). Bioremediation of heavy metals by a novel bacterial strain Enterobacter cloacae and its antioxidant enzyme activity, flocculant production, and protein expression in presence of lead, cadmium, and nickel. *Water, Air, & Soil Pollution*, *226*(4), 91.

Bankevich, A., Nurk, S., Antipov, D., Gurevich, A. A., Dvorkin, M., Kulikov, A. S., Lesin, V.M., Nikolenko, S.I., Pham, S., Prjibelski, A.D., and Pyshkin, A. V. (2012). SPAdes: a new genome assembly algorithm and its applications to single-cell sequencing. *Journal of Computational Biology, 19*(5), 455-477.

Barber, D. J., and Freestone, I. C. (1990). An investigation of the origin of the colour of the Lycurgus Cup by analytical transmission electron microscopy. *Archaeometry*, *32*(1), 33-45.

Bharde, A., Kulkarni, A., Rao, M., Prabhune, A., and Sastry, M. (2007). Bacterial enzyme mediated biosynthesis of gold nanoparticles. *Journal of Nanoscience and Nanotechnology*, *7*(12), 4369-4377.

Bi, Y., and Lu, G. (2008). Morphological controlled synthesis and catalytic activities of gold nanocrystals. *Materials Letters*, *62*(17), 2696-2699.

Blomqvist, K., Nikkola, M., Lehtovaara, P., Suihko, M. L., Airaksinen, U., Stråby, K. B., Knowles, J. K., and Penttilä, M. E. (1993). Characterization of the genes of the 2, 3-butanediol operons from *Klebsiella terrigena* and *Enterobacter aerogenes*. *Journal of Bacteriology*, *175*(5), 1392-1404.

Bondarczuk, K., and Piotrowska-Seget, Z. (2013). Molecular basis of active copper resistance mechanisms in Gram-negative bacteria. *Cell Biology and Toxicology*, *29*(6), 397-405.

Borremans, B., Hobman, J. L., Provoost, A., Brown, N. L., and van Der Lelie, D. (2001). Cloning and functional analysis of thepbr lead resistance determinant of Ralstonia metallidurans CH34. *Journal of bacteriology*, *183*(19), 5651-5658.

Bosi, E., Donati, B., Galardini, M., Brunetti, S., Sagot, M. F., Lió, P., Crescenzi, P., Fani, R and Fondi, M. (2015). MeDuSa: a multi-draft based scaffolder. *Bioinformatics, 31*(15), 2443-2451.

Bourzac, K. (2013). Quantum dots go on display: Adoption by TV makers could expand the market for light-emitting nanocrystals. *Nature, 493*(7432), 283-284.

Brenner D.J., and Farmer J.J. (2005). Family I *Enterobacteriaceae*. In Bergey's Manual of Systematic Bacteriology, 2nd ed. Vol 2. The *Proteobacteria* part B: the *Gammaproteobacteria*. Brenner D, Kriger N. R, Staley J. T, Garrity G. M. Springer, New York, pp 587-607.

Brown, S.D., Nativo, P., Smith, J.A., Stirling, D., Edwards, P.R., Venugopal, B., Flint, D.J., Plumb, J.A., Graham, D., and Wheate, N.J. (2010). Gold nanoparticles for the improved anticancer drug delivery of the active component of oxaliplatin. *Journal of the American Chemical Society*, *132*(13), 4678-4684.

Burrows, N. D., Vartanian, A. M., Abadeer, N. S., Grzincic, E. M., Jacob, L. M., Lin, W., Li, J., Dennison, J.M., Hinman, J.G., and Murphy, C. J. (2016). Anisotropic nanoparticles and anisotropic surface chemistry. *The Journal of Physical Chemistry Letters, 7*(4), 632-641.

Burrus, V., Pavlovic, G., Decaris, B., and Guédon, G. (2002). Conjugative transposons: the tip of the iceberg. *Molecular Microbiology*. 46, 601–610.

Chandran, K., Song, S., and Yun, S. (2014). Effect of size and shape controlled biogenic synthesis of gold nanoparticles and their mode of interactions against food borne bacterial pathogens. *Arabian Journal of Chemistry*. doi:10.1016/j.arabjc.2014.11.041.

Chandran, S. P., Chaudhary, M., Pasricha, R., Ahmad, A., and Sastry, M. (2006). Synthesis of gold nanotriangles and silver nanoparticles using *Aloe vera* plant extract. *Biotechnology Progress*, *22*(2), 577-583.

Checa, S. K., Espariz, M., Audero, M. E. P., Botta, P. E., Spinelli, S. V., and Soncini, F. C. (2007). Bacterial sensing of and resistance to gold salts. *Molecular Microbiology*, *63*(5), 1307-1318.

Chen, C. C., Lin, Y. P., Wang, C. W., Tzeng, H. C., Wu, C. H., Chen, Y. C., Chen, C.P., Chen, L.C and Wu, Y. C. (2006). DNA− gold nanorod conjugates for remote control of localized gene expression by near infrared irradiation. *Journal of the American Chemical Society*, *128*(11), 3709-3715.

Chen, Y., Preece, J. A., and Palmer, R. E. (2008). Processing and characterization of gold nanoparticles for use in plasmon probe spectroscopy and microscopy of biosystems. *Annals of the New York Academy of Sciences*, *1130*(1), 201-206.

Chinhoga, N. (2016). *Defining a spectrum of metals biosorbed by Paenibacillus castaneae with respect to heavy metal contamination in Gauteng*. (Master's dissertation) Retrieved from WIReDSpace database. (http://hdl.handle.net/10539/21732).

Correa-Llantén, D.N., Muñoz-Ibacache, S.A., Castro, M.E., Muñoz, P.A., and Blamey, J.M. (2013). Gold nanoparticles synthesized by *Geobacillus* sp. strain ID17 a thermophilic bacterium isolated from Deception Island. *Microbial Cell Factories 12*, 75.

Dai, X., and Compton, R. G. (2006). Direct electrodeposition of gold nanoparticles onto indium tin oxide film coated glass: application to the detection of arsenic (III). *Analytical Sciences*, *22*(4), 567-570.

Daniel, M. C., and Astruc, D. (2004). Gold nanoparticles: assembly, supramolecular chemistry, quantum-size-related properties, and applications toward biology, catalysis, and nanotechnology. *Chemical Reviews*, *104*(1), 293-346.

Darling, A. E., Tritt, A., Eisen, J. A., and Facciotti, M. T. (2011). Mauve assembly metrics. *Bioinformatics*, *27*(19), 2756-2757.

Das, N., Vimala, R, and Karthika, P. (2008). Biosorption of heavy metals – An overview. *Indian Journal of Biotechnology*, *7*, 159-169.

Das, S. K., Das, A. R., and Guha, A. K. (2010). Microbial Synthesis of Multishaped Gold Nanostructures. *Small*, *6*(9), 1012-1021.

Dasary, S. S., Singh, A. K., Senapati, D., Yu, H., and Ray, P. C. (2009). Gold nanoparticle based label-free SERS probe for ultrasensitive and selective detection of trinitrotoluene. *Journal of the American Chemical Society*, *131*(38), 13806-13812.

De Maayer, P., Chan, W. Y., Martin, D. A., Blom, J., Venter, S. N., Duffy, B., Cowan, D.A., Smits, T.H., and Coutinho, T. A. (2015). Integrative conjugative elements of the ICEPan family play a potential role in *Pantoea ananatis* ecological diversification and antibiosis. *Frontiers in Microbiology*, *6*, 576.

DeAngelis, K. M., D'Haeseleer, P., Chivian, D., Fortney, J. L., Khudyakov, J., Simmons, B., Woo, H., Arkin, A.P., Davenport, K.W., Goodwin, L., and Chen, A. (2011). Complete genome sequence of "*Enterobacter lignolyticus*" SCF1. *Standards in Genomic Sciences*, *5*(1), 69-85.

Dell'Aglio, M., Mangini, V., Valenza, G., De Pascale, O., De Stradis, A., Natile, G., Arnesano, F., and De Giacomo, A. (2016). Silver and gold nanoparticles

produced by pulsed laser ablation in liquid to investigate their interaction with ubiquitin. *Applied Surface Science*, *374*, 297-304.

Deplanche, K., and Macaskie, L. E. (2008). Biorecovery of gold by *Escherichia coli* and *Desulfovibrio desulfuricans*. *Biotechnology and Bioengineering*, *99*(5), 1055-1064.

Dhand, C., Dwivedi, N., Loh, X. J., Ying, A. N. J., Verma, N. K., Beuerman, R. W., Lakshmi, R., and Ramakrishna, S. (2015). Methods and strategies for the synthesis of diverse nanoparticles and their applications: a comprehensive overview. *RSC Advances*, *5*(127), 105003-105037.

Diaz-Ravina, M., and Baath, E. (1996). Development of metal tolerance in soil bacterial communities exposed to experimentally increased metal levels. *Applied and Environmental Microbiology*, *62*(8), 2970-2977.

Dong, H., Gao, Y., Sinko, P. J., Wu, Z., Xu, J., and Jia, L. (2016). The nanotechnology race between China and the United States. *Nano Today*, *11*(1), 7-12.

Dreaden, E. C., Alkilany, A. M., Huang, X., Murphy, C. J., and El-Sayed, M. A. (2012). The golden age: gold nanoparticles for biomedicine. *Chemical Society Reviews*, *41*(7), 2740-2779.

Du, L., Jiang, H., Liu, X., and Wang, E. (2007). Biosynthesis of gold nanoparticles assisted by Escherichia coli DH5a and its application on direct electrochemistry of haemoglobin. *Electrochemistry Communications 9*: 1165–1170

Dubey, S. P., Lahtinen, M., and Sillanpää, M. (2010). Tansy fruit mediated greener synthesis of silver and gold nanoparticles. *Process Biochemistry*, *45*(7), 1065-1071.

Durán, N., Marcato, P. D., Durán, M., Yadav, A., Gade, A., and Rai, M. (2011). Mechanistic aspects in the biogenic synthesis of extracellular metal nanoparticles by peptides, bacteria, fungi, and plants. *Applied Microbiology and Biotechnology*, *90*(5), 1609-1624.

Elbakry, A., Zaky, A., Liebl, R., Rachel, R., Goepferich, A., and Breunig, M. (2009). Layer-by-layer assembled gold nanoparticles for siRNA delivery. *Nano Letters*, *9*(5), 2059-2064.

El-Deeb, B., Mostafa, N. Y., Tork, S., and El-Memoni, N. (2014). Optimization of green synthesis of gold nanoparticles using bacterial strain *Alcaligenes faecalis*. *Nanoscience and Nanotechnology Letters*, *6*(5), 372-384.

Eminoğlu, A., Vullo, D., Aşık, A., Çolak, D. N., Supuran, C. T., Çanakçı, S., and Osman Beldüz, A. (2016). Cloning, expression and biochemical characterization of a β-carbonic anhydrase from the soil bacterium Enterobacter sp. B13. *Journal of Enzyme Inhibition and Medicinal chemistry*, *31*(6), 1111-1118.

Enustun, B.V., and Turkevich, J. (1963). Coagulation of Colloidal Gold. *Journal of the American Chemical Society. 85*:3317–3328.

Erasmus, M., Cason, E. D., van Marwijk, J., Botes, E., Gericke, M., and van Heerden, E. (2014). Gold nanoparticle synthesis using the thermophilic bacterium *Thermus scotoductus* SA-01 and the purification and characterization of its unusual gold reducing protein. *Gold Bulletin*, *47*(4), 245-253.

Eustis, S., and El-Sayed, M. A. (2006). Why gold nanoparticles are more precious than pretty gold: noble metal surface plasmon resonance and its enhancement of the radiative and nonradiative properties of nanocrystals of different shapes. *Chemical Society Reviews*, *35*(3), 209-217.

Faraday, M. (1857). The Bakerian lecture: experimental relations of gold (and other metals) to light. *Philosophical Transactions of the Royal Society of London*, *147*, 145-181.

Fashola, M. O., Ngole-Jeme, V. M., and Babalola, O. O. (2016). Heavy metal pollution from gold mines: environmental effects and bacterial strategies for resistance. *International Journal of Environmental Research and Public Health*, *13*(11), 1047.

Feng, Y., Yu, Y., Wang, Y., and Lin, X. (2007) Biosorption and Bioreduction of Trivalent Aurum by Photosynthetic Bacteria *Rhodobacter capsulatus*. *Current Microbiology*, *55*, 402–408.

Feynman, R. P. (1960). There's plenty of room at the bottom. *Engineering and Science*, *23*(5), 22-36.

Freestone, I., Meeks, N., Sax, M., and Higgitt, C. (2007). The Lycurgus cup—a roman nanotechnology. *Gold Bulletin*, *40*(4), 270-277.

Gajigo, O., Mutambatsere, E., & Mdiaye, G. (2012). Gold mining in Africa: Maximizing economic returns for countries. African Development Bank. Working paper 147

Gericke, M., and Pinches, A. (2006). Biological synthesis of metal nanoparticles. *Hydrometallurgy*, *83*(1), 132-140.

Ghosh, S., Patil, S., Ahire, M., Kitture, R., Gurav, D. D., Jabgunde, A. M., Kale, S., Pardesi, K., Shinde, V., Bellare, J., and Dhavale, D. D. (2012). *Gnidia glauca* flower extract mediated synthesis of gold nanoparticles and evaluation of its chemocatalytic potential. *Journal of Nanobiotechnology*, *10*(1), 17.

Gole, A., Dash, C., Ramakrishnan, V., Sainkar, S. R., Mandale, A. B., Rao, M., and Sastry, M. (2001). Pepsin− gold colloid conjugates: preparation, characterization, and enzymatic activity. *Langmuir*, *17*(5), 1674-1679.

Grant, J. R., and Stothard, P. (2008). The CGView Server: a comparative genomics tool for circular genomes. *Nucleic acids research*, *36*, W181-W184.

Grimont, F., and Grimont, P. A. (2006). The genus *Enterobacter*. *Prokaryotes*, *6*, 197-214.

Grisel, R., Weststrate, K. J., Gluhoi, A., and Nieuwenhuys, B. E. (2002). Catalysis by gold nanoparticles. *Gold Bulletin*, *35*(2), 39-45.

Grzelczak, M., Pérez-Juste, J., Mulvaney, P., and Liz-Marzán, L. M. (2008). Shape control in gold nanoparticle synthesis. *Chemical Society Reviews*, *37*(9), 1783-1791.

Gu, C. T., Li, C. Y., Yang, L. J., and Huo, G. C. (2014). *Enterobacter xiangfangensis* sp. nov., isolated from Chinese traditional sourdough, and reclassification of Enterobacter sacchari Zhu *et al*. 2013 as Kosakonia sacchari comb. nov. *International Journal of Systematic and Evolutionary microbiology*, *64*(8), 2650-2656.

Gupta, A., Matsui, K., Lo, J. F., and Silver, S. (1999). Molecular basis for resistance to silver cations in Salmonella. *Nature Medicine*, *5*(2), 183.

Haefeli, C., Franklin, C., and Hardy, K. (1984). Plasmid-determined silver resistance in *Pseudomonas stutzeri* isolated from a silver mine. *Journal of Bacteriology*, *158*(1), 389-392.

Haiss, W., Thanh, N. T., Aveyard, J., and Fernig, D. G. (2007). Determination of size and concentration of gold nanoparticles from UV− Vis spectra. *Analytical Chemistry*, *79*(11), 4215-4221.

Hall, T. A. (1999). BioEdit: a user-friendly biological sequence alignment editor and analysis program for Windows 95/98/NT. *Nucleic Acids Symposium Series 41*(41) 95-98.

Haruta, M. (2003). When gold is not noble: catalysis by nanoparticles. *The Chemical Record*, *3*(2), 75-87.

Haruta, M. (2005). Catalysis: gold rush. *Nature*, *437*(7062), 1098-1099.

He, S., Guo, Z., Zhang, Y., Zhang, S., Wang, J., and Gu, N. (2007). Biosynthesis of gold nanoparticles using the bacteria *Rhodopseudomonas capsulata*. *Materials Letters*, *61*(18), 3984-3987.

He, S., Zhang, Y., Guo, Z., and Gu, N. (2008). Biological synthesis of gold nanowires using extract of *Rhodopseudomonas capsulata*. *Biotechnology Progress*, *24*(2), 476-480.

Herizchi, R., Abbasi, E., Milani, M., and Akilobasesarzadeh, A. (2016). Current methods for synthesis of gold nanoparticles. *Artificial Cells, Nanomedicine, and Biotechnology*, *44*(2), 596-602.

Hiebner, D. (2017) Biosynthesis and Characterization of Metallic Nanoparticles Produced by *Paenibacillus castaneae.* (Master's dissertation)

Hiramatsu, H., and Osterloh, F. E. (2004). A simple large-scale synthesis of nearly monodisperse gold and silver nanoparticles with adjustable sizes and with exchangeable surfactants. *Chemistry of Materials*, *16*(13), 2509-2511.

Holmes, J. D., Smith, P. R., Evans-Gowing, R., Richardson, D. J., Russell, D. A., and Sodeau, J. R. (1995). Energy-dispersive X-ray analysis of the extracellular cadmium sulfide crystallites of Klebsiella aerogenes. *Archives of microbiology*, *163*(2), 143-147.

Huang, D., Liao, F., Molesa, S., Redinger, D., and Subramanian, V. (2003). Plastic-compatible low resistance printable gold nanoparticle conductors for flexible electronics. *Journal of the Electrochemical Society*, *150*(7), G412-G417.

Huang, S. H. (2006). Gold nanoparticle-based immunochromatographic test for identification of Staphylococcus aureus from clinical specimens. *Clinica Chimica Acta*, *373*(1), 139-143.

Huang, X., and El-Sayed, M. A. (2010). Gold nanoparticles: optical properties and implementations in cancer diagnosis and photothermal therapy. *Journal of Advanced Research*, *1*(1), 13-28.

Huffman, D. L., Huyett, J., Outten, F. W., Doan, P. E., Finney, L. A., Hoffman, B. M., and O'Halloran, T. V. (2002). Spectroscopy of Cu (II)-PcoC and the multicopper oxidase function of PcoA, two essential components of *Escherichia coli* pco copper resistance operon. *Biochemistry*, *41*(31), 10046-10055.

Isomaa, B., Reuter, J., and Djupsund, B. M. (1976). The subacute and chronic toxicity of cetyltrimethylammonium bromide (CTAB), a cationic surfactant, in the rat. *Archives of Toxicology*, *35*(2), 91-96.

Issa, B., Obaidat, I. M., Albiss, B. A., and Haik, Y. (2013). Magnetic nanoparticles: surface effects and properties related to biomedicine applications. *International Journal of Molecular Sciences*, *14*(11), 21266-21305.

Iyer A, Mody K and Jha B (2004). Accumulation of hexavalent chromium by an exopolysaccharide producing marine *Enterobacter cloaceae*. *Marine Pollution Bulletin 49*: 974-977

Iyer A, Mody K and Jha B (2005).Characterization of an exopolysaccharide produced by a marine *Enterobacter cloacae*. *Indian Journal of Experimental Biology*, *43*, 467-471.

Jain, P. K., Lee, K. S., El-Sayed, I. H., and El-Sayed, M. A. (2006). Calculated absorption and scattering properties of gold nanoparticles of different size, shape, and composition: applications in biological imaging and biomedicine. *The Journal of Physical Chemistry B*, *110*(14), 7238-7248.

Javier, D. J., Castellanos-Gonzalez, A., Weigum, S. E., White, A. C., and Richards-Kortum, R. (2009). Oligonucleotide-gold nanoparticle networks for detection of *Cryptosporidium parvum* heat shock protein 70 mRNA. *Journal of Clinical Microbiology*, *47*(12), 4060-4066.

Jeng, S. L., Lu, J. C., and Wang, K. (2007). A review of reliability research on nanotechnology. *IEEE Transactions on Reliability*, *56*(3), 401-410.

Ji, G., and Silver, S. (1992). Reduction of arsenate to arsenite by the ArsC protein of the arsenic resistance operon of *Staphylococcus aureus* plasmid pI258. *Proceedings of the National Academy of Sciences*, *89*(20), 9474-9478.

Johnson, C. M., and Grossman, A. D. (2015). Integrative and conjugative elements (ICEs): what they do and how they work. *Annual Review of Genetics*, *49*, 577-601.

Johnston, C. W., Wyatt, M. A., Li, X., Ibrahim, A., Shuster, J., Southam, G., and Magarvey, N. A. (2013). Gold biomineralization by a metallophore from a gold-associated microbe. *Nature Chemical Biology*, *9*(4), 241-243.

Kabashin, A. V., Meunier, M., Kingston, C., and Luong, J. H. (2003). Fabrication and characterization of gold nanoparticles by femtosecond laser ablation in an aqueous solution of cyclodextrins. *The Journal of Physical Chemistry B*, *107*(19), 4527-4531.

Kalishwaralal, K., Deepak, V., Pandian, S. R. K., Kottaisamy, M., BarathManiKanth, S., Kartikeyan, B., and Gurunathan, S. (2010). Biosynthesis of silver and gold nanoparticles using *Brevibacterium casei*. *Colloids and Surfaces B: Biointerfaces*, *77*(2), 257-262.

Karthikeyan, S., and Beveridge, T. J. (2002). *Pseudomonas aeruginosa* biofilms react with and precipitate toxic soluble gold. *Environmental Microbiology*, *4*(11), 667-675.

Kim, D., Park, S., Lee, J. H., Jeong, Y. Y., and Jon, S. (2007). Antibiofouling polymer-coated gold nanoparticles as a contrast agent for in vivo X-ray computed tomography imaging. *Journal of the American Chemical Society*, *129*(24), 7661-7665.

Klumpp, S., Zhang, Z., and Hwa, T. (2009). Growth rate-dependent global effects on gene expression in bacteria. *Cell*, *139*(7), 1366-1375.

Kondiah, K. (2013). *Investigation of metallophiles for use in bioremediation of acid mine drainage.*

Konishi, Y., Tsukiyama, T., Tachimi, T., Saitoh, N., Nomura, T., and Nagamine, S. (2007). Microbial deposition of gold nanoparticles by the metal-reducing bacterium *Shewanella algae*. *Electrochimica Acta*, *53*(1), 186-192.

Kumari, M., Mishra, A., Pandey, S., Singh, S. P., Chaudhry, V., Mudiam, M. K. R., Shukla, S., Kakkar, P. and Nautiyal, C. S. (2016). Physico-chemical condition

optimization during biosynthesis lead to development of improved and catalytically efficient gold nano particles. *Scientific Reports*, *6*, 27575.

LaMer, V.K. (1952). Nucleation in Phase Transitions. *Industrial and Engineering Chemistry Research. 44*, 1270–1277.

LaMer, V.K., and Dinegar, R.H. (1950). Theory, Production and Mechanism of Formation of Monodispersed Hydrosols *Journal of the American Chemical Society 72*, 4847–4854.

Lau, I. P., Chen, H., Wang, J., Ong, H. C., Leung, K. C. F., Ho, H. P., and Kong, S. K. (2012). In vitro effect of CTAB-and PEG-coated gold nanorods on the induction of eryptosis/erythroptosis in human erythrocytes. *Nanotoxicology*, *6*(8), 847-856.

Levy, S. B. (1992). Active efflux mechanisms for antimicrobial resistance. *Antimicrobial Agents and Chemotherapy*, *36*(4), 695.

Li, C., Cai, W., Kan, C., Fu, G., and Zhang, L. (2004). Ultrasonic solvent induced morphological change of Au colloids. *Materials Letters*, *58*(1-2), 196-199.

Li, N., Zhao, P., and Astruc, D. (2014). Anisotropic gold nanoparticles: synthesis, properties, applications, and toxicity. *Angewandte Chemie International Edition*, *53*(7), 1756-1789.

Li, X., Xu, H., Chen, Z. S., and Chen, G. (2011). Biosynthesis of nanoparticles by microorganisms and their applications. *Journal of Nanomaterials*, *2011*, 1-16.

Li, Y., Li, Y., Li, Q., Fan, X., Gao, J., and Luo, Y. (2016). Rapid biosynthesis of gold nanoparticles by the extracellular secretion of *Bacillus niabensis* 45: characterization and antibiofilm activity. *Journal of Chemistry*, *2016*, 1-7.

Li, Y., Wang, H., Feng, Q., Zhou, G., and Wang, Z. S. (2013). Gold nanoparticles inlaid TiO 2 photoanodes: a superior candidate for high-efficiency dye-sensitized solar cells. *Energy and Environmental Science*, *6*(7), 2156-2165.

Lin, N., Huang, J., and Dufresne, A. (2012). Preparation, properties and applications of polysaccharide nanocrystals in advanced functional nanomaterials: a review. *Nanoscale*, *4*(11), 3274-3294.

Link, S., and El-Sayed, M. A. (1999). Size and temperature dependence of the plasmon absorption of colloidal gold nanoparticles. *The Journal of Physical Chemistry B*, *103*(21), 4212-4217.

Liu, J., and Lu, Y. (2006). Fast colorimetric sensing of adenosine and cocaine based on a general sensor design involving aptamers and nanoparticles. *Angewandte Chemie*, *118*(1), 96-100.

Lopez, N., Janssens, T. V. W., Clausen, B. S., Xu, Y., Mavrikakis, M., Bligaard, T., and Nørskov, J. K. (2004). On the origin of the catalytic activity of gold nanoparticles for low-temperature CO oxidation. *Journal of Catalysis*, *223*(1), 232-235.

Low, S. X. Z., Aw, Z. Q., Loo, B. Z. L., Lee, K. C., Oon, J. S. H., Lee, C. H., and Ling, M. H. T. (2013). Viability of *Escherichia coli* ATCC 8739 in nutrient broth, luria-bertani broth and brain heart infusion over 11 weeks. *Electronic Physician*, *5*(1), 576.

Lu, M., Li, Z., Liang, J., Wei, Y., Rensing, C., and Wei, G. (2016). Zinc resistance mechanisms of P 1B-type ATPases in *Sinorhizobium meliloti* CCNWSX0020. *Scientific Reports*, *6*, 29355.

Lu, Y. C., Xu, Z., Gasteiger, H. A., Chen, S., Hamad-Schifferli, K., and Shao-Horn, Y. (2010). Platinum− gold nanoparticles: a highly active bifunctional

electrocatalyst for rechargeable lithium− air batteries. *Journal of the American Chemical Society*, *132*(35), 12170-12171.

Luo, F., Zheng, L., Chen, S., Cai, Q., Lin, Z., Qiu, B., and Chen, G. (2012). An aptamer-based fluorescence biosensor for multiplex detection using unmodified gold nanoparticles. *Chemical Communications*, *48*(51), 6387-6389.

Luo, J., Wang, L., Mott, D., Njoki, P. N., Lin, Y., He, T., Xu, Z., Wanjana, B.N., Lim, I., Im, S., and Zhong, C. J. (2008). Core/shell nanoparticles as electrocatalysts for fuel cell reactions. *Advanced Materials*, *20*(22), 4342-4347.

Mafuné, F., Kohno, J. Y., Takeda, Y., Kondow, T., and Sawabe, H. (2001). Formation of gold nanoparticles by laser ablation in aqueous solution of surfactant. *The Journal of Physical Chemistry B*, *105*(22), 5114-5120.

Menon, S., Rajeshkumar, S., and Kumar, V. (2017). A review on biogenic synthesis of gold nanoparticles, characterization, and its applications. *Resource-Efficient Technologies*, *3*(4), 516-527.

Monchy, S., Benotmane, M. A., Wattiez, R., Van Aelst, S., Auquier, V., Borremans, B., M., Taghavi, S., Van der Lelie, D., and Vallaeys, T. (2006). Transcriptomic and proteomic analyses of the pMOL30-encoded copper resistance in *Cupriavidus metallidurans* strain CH34. *Microbiology*, *152*(6), 1765-1776.

Murdoch, M. G. I. N., Waterhouse, G. I. N., Nadeem, M. A., Metson, J. B., Keane, M. A., Howe, R. F., Llorca, J., and Idriss, H. (2011). The effect of gold loading and particle size on photocatalytic hydrogen production from ethanol over Au/TiO 2 nanoparticles. *Nature Chemistry*, *3*(6), 489.

Murphy, C. (2014, June 10) *Two Ways to Make Nanoparticles.* Retrieved from http://sustainable-nano.com/2014/06/10/two-ways-to-make-nanoparticles/

Nakashimada, Y., Rachman, M. A., Kakizono, T., and Nishio, N. (2002). Hydrogen production of *Enterobacter aerogenes* altered by extracellular and intracellular redox states. *International Journal of Hydrogen Energy*, *27*(11), 1399-1405.

Nangia, Y., Wangoo, N., Goyal, N., Shekhawat, G., and Suri, C. R. (2009). A novel bacterial isolate *Stenotrophomonas maltophilia* as living factory for synthesis of gold nanoparticles. *Microbial Cell Factories*, *8*(1), 39.

Narayanan, K. B., and Sakthivel, N. (2010). Biological synthesis of metal nanoparticles by microbes. *Advances in colloid and interface science*, *156*(1-2), 1-13.

Narayanan, S., Sathy, B. N., Mony, U., Koyakutty, M., Nair, S. V., and Menon, D. (2011). Biocompatible magnetite/gold nanohybrid contrast agents via green chemistry for MRI and CT bioimaging. *ACS Applied Materials and Interfaces*, *4*(1), 251-260.

Ndeh, N. T., Maensiri, S., and Maensiri, D. (2017). The effect of green synthesized gold nanoparticles on rice germination and roots. *Advances in Natural Sciences: Nanoscience and Nanotechnology*, *8*(3), 035008.

Nies, D. H. (2003). Efflux-mediated heavy metal resistance in prokaryotes. *FEMS Microbiology Reviews*, *27*(2-3), 313-339.

Nies, D. H., and Herzberg, M. (2013). A fresh view of the cell biology of copper in *Enterobacteria*. *Molecular microbiology*, *87*(3), 447-454.

Niikura, K., Matsunaga, T., Suzuki, T., Kobayashi, S., Yamaguchi, H., Orba, Y., awaguchi, A., Hasegawa, H., Kajino, K., Ninomiya, T., and Ijiro, K. (2013). Gold nanoparticles as a vaccine platform: influence of size and shape on immunological responses in vitro and in vivo. *ACS Nano*, *7*(5), 3926-3938.

Nikoobakht, B., and El-Sayed, M. A. (2003). Preparation and growth mechanism of gold nanorods (NRs) using seed-mediated growth method. *Chemistry of Materials*, *15*(10), 1957-1962.

Nirbhavane, H. M., Bagde, U. S., Nirbhavane, H. M., Bagde, U. S., and Nirbhavane, H. M. (2017). Resistance by *Enterobacter* spp. towards several antimicrobial drugs and heavy metals: A review. *African Journal of Biotechnology*, *16*(16), 826-841.

Noruzi, M., Zare, D., Khoshnevisan, K., and Davoodi, D. (2011). Rapid green synthesis of gold nanoparticles using *Rosa hybrida* petal extract at room temperature. *Spectrochimica Acta Part A: Molecular and Biomolecular Spectroscopy*, *79*(5), 1461-1465.

Ogi, T., Saitoh, N., Nomura, T., and Konishi, Y. (2010). Room-temperature synthesis of gold nanoparticles and nanoplates using *Shewanella algae* cell extract. *Journal of Nanoparticle Research*, *12*(7), 2531-2539.

Oliveira, J. P., Prado, A. R., Keijok, W. J., Ribeiro, M. R., Pontes, M. J., Nogueira, B. V., and Guimarães, M. C. (2017). A helpful method for controlled synthesis of monodisperse gold nanoparticles through response surface modeling. *Arabian Journal of Chemistry*. https://doi.org/10.1016/j.arabjc.2017.04.003

Ordóñez, E., Letek, M., Valbuena, N., Gil, J. A., and Mateos, L. M. (2005). Analysis of genes involved in arsenic resistance in *Corynebacterium glutamicum* ATCC 13032. *Applied and Environmental Microbiology*, *71*(10), 6206-6215.

Paknikar KM, Pethkar AV and Puranik PR (2003). Bioremediation of metalliferous wastes and products using inactivated microbial biomass. *Indian Journal of Biotechnology*, *2*, 426-443.

Palmgren, M. G., and Nissen, P. (2011). P-type ATPases. *Annual Review of Biophysics*, *40*, 243-266.

Pantidos, N., and Horsfall, L. E. (2014). Biological synthesis of metallic nanoparticles by bacteria, fungi and plants. *Journal of Nanomedicine & Nanotechnology*, *5*(5), 1-10.

Park, B., Cho, K., Kim, H., and Kim, S. (2006). Capacitance characteristics of MOS capacitors embedded with colloidally synthesized gold nanoparticles. *Semiconductor Science and Technology*, *21*(7), 975-979.

Park, J. S., Lee, S. J., Rhie, H. G., and Lee, H. S. (2008). Characterization of a chromosomal nickel resistance determinant from Klebsiella oxytoca CCUG 15788. *Journal of Microbiology and Biotechnology*, *18*(6), 1040-1043.

Percival, S. L., Woods, E., Nutekpor, M., Bowler, P., Radford, A., and Cochrane, C. (2008). Prevalence of silver resistance in bacteria isolated from diabetic foot ulcers and efficacy of silver-containing wound dressings. *Ostomy/wound Management*, *54*(3), 30-40.

Pimprikar, P. S., Joshi, S. S., Kumar, A. R., Zinjarde, S. S., and Kulkarni, S. K. (2009). Influence of biomass and gold salt concentration on nanoparticle synthesis by the tropical marine yeast Yarrowia lipolytica NCIM 3589. *Colloids and Surfaces B: Biointerfaces*, *74*(1), 309-316.

Pissuwan, D., Niidome, T., and Cortie, M. B. (2011). The forthcoming applications of gold nanoparticles in drug and gene delivery systems. *Journal of controlled release*, *149*(1), 65-71.

Polte J., Herder M., Erler R., Rolf S, Fischer A., Würth C., Thünemann A.F., Kraehnert R., and Emmerling F. (2010). Mechanistic insights into seeded growth processes of gold nanoparticles. *Nanoscale. 2*:2463-9.

Pontel, L. B., Audero, M. E. P., Espariz, M., Checa, S. K., and Soncini, F. C. (2007). GolS controls the response to gold by the hierarchical induction of *Salmonella*-specific genes that include a CBA efflux-coding operon. *Molecular Microbiology*, *66*(3), 814-825.

Pudge, I. B., Daugulis, A. J., and Dubois, C. (2003). The use of *Enterobacter cloacae* ATCC 43560 in the development of a two-phase partitioning bioreactor for the destruction of hexahydro-1, 3, 5-trinitro-1, 3, 5-s-triazine (RDX). *Journal of Biotechnology*, *100*(1), 65-75.

Rajbanshi, A. (2008). Study on Heavy Metal Resistant Bacteria in Guheswori Sewage Treatment Plant. *Our Nature*, *6*(1), 52-57.

Ramanathan, R., Field, M. R., O'Mullane, A. P., Smooker, P. M., Bhargava, S. K., and Bansal, V. (2013). Aqueous phase synthesis of copper nanoparticles: a link between heavy metal resistance and nanoparticle synthesis ability in bacterial systems. *Nanoscale*, *5*(6), 2300-2306.

Randall, C. P., Gupta, A., Jackson, N., Busse, D., and O'neill, A. J. (2015). Silver resistance in Gram-negative bacteria: a dissection of endogenous and exogenous mechanisms. *Journal of Antimicrobial Chemotherapy*, *70*(4), 1037-1046.

Rastogi, G., Osman, S., Kukkadapu, R., Engelhard, M., Vaishampayan, P. A., Andersen, G. L., and Sani, R. K. (2010). Microbial and mineralogical characterizations of soils collected from the deep biosphere of the former Homestake gold mine, South Dakota. *Microbial Ecology*, *60*(3), 539-550.

Ratchford, D. C., Dunkelberger, A. D., Vurgaftman, I., Owrutsky, J. C., and Pehrsson, P. E. (2017). Quantification of efficient plasmonic hot-electron injection in gold nanoparticle–TiO2 films. *Nano Letters*, *17*(10), 6047-6055.

Reith, F. *et*schmann, B., Grosse, C., Moors, H., Benotmane, M. A., Monsieurs, P., Grass, G., Doonan, C., Vogt, S., Lai, B., and Martinez-Criado, G. (2009). Mechanisms of gold biomineralization in the bacterium *Cupriavidus metallidurans*. *Proceedings of the National Academy of Sciences*, *106*(42), 17757-17762.

Ren, Y., Ren, Y., Zhou, Z., Guo, X., Li, Y., Feng, L., and Wang, L. (2010). Complete genome sequence of *Enterobacter cloacae* subsp. cloacae type strain ATCC 13047. *Journal of Bacteriology*, *192*(9), 2463-2464.

Rezaei, F., Xing, D., Wagner, R., Regan, J. M., Richard, T. L., and Logan, B. E. (2009). Simultaneous cellulose degradation and electricity production by *Enterobacter cloacae* in a microbial fuel cell. *Applied and Environmental Microbiology*, *75*(11), 3673-3678.

Rice, S. B., Chan, C., Brown, S. C., Eschbach, P., Han, L., Ensor, D. S., A.B., Bonevich, J., Vladár, A.E., Walker, A.R.H., and Zheng, J. (2013). Particle size distributions by transmission electron microscopy: an interlaboratory comparison case study. *Metrologia*, *50*(6), 663-678.

Roco, M. C. (2011). The long view of nanotechnology development: the National Nanotechnology Initiative at 10 years. *Journal of Nanoparticle Research*, *13*(2), 427-445.

Rojanathanes, R., Sereemaspun, A., Pimpha, N., Buasorn, V., Ekawong, P., and Wiwanitkit, V. (2008). Gold nanoparticle as an alternative tool for a urine pregnancy test. *Taiwanese Journal of Obstetrics and Gynecology*, *47*(3), 296-299.

Rosseler, O., Shankar, M. V., Karkmaz-Le Du, M., Schmidlin, L., Keller, N., and Keller, V. (2010). Solar light photocatalytic hydrogen production from water over Pt and Au/TiO 2 (anatase/rutile) photocatalysts: influence of noble metal and porogen promotion. *Journal of Catalysis*, *269*(1), 179-190.

Rouch, D. A., and Brown, N. L. (1997). Copper-inducible transcriptional regulation at two promoters in the *Escherichia coli* copper resistance determinant pco. *Microbiology*, *143*(4), 1191-1202.

Ruivo, A., Gomes, C., Lima, A., Botelho, M. L., Melo, R., Belchior, A., and de Matos, A. P. (2008). Gold nanoparticles in ancient and contemporary ruby glass. *Journal of Cultural Heritage*, *9*, e134-e137.

Sajanlal, P. R., Sreeprasad, T. S., Samal, A. K., and Pradeep, T. (2011). Anisotropic nanomaterials: structure, growth, assembly, and functions. *Nano reviews*, *2*(1), 5883.

Sastry, M., Ahmad, A., Khan, M. I., and Kumar, R. (2003). Biosynthesis of metal nanoparticles using fungi and actinomycete. *Current Science*, *85*(2), 162-170.

Sau, T. K., Pal, A., Jana, N. R., Wang, Z. L., and Pal, T. (2001). Size controlled synthesis of gold nanoparticles using photochemically prepared seed particles. *Journal of Nanoparticle Research*, *3*(4), 257-261.

Sau, T. K., Rogach, A. L., Jäckel, F., Klar, T. A., and Feldmann, J. (2010). Properties and applications of colloidal nonspherical noble metal nanoparticles. *Advanced Materials*, *22*(16), 1805-1825.

Scott, M., Gunderson, C. W., Mateescu, E. M., Zhang, Z., and Hwa, T. (2010). Interdependence of cell growth and gene expression: origins and consequences. *Science*, *330*(6007), 1099-1102.

Seemann, T. (2014). Prokka: rapid prokaryotic genome annotation. *Bioinformatics*, *30*(14), 2068-2069.

Shahverdi, A. R., Minaeian, S., Shahverdi, H. R., Jamalifar, H., and Nohi, A. A. (2007). Rapid synthesis of silver nanoparticles using culture supernatants of *Enterobacteria*: a novel biological approach. *Process Biochemistry*, *42*(5), 919-923.

Shaker, R., Osaili, T., Al-Omary, W., Jaradat, Z., and Al-Zuby, M. (2007). Isolation of *Enterobacter sakazakii* and other *Enterobacter* sp. from food and food production environments. *Food Control*, *18*(10), 1241-1245.

Shang, L., Jin, L., and Dong, S. (2009). Sensitive turn-on fluorescent detection of cyanide based on the dissolution of fluorophore functionalized gold nanoparticles. *Chemical Communications*, (21), 3077-3079.

Shantkriti, S., and Rani, P. (2014). Biological synthesis of copper nanoparticles using *Pseudomonas fluorescens*. *International Journal of Current Microbiology and Applied Sciences*, *3*(9), 374-383.

Sharma, N., Pinnaka, A. K., Raje, M., Ashish, F. N. U., Bhattacharyya, M. S., and Choudhury, A. R. (2012). Exploitation of marine bacteria for production of gold nanoparticles. *Microbial Cell Factories*, *11*(1), 86.

Shedbalkar, U., Singh, R., Wadhwani, S., Gaidhani, S., and Chopade, B. A. (2014). Microbial synthesis of gold nanoparticles: current status and future prospects. *Advances in Colloid and Interface Science*, *209*, 40-48.

Shin, S. H., Kim, S., Kim, J. Y., Lee, S., Um, Y., Oh, M. K., Kim, Y.R., Lee, J.and Yang, K. S. (2012). Complete genome sequence of *Enterobacter aerogenes* KCTC 2190. *Journal of Bacteriology*, *194*(9), 2373-2374.

Silver, S. (2003). Bacterial silver resistance: molecular biology and uses and misuses of silver compounds. *FEMS Microbiology Reviews*, *27*(2-3), 341-353.

Singh, A. K., and Srivastava, O. N. (2015). One-step green synthesis of gold nanoparticles using black cardamom and effect of pH on its synthesis. *Nanoscale Research Letters*, *10*(1), 353.

Singh, B. K., Walker, A., Morgan, J. A. W., and Wright, D. J. (2004). Biodegradation of chlorpyrifos by *Enterobacter* strain B-14 and its use in bioremediation of contaminated soils. *Applied and Environmental Microbiology*, *70*(8), 4855-4863.

Sinha, A. K., Seelan, S., Tsubota, S., and Haruta, M. (2004). Catalysis by gold nanoparticles: epoxidation of propene. *Topics in Catalysis*, *29*(3), 95-102.

Slocik, J. M., Naik, R. R., Stone, M. O., and Wright, D. W. (2005). Viral templates for gold nanoparticle synthesis. *Journal of Materials Chemistry*, *15*(7), 749-753.

Song, J. Y., and Kim, B. S. (2009). Rapid biological synthesis of silver nanoparticles using plant leaf extracts. *Bioprocess and Biosystems Engineering*, *32*(1), 79-84.

Sönnichsen, C., Franzl, T., Wilk, T., von Plessen, G., Feldmann, J., Wilson, O. V., and Mulvaney, P. (2002). Drastic reduction of plasmon damping in gold nanorods. *Physical Review Letters*, *88*(7), 077402.

Spaans, S. K., Weusthuis, R. A., Van Der Oost, J., and Kengen, S. W. (2015). NADPH-generating systems in bacteria and archaea. *Frontiers in Microbiology*, *6*, 742.

Srinath, B. S., and Rai, R. V. (2015). Biosynthesis of gold nanoparticles using extracellular molecules produced by *Enterobacter aerogenes* and their catalytic study. *Journal of Cluster Science*, *26*(5), 1483-1494.

Srivastava, N., and Mukhopadhyay, M. (2015). Biosynthesis and characterization of gold nanoparticles using *Zooglea ramigera* and assessment of its antibacterial property. *Journal of Cluster Science*, *26*(3), 675-692.

Su, R., Tiruvalam, R., Logsdail, A. J., He, Q., Downing, C. A., Jensen, M. T., Dimitratos, N., Kesavan, L., Wells, P.P., Bechstein, R., and Jensen, H. H. (2014). Designer titania-supported Au–Pd nanoparticles for efficient photocatalytic hydrogen production. *ACS Nano*, *8*(4), 3490-3497.

Su, Y. H., Ke, Y. F., Cai, S. L., and Yao, Q. Y. (2012). Surface plasmon resonance of layer-by-layer gold nanoparticles induced photoelectric current in environmentally-friendly plasmon-sensitized solar cell. *Light: Science and Applications*, *1*(6), e14.

Sugunan, A., Thanachayanont, C., Dutta, J., and Hilborn, J. G. (2005). Heavy-metal ion sensors using chitosan-capped gold nanoparticles. *Science and Technology of Advanced Materials*, *6*(3), 335-340.

Suresh, A. K., Pelletier, D. A., Wang, W., Broich, M. L., Moon, J. W., Gu, B., Allison, D.P., Joy, D.C., Phelps, T.J and Doktycz, M. J. (2011). Biofabrication of discrete spherical gold nanoparticles using the metal-reducing bacterium *Shewanella oneidensis*. *Acta Biomaterialia*, *7*(5), 2148-2152.

Sütterlin, S., Edquist, P., Sandegren, L., Adler, M., Tängdén, T., Drobni, M., Olsen, B and Melhus, Å. (2014). Silver resistance genes are overrepresented among Escherichia coli isolates with CTX-M production. *Applied and Environmental Microbiology*, *80*(22), 6863-6869.

Tan, Y., Liu, Y., Kong, L., Kang, L., and Ran, F. (2017). Supercapacitor electrode of nano-Co3O4 decorated with gold nanoparticles via in-situ reduction method. *Journal of Power Sources*, *363*, 1-8.

Thakkar, K. N., Mhatre, S. S., and Parikh, R. Y. (2010). Biological synthesis of metallic nanoparticles. *Nanomedicine: Nanotechnology, Biology and Medicine*, *6*(2), 257-262.

Thanh, N. T., Maclean, N., and Mahiddine, S. (2014). Mechanisms of nucleation and growth of nanoparticles in solution. *Chemical Reviews*, *114*(15), 7610-7630.

Timoszyk, A., Niedbach, J., Śliżewska, P., Mirończyk, A., and Kozioł, J. J. (2017). Eco-Friendly and Temperature Dependent Biosynthesis of Gold Nanoparticles Using the Bacterium *Pseudomonas aeruginosa*: Characterization and Antibacterial Activity. *Journal of Nano Research 48*, 114-124.

Tiwari, P. M., Vig, K., Dennis, V. A., and Singh, S. R. (2011). Functionalized gold nanoparticles and their biomedical applications. *Nanomaterials*, *1*(1), 31-63.

Tran, Q. H., and Le, A. T. (2013). Silver nanoparticles: synthesis, properties, toxicology, applications and perspectives. *Advances in Natural Sciences: Nanoscience and Nanotechnology*, *4*(3), 033001.

Tweney, R. D. (2006). Discovering discovery: How Faraday found the first metallic colloid. *Perspectives on Science, 14*(1), 97-121.

Vallabh, B. (2017) Defining the factors that influence the biosorption of lead by *Paenibacillus castaneae* and *Micrococcus luteus*. (Master's dissertation) Retrieved from WIReDSpace database (http://hdl.handle.net/10539/22730).

van Marwijk, J., Opperman, D. J., Piater, L. A., and van Heerden, E. (2009). Reduction of vanadium (V) by *Enterobacter cloacae* EV-SA01 isolated from a South African deep gold mine. *Biotechnology Letters*, *31*(6), 845-849.

Vance, M. E., Kuiken, T., Vejerano, E. P., McGinnis, S. P., Hochella Jr, M. F., Rejeski, D., and Hull, M. S. (2015). Nanotechnology in the real world: Redeveloping the nanomaterial consumer products inventory. *Beilstein Journal of Nanotechnology, 6*, 1769-1780.

Varia J.C., Zegeye A., Velasquez-Orta S., and Bull S. (2016). Process analysis of $AuCl_4^-$ sorption leading to gold nanoparticle synthesis by *Shewanella putrefaciens*. *Chemical Engineering Journal, 288*, 482-488.

Vijayaraghavan, K., and Yun, Y. S. (2008). Bacterial biosorbents and biosorption. *Biotechnology Advances, 26*(3), 266-291.

Wadhwani, S. A., Shedbalkar, U. U., Singh, R., Karve, M. S., and Chopade, B. A. (2014). Novel polyhedral gold nanoparticles: green synthesis, optimization and characterization by environmental isolate of *Acinetobacter* sp. SW30. *World Journal of Microbiology and Biotechnology*, *30*(10), 2723-2731.

Wang, Y., and Xia, Y. (2004). Bottom-up and top-down approaches to the synthesis of monodispersed spherical colloids of low melting-point metals. *Nano letters*, *4*(10), 2047-2050.

Wei, Z., and Zamborini, F. P. (2004). Directly monitoring the growth of gold nanoparticle seeds into gold nanorods. *Langmuir, 20*(26), 11301-11304.

Wiesemann, N., Mohr, J., Grosse, C., Herzberg, M., Hause, G., Reith, F., and Nies, D. H. (2013). Influence of copper resistance determinants on gold transformation by *Cupriavidus metallidurans* strain CH34. *Journal of Bacteriology*, *195*(10), 2298-2308.

Woods, E. J., Cochrane, C. A., and Percival, S. L. (2009). Prevalence of silver resistance genes in bacteria isolated from human and horse wounds. *Veterinary Microbiology*, *138*(3-4), 325-329.

Wozniak, R.A. F., and Waldor, M.K. (2010). Integrative and conjugative elements: mosaic mobile genetic elements enabling dynamic lateral gene flow. *Nature Reviews Microbiology*. *8*, 552–563

Wu, B., Liu, D., Mubeen, S., Chuong, T. T., Moskovits, M., and Stucky, G. D. (2016). Anisotropic growth of TiO2 onto gold nanorods for plasmon-enhanced hydrogen production from water reduction. *Journal of the American Chemical Society*, *138*(4), 1114-1117.

Wuithschick, M., Birnbaum, A., Witte, S., Sztucki, M., Vainio, U., Pinna, N., Rademann, K., Emmerling, F., Kraehnert, R., and Polte, J. (2015). Turkevich in new robes: key questions answered for the most common gold nanoparticle synthesis. *ACS Nano*, *9*(7), 7052-7071.

Xia, F., Zuo, X., Yang, R., Xiao, Y., Kang, D., Vallée-Bélisle, A., Gong, X., Yuen, J.D., Hsu, B.B., Heeger, A.J. and Plaxco, K.W., 2010. Colorimetric detection of DNA, small molecules, proteins, and ions using unmodified gold nanoparticles and conjugated polyelectrolytes. *Proceedings of the National Academy of Sciences*, *107*(24), 10837-10841.

Xie, J., Lee, J. Y., Wang, D. I., and Ting, Y. P. (2007). Identification of active biomolecules in the high-yield synthesis of single-crystalline gold nanoplates in algal solutions. *Small*, *3*(4), 672-682.

Xiong, Z., Zhang, L. L., Ma, J., and Zhao, X. S. (2010). Photocatalytic degradation of dyes over graphene–gold nanocomposites under visible light irradiation. *Chemical Communications*, *46*(33), 6099-6101.

Yang, H. C., and Rosen, B. P. (2016). New mechanisms of bacterial arsenic resistance. *Biomedical Journal*, *39*(1), 5-13

Yang, H. C., Cheng, J., Finan, T. M., Rosen, B. P., and Bhattacharjee, H. (2005b). Novel pathway for arsenic detoxification in the legume symbiont *Sinorhizobium meliloti*. *Journal of Bacteriology, 187*(20), 6991-6997.

Yang, H. C., Fu, H. L., Lin, Y. F., and Rosen, B. P. (2012). Pathways of arsenic uptake and efflux. *Current Topics in Membranes 69*, 325-358.

Yang, P. H., Sun, X., Chiu, J. F., Sun, H., and He, Q. Y. (2005a). Transferrin-mediated gold nanoparticle cellular uptake. *Bioconjugate Chemistry, 16*(3), 494-496.

Zeng, S., Yong, K. T., Roy, I., Dinh, X. Q., Yu, X., and Luan, F. (2011). A review on functionalized gold nanoparticles for biosensing applications. *Plasmonics, 6*(3), 491-506.

Zimmermann, M., Udagedara, S. R., Sze, C. M., Ryan, T. M., Howlett, G. J., Xiao, Z., and Wedd, A. G. (2012). PcoE—A metal sponge expressed to the periplasm of copper resistance *Escherichia coli.* Implication of its function role in copper resistance. *Journal of Inorganic Biochemistry, 115*, 186-197.

Zonooz, N. F., Salouti, M., Shapouri, R., and Nasseryan, J. (2012). Biosynthesis of gold nanoparticles by *Streptomyces* sp. ERI-3 supernatant and process optimization for enhanced production. *Journal of Cluster Science, 23*(2), 375-382.